BYG • DTU

DANMARKS
TEKNISKE
UNIVERSITET

Nicky Viebæk Petersen

Numerical Modeling of Reinforced Concrete Beam Structures Applying a Hinge Model

Master Thesis
DTU Civil Engineering
January 2010

Numerical Modeling of Reinforced Concrete Beam Structures Applying a Hinge Model

Nicky Viebæk Petersen

Master Thesis

Department of Civil Engineering
Technical University of Denmark

January 2010

Numerical Modeling of Reinforced Concrete Beam Structures
Applying a Hinge Model

Department of Civil Engineering
Technical University of Denmark

Preface

This thesis is submitted as a partial fulfilment of the requirements for the Danish master degree in civil engineering at the Technical University of Denmark. The thesis represents 30 ECTS-point and is carried out in the period from 15/8 2009 to 15/1 2010.

Kgs. Lyngby, January 2010

Nicky Viebæk Petersen, s042030

Acknowledgements

The author gratefully acknowledges the support of his supervisors associate professor Peter Noe Poulsen and associate professor John Forbes Olesen, both from the Technical University of Denmark - Department of Civil Engineering.

A special acknowledgement is given to Thomas Olsen with whom I have enjoyed many fruitful discussions during the work with the thesis.

Also a special thanks to the people that helped me with the final copy-editing.

Finally an extraordinary thanks is given to my girlfriend, family and friends for their support during the time of the project.

Abstract

A non-linear adaptive cracked hinge model is developed and the extension of the model to cover a simple reinforced non-linear adaptive cracked hinge is handled. The model is based on the fracture mechanics concepts of the fictitious crack model with a linear stress-crack opening relation. The non-linear adaptive cracked hinge model is compared to a finite element model and an explicit formulation for a cracked hinge model with constant width.

The non-linear adaptive cracked hinge model is inspired by observations done in the established finite element model and differs in its nature from existing hinge models. With use of a numerical solution the model is not restricted in the same way as an explicit formulation allowing a more exact description of the mechanisms present in an adaptive cracked hinge to be implemented. The basic idea of the non-linear adaptive cracked hinge model is to separate the hinge into a two-beam model constrained by kinematic relations and allow deformation of the hinge in both the axial and the vertical direction. The non-linear adaptive cracked hinge model is limited to cover the case where stresses are present all over the crack length.

With the finite element model as a basis for comparison it is shown that the bending stiffness relation in terms of a moment-curvature curve, and the crack mouth opening displacement relative to the curvature is better described by the non-linear adaptive cracked hinge model than the cracked hinge model with constant width. Especially after peak the difference between the non-linear adaptive cracked hinge model and the explicit formulation is entirely different in their nature. This is interesting considering statically undetermined concrete beam structures, since the forces will redistribute when the stiffness changes. But pure concrete structure are not constructed so the primary interest lies in the extension of the model to a reinforced adaptive cracked hinge model.

With the implementation of a simple reinforcement bar into the non-linear adaptive cracked hinge model it is shown that an extend of the presented model seems fairly easy to implement. Comparison of the established simple reinforced cracked hinge model with an elastic solution for a cracked cross section, with different values of the mechanical reinforcement degree, shows that the intended behavior of the simple reinforced adaptive cracked hinge is achieved. The solution begin to converge towards the elastic solution, but the results is limited to describe the behavior until a stress free crack mouth is reached.

The case of a non-zero normal force will not require further development, though this is not handled in this thesis, due to time limitations.

Resumé

En ikke-lineær adaptiv revnet hængselsmodel bliver udviklet og udvidelsen af modellen til at dække et simpelt armeret ikke-lineært adaptivt hængsel håndteres. Modellen er baseret på det brudmekaniske princip om en fiktiv revne "fictitious crack model" med en lineær spændings revnerelation. Den adaptive hængsels model sammenlignes med en elementmetodemodel og en explicit formulering for et hængsel med konstant hængselsbredde på lukket form.

Den adaptive hængselsmodel er inspireret af observationer fra elementmetodemodellen og afviger grundlæggende fra eksisterende hængselsmodeller. Ved brug af numeriske løsningsmetoder har modellen ikke de samme begrænsninger som en analytisk formulering og tillader derved en mere nøjagtig beskrivelse af de mekanismer, der findes i et adaptivt hængsel. Den grundlæggende ide for den nye model er at dele hængslet op i en sammensat bjælkemodel bestående af to bjælker der, samvirker som følge af kinematiske restriktioner. Deformation af begge bjælker i både vandret og lodret retning tillades.

Med finite elementmodellen som udgangspunkt for en sammeligning, vises det at for bøjningsstivheden i form af en moment-krumningsrelation og for revneåbningen ved hængslets bund relativt til krumningen, er bedre beskrevet med den adaptive hængselsmodel end hængselsmodellen for et hængsel med konstant bredde. Specielt efter den maksimale bæreevne ses en forskel på responset fra den adaptive hængselsmodel og modellen med fast hængselsbredde. Det er interessant for statisk ubestemte bjælkekonstruktioner, hvor krafterne vil omfordele sig når stivheden af konstruktionen ændres, men da sådanne konstruktioner ikke bygges ligger den primære interesse i udvidelsen af modellen til en armeret adaptiv hængselsmodel.

Med implementeringen af en simpel armeringsstang i den adaptive hængselsmodel illustreres at en udvidelse af den adaptive hængselsmodel ser rimelig tilgængelig ud. Sammenligning af den etablerede simple armerede adaptive revnede hængselsmodel med en elastisk løsning for et revnet tværsnit, viser de forventede karakteristika. Løsningen for det armerede adaptive hængsel konvergerer mod den elastiske løsning, men løsningen for det armerede adaptive hængsel er begrænset til at beskrive udviklingen indtil det yderste punkt i revnen bliver spændingsfrit.

Tilfældet med en normalkraft der er forskellig fra nul vil ikke kræve en videreudvikling af modellen, men undersøgelser af modellen med normalkraft forskellig fra nul er ikke nået inden for tidsrammen af dette projekt.

Table of Contents

List of Symbols

a length of the uncracked height of the hinge

A cross sectional area

A_0 representative shear cross sectional area

A_s cross sectional reinforcement area

c crack length

$CMOD$ crack mouth opening displacement

d distance from the top of the hinge to the reinforcement bar

D diameter of the reinforcement bar

E_c modulus of elasticity for the concrete

E_s modulus of elasticity for the reinforcement bar

$f(x)$ function describing the vertical normal stress distribution at the crack tip level

$F(x)$ Matlab function

F_{bar} force representing the reinforcement bar

f_c compression strength

f_t tensile strength

f_y yield strength for the reinforcement

G elastic shear modulus

G_F fracture energy

h hinge height

I_{vb} moment of inertia of the vertical beam used to derive horizontal displacements

M moment

M'	normalized moment
M_{bb}	moment at the boundary for the lower beam part B
M_{bt}	moment at the boundary for the upper beam part A
M_{cb}	moment at the mid-section for the lower beam part B
M_{ct}	moment at the mid-section for the upper beam part A
M_{c1}	cracking moment 1, used for illustration
M_{c2}	cracking moment 2, used for illustration
$M_0(y)$	resulting moment distribution used for virtual work calculation
$M_1(y)$	moment distribution from a virtual unit force
M_E	elastic moment
M_v	resulting moment from the vertical normal stress distribution
N	normal force
N_{bb}	normal force at the boundary for the lower beam part B
N_{bt}	normal force at the boundary for the upper beam part A
N_{cb}	normal force at the mid-section for the lower beam part B
N_{ct}	normal force at the mid-section for the upper beam part A
s	half hinge width
t	thickness of the hinge
$TolFun$	stop criteria for `fsolve` concerning function values
$TolX$	stop criteria for `fsolve` concerning the unknown varables
u_{bt}	total vertical displacement of the lower beam part B
$u_{V,b}$	vertical shear displacement of the lower beam part B
$u_{V,t}$	vertical shear displacement of the upper beam part A
u_b	vertical bending deflection of the lower beam part B
u_r	vertical displacement of the lower beam part B, due to rotation
u_t	bending deflection of the upper beam part A
u_tt	total displacement of the upper beam part A
$V_0(y)$	resulting shear force distribution used for virtual work calculation

$V_1(y)$	shear force distribution from a virtual unit force
w	half of the crack opening
w_0	half of the crack mouth opening displacement
w_1	half stress free crack opening
w_{01}	total horizontal displacement of lower beam part B, due to bending and shear displacement
$w_{01,a}$	bending contribution to horizontal displacement
$w_{01,b}$	shear contribution to horizontal displacement
w_{02}	horizontal displacement due to rotation of the horizontal support
x	x-direction, used for function description
$\mathbf{x}$	vector with unknown parameters
$\mathbf{x}_0$	vector with initial guess for unknown parameters
$\mathbf{x}_{new}$	vector with new prediction of the unknowns
y	y-direction, used for function description

Greek letters

α	relative crack length in the hinge model with constant width
β	dimensionless parameter
ΔN_b	normal force difference for the lower beam part B
ΔN_t	normal force difference for the upper beam part A
κ'	normalized curvature
κ_E	curvature corresponding to the elastic moment
μ	normalization of the moment for the hinge with constant width
ν	poisons ratio
Φ	mechanical reinforcement degree
Φ_{bal}	mechanical reinforcement degree for balanced reinforced cross section
Φ_{min}	mechanical reinforcement degree corresponding to minimum reinforcement
σ	stress

σ_{0b} stress at the bottom of the boundary

σ_{0c} stress at the bottom of the mid-section

σ_{1b} stress at the boundary at the crack tip level

σ_{1c} stress at the mid-section at the crack tip level

σ_{2b} stress at the top of the boundary

σ_{2c} stress at the top of the mid-section

$\sigma_{mid-section}$ stress distribution at the mid-section

σ_w stress-crack opening relation

σ_{xx} normal stress in the global x-direction

σ_{xy} shear stress in the global xy-direction

σ_{yy} normal stress in the global y-direction

σ_{yc} vertical tensile stress at the crack tip

$\sigma_{yy}(x)$ represents the vertical normal stress distribution observed in finite element model

τ_{1t} uniform shear stress given by the normal force differences at the bottom of beam part A

τ_{1b} uniform shear stress given by the normal force differences at the top of beam part B

Θ normalization of the angular deformation in the hinge model with constant width

ε'_b mean strain at the bottom of the hinge

ε'_c mean strain at the crack tip level

ε'_d mean strain at the level of the reinforcement

ε'_m mean strain at half the hinge height

ε'_t mean strain at the top of the hinge

ε_{cu} strain corresponding to crushing of the concrete

ε_y yield strain for the reinforcement

Chapter 1

Introduction

1.1 Introduction

Concrete is used in large amounts and is probably the most important construction material in the world. In Denmark alone about 8 million tons of concrete is used every year (year 2000). And still calculation methods are commonly based on simplified models based on empirical reseach. Crack formation and crack growth have an important role considering the performance of unreinforced and reinforced concrete. Especially the crack spacing and crack width in bending together with the bearing capacity of reinforced and unreinforced cracking beams have the interest of the current work. When Hillerberg presented the fictitious crack model in 1976, he demonstrated that with the concepts of the fictitious crack model it is possible to explain the variation of bending strength with beam depth, commonly referred to as size effects. With the concepts of the fictitious crack model, among other fracture mechanical concepts in combination with the advances in the area of the finite element method, it was possible to study the complicated cases of crack formation and crack growth. Today, history has shown that very moderate progress has been done in the area of establishing procedures easy to use that include crack formation and crack growth in unreinforced and reinforced concrete beams. Modern finite element analysis programs present features to model crack formation and crack growth, but it is rather time consuming to establish these models, and they are therefore often used with a scientific purpose. With the presentation of an analytical solution for load-displacement curves of concrete beams by Ulfkjaer et al. [1995], later referred to as a hinge model, it became possible by simple means to model the bending failure of concrete beams, described by load-displacement curves. For concrete beams, this model presented a method to describe the bending failure including the softening behavior. Considering undeterminate beam structures estimation of the bending stiffness is important since the forces might redistribute when the stiffness locally changes due to the softening behavior of a cracking section. For this purpose an explicit formulation for a reinforced adaptive cracked hinge was presented by Olesen, which was able, with rough definitions of the crack, to model the interaction between a cracking hinge and a reinforcement bar. A hinge can be interpreted as the length of a beam which is affected by the crack, and with a reinforcement bar this length was assumed equal to the length of the reinforcement de-bonding. Since this length will vary as the crack develop, an adaptive hinge is needed. In order to refine the reinforced adaptive cracked hinge model, a more exact description of the crack and de-bonding is necessary. Stepping from analytical solutions to numerical solutions allow a higher degree of freedom considering the parameters describing a reinforced hinge. In the present work the initial step to such a numerical description is presented in terms of a non-linear adaptive cracked hinge model. As inspiration for further work and to illustrate how to extend the presented model, a simple reinforcement bar will also be introduced.

1.2 Scope of the Thesis

The scope of this master thesis is to establish a non-linear adaptive cracked hinge model and present a numerical solution. The purpose of such a model is to establish the initial step towards a numerical solution for a reinforced adaptive cracked hinge model. Extension of the model is exemplified with the introduction of a simple reinforcement. The aim of such models is to present simple procedures to predict the bending stiffness relation in terms of a moment-curvature relation for unreinforced and reinforced concrete beam structures. Knowing the moment-curvature relation it is possible with existing commercial finite element analysis programs as for example ABAQUS, which is a general purpose finite element program, to implement this behavior in simple beam elements. This feature is originally designed for implementation of experimental results, but can be equivalently used with such a numerically obtained stiffness relation. With this new numerical solution for an adaptive cracked hinge it is possible to model the behavior of cracking concrete beam structures without using the more detailed time consuming finite element analysis.

1.3 Limitations

The work with the finite element analysis program DIANA has been limited by the restrictions of the DIANA teacher license, which has a restriction of 1000 elements.

1.4 Theoretical Background

The presented adaptive cracked hinge model is based on the fracture mechanics concept of the fictitious crack model with a linear stress crack opening relationship. The fictitious crack model for plain concrete was originally presented by Hillerborg et al. [1976]. In the concept of the fictitious crack model the material is assumed to be linear elastic until the tensile strength f_t whereafter a crack is assumed to propagate at the crack tip or tensile side of a bending beam. It is assumed that some aggregate interaction remains that can transfer stresses when the crack opens - this is referred to as bridging stresses since they connect the two crack faces. The principles of the fictitious crack model is illustrated in figure 1.1. The figure illustrates the crack opening with a smooth closure at the crack tip which illustrates another model assumption that the stress concentration at the crack tip is eliminated by the stresses on the crack faces so that the propagation of the crack is governed by the tensile strength f_t. The crack length is the sum of the stress free crack (visible crack) and the crack part where bridging stresses are still present.

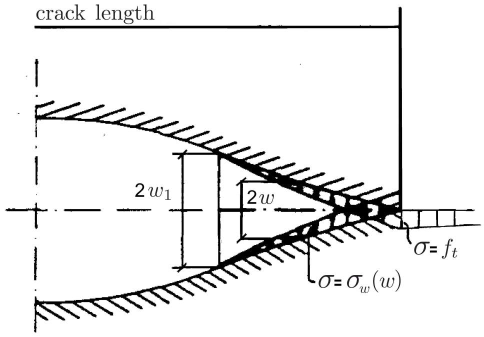

Figure 1.1: Concept of the fictitious crack model. The figure illustrates the smooth closure of the crack. Illustration from Hillerborg et al. [1976], slightly modified.

The stresses σ are assumed to decrease with increasing crack opening which, in the presented model, is represented by the linear stress-crack opening relation σ_w illustrated in figure 1.2 and represented by the function (1.1).

$$\sigma_w(w) = f_t - f_t \frac{w}{w_1} \tag{1.1}$$

where $\sigma_w(w)$ is the stress-crack opening relation as a function of half the crack opening w. w_1 is half the crack opening limit where the crack become stress free and f_t is the tensile strength.

While opening the crack, energy is absorbed. This energy is commonly known as the fracture energy G_F and can be defined as the absorbed energy per unit crack area in widening the crack from zero to halg the stress free opening w_1 in figure 1.1, according to Hillerborg et al. [1976]. The fracture energy corresponds to the area underneath the curve in figure 1.2 and is defined by (1.2).

$$G_F = \int_0^{w_1} \sigma_w(w) dw \tag{1.2}$$

In the presented model it must be emphasized that it is half the hinge that is considered and the parameters w and w_1 refer to half the crack opening and half the stress free crack opening respectively, see section 1.6 on page 5 for an illustrative presentation of the hinge and definition of a half hinge.

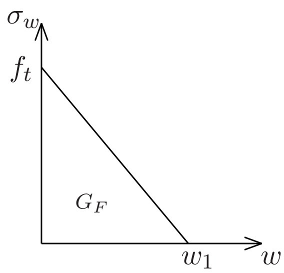

Figure 1.2: Linear stress-crack opening relationship.

1.5 Hinge Definition

When a concrete beam loaded with a constant moment reaches the elastic bearing capacity, multiple cracks will develop at the tension side of the beam. These cracks will unload the material next to the cracks as the bridging stress will decrease with increasing crack opening, as illustrated in figure 1.2. Due to inhomogeneities in the material, some of the cracks will develop faster than others, some of the cracks will increase in size while others will close as seen in figure 1.3.

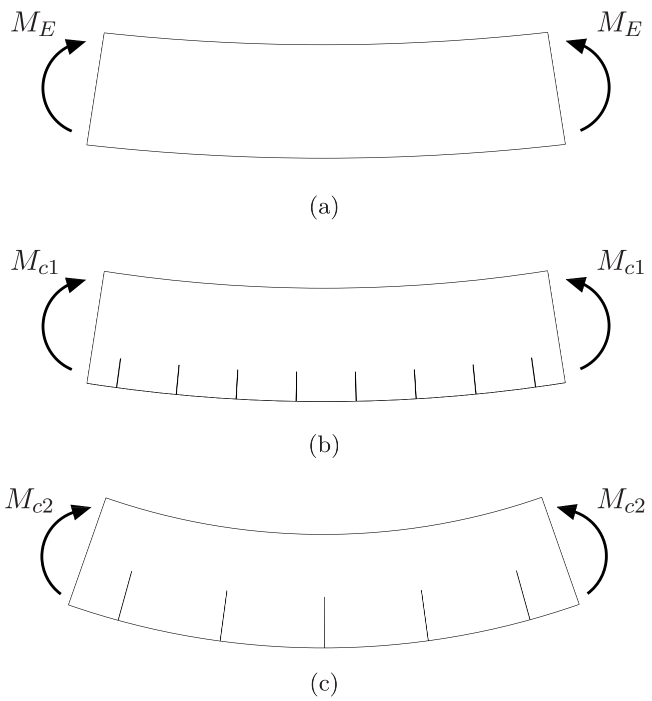

Figure 1.3: Beam model illustrating a cracking beam. (a) Elastic moment M_E - no cracks. (b) and (c) Moments M_{c1} and M_{c2} correspond to curvatures greater than the elastic curvature κ_E - multiple cracks. (c) illustrates that with a larger curvature follow fewer but longer, more open cracks and greater distance between the cracks.

At any curvature greater than the elastic curvature, a number of cracks are formed. To model this state a multiple number of hinges with a width equal to the space between the cracks is necessary. Such a state is illustrated in figure 1.4 where the stippled line indicates the internal hinge boundaries.

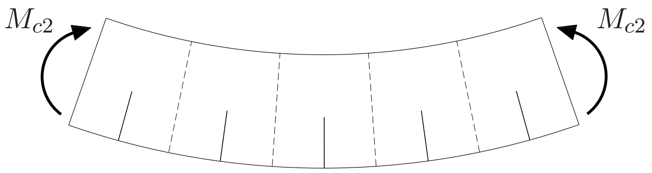

Figure 1.4: Cracked beam with indication of the hinges needed to model this exact state.

The model that will be presented will concern one of these hinges, and definition of the geometry and positive load directions are given in figure 1.5. It is emphasized that the illustrated hinge only exist in a deformed state and the undeformed illustration is used, since the geometry definitions refer to such an undeformed hinge. In the figure M and N represents the moment and normal force, h is the hinge height, t is the thickness of the hinge, s is the half hinge width and c is the crack length.

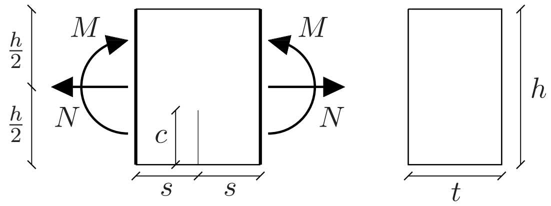

Figure 1.5: Undeformed hinge with geometry and load definitions.

1.6 Adaptive Cracked Hinge

An adaptive hinge can be defined as a hinge that will adapt its width to the present kinematic state. With such a definition of a finite hinge follows a boundary assumption. In common calculation methods for cracked concrete beam cross sections it is assumed that the tensile strength equals zero. With that assumption the stress equals zero in the crack plane from the crack mouth to the crack tip, see definitions of crack mouth and crack tip in the following figure 1.6. At the bottom of the beam the stress is assumed to increase from zero at the crack (point p1 in figure 1.6b) to an upper limit equal to the tensile strength right between to cracks (point p6 in figure 1.6b), see e.g. Heshe et al. [2005]. In continuation of such an assumption it seems reasonable to assume that the hinge boundary can be defined as the cross section where the tension stress in the bottom (point p6 in figure 1.6b) equals the tensile strength. The kinematic relation for the boundary is restricted by the adjacent hinges or beam in the sense that the boundary must remain plane throughout the deformation of the hinge. These rigid boundaries together with the overall deformation principle and a definition of the crack tip level are illustrated in figure 1.6a. Figure 1.6b defines half of the hinge with definition of six characteristic points and the cross sections mid-section and boundary, and half the crack opening w_0. Figure 1.6c illustrates the principle of the established model where the hinge is modeled as two independent beam parts, in the figure part A and part B, where the deformation of the two beam parts are internally restricted by the rigid boundary and an equal vertical displacement at the crack tip, point p2.

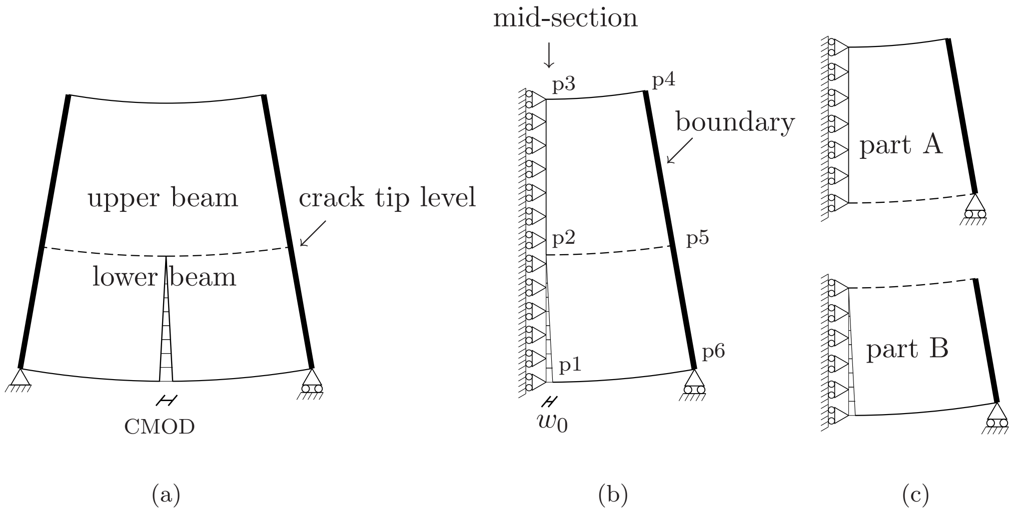

Figure 1.6: Definition of characteristic points, cross sections and the level of the crack tip. (a) deformed hinge where the stippled line indicates the crack tip level which also defines the limit between the upper and lower beam. The boundaries are shown with thick lines to indicate that they are rigid. (b) right beam half with definition of the mid-section, boundary and the six points p1-p6. (c) right beam half separated into the two beam parts (part A and part B) with indication of equivalent supports. The horizontal lines across the crack illustrate that there is still a connection.

In the following, descriptions of the geometric properties defined in figure 1.6 are given.

CMOD	Crack Mouth Opening Displacement
w_0	Half of the crack opening at point p1, $w_0 = \frac{1}{2}$ CMOD
p1	Crack mouth
p2	Crack tip
p3	Top of mid-section
p4	Top of boundary
p5	Point at crack tip level at the boundary
p6	Bottom point at the boundary
upper beam	Part of hinge above the crack tip level
lower beam	Part of hinge below the crack tip level
crack tip level	a level placed a crack length away from the bottom
mid-section	cracking cross section
boundary	boundary of the hinge (rigid)
part A	the right beam part of the upper beam
part B	the right beam part of the lower beam

It should be emphasized that throughout the report it is the hinge half to the right that is considered. The specific crack opening at the bottom of the mid-section w_0 refer to half of the crack opening.

Chapter 2

Finite Element Model

In this chapter, the finite element analysis program DIANA is used to gain information about the internal stress distributions present in an adaptive cracking hinge. To model the behavior of an adaptive cracking hinge, a model for each hinge width is necessary. This is done in order to achieve the correct boundary conditions.

Investigations using interface cohesive crack elements by Stang et al. [2007] show that smooth crack closure is automatically achieved in a finite element formulation with a stress criterion when a sufficient numbers of elements are applied. It has been observed that DIANA might find equilibrium state where the stresses near the crack tip are not as smooth as wanted. In order to confirm the reliability of the results gained from the finite element model, it is graphically controlled that the stress distribution in the mid-section and especially at the crack tip is smooth, though this is not documented.

There will be referred to DIANA which is the finite element analysis program and iDIANA which is the graphical user interface which is used while establishing the finite element model. DIANA is chosen for the finite element analysis since fracture mechanics were one of the original features of this finite element analysis program.

In this chapter only the main characteristics of the finite element model parameters will be described, and a more technical description is given in appendix B.

2.1 Finite Element Model Parameters

Several finite element models are constructed and for each model only one load step is considered to be correct concerning the boundary assumption for the adaptive hinge. The load step where the tensile strength in the bottom of the boundary (point p6 in figure 1.6b) is equal to the tensile strength. To refresh the concept of an adaptive hinge, it can be interpret as a hinge with a new hinge width for each increment of the curvature. When a finite element model with a given geometry is analyzed the model is deformed from zero curvature until failure, and for each increment of the curvature the model should consist of a multiple number of hinges, and therefore only the load step where the stress at the boundary bottom point equals the tensile strength, corresponding to exactly one hinge, is retrieved as a correct result.

The finite element model is defined through the following points: Geometry, mesh, elements, load and boundary conditions and material parameters.

2.1.1 Geometry

The adaptive hinge is a symmetric assuming that the crack will develop in the mid-cross section. Due to this symmetry assumption only half of the hinge is modeled with DIANA. The variable half hinge width is named s, the height is $h = 100\,\text{mm}$ and the thickness $t = 100\,\text{mm}$.

2.1.2 Mesh

The current work is done with the limited DIANA Teacher Licence with a limit of 1000 elements. A minimum of 32 elements over the height has been used for all models. The mesh for the adaptive hinge with width $s = 40\,\text{mm}$ is illustrated in figure 2.1.

2.1.3 Elements

The model is discretized with interface cohesive crack elements with a linear tension softening behavior for the crack. Eight-node quadrilateral isoparametric plane stress elements are used to model the elastic behavior of the concrete from the mid-section to the boundary. The beam element is a curved 3 nodes beam element based on the Mindlin-Reissner theory. The beam element is based on an isoparametric formulation which assumes that the displacements and rotations of the beam axis normals are independent and are respectively interpolated from the nodal displacements and rotations.

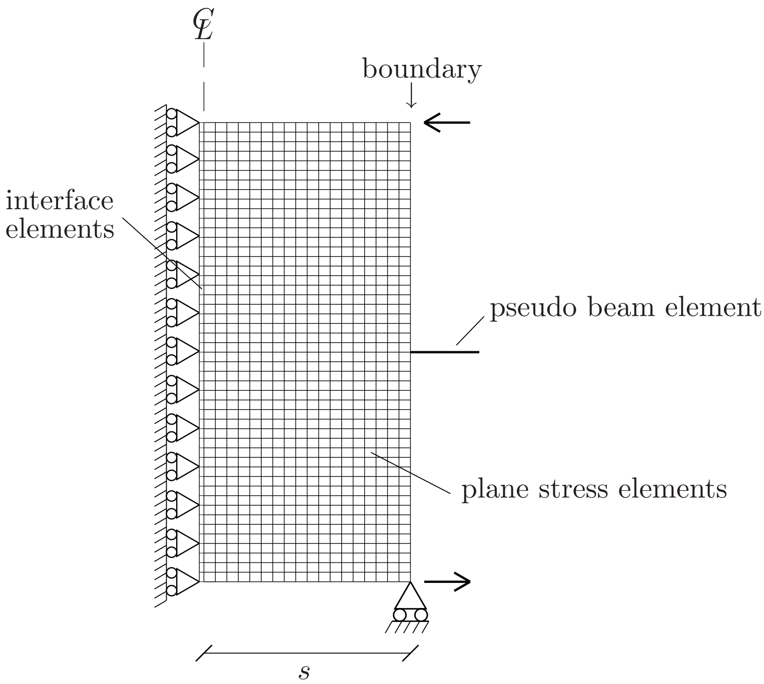

Figure 2.1: Finite element mesh, representing a model with half hinge width $s = 40\,\mathrm{mm}$. The interface elements are illustrated with a finite width, but are reduced to line elements in the finite element model.

2.1.4 Load and Boundary Conditions

The finite element model is supported horizontally at the mid-section and has a vertical support at the boundary. For the adaptive cracked hinge model presented in the proceeding chapter the boundary is assumed to remain plane. Therefore a translational constraint of the boundary in the finite element model is established. The pseudo beam element illustrated in figure 2.1 has both translational and rotational degrees of freedom. By means of a build in semi-automatic constraint in the finite element program it is possible to constraint the translational degree of freedom of the plane stress elements to the rotational degree of freedom of the pseudo beam element. The effect of this constraint is that all the element nodes which are placed on the boundary line will follow the rotation of the pseudo beam node on the boundary line. With this boundary constraint a constant moment with a linear stress distribution over the hinge height is achieved through the two concentrated loads, indicated with arrows in opposite direction in figure 2.1. Further description and illustrations are given in appendix B.1.4.

2.1.5 Material Parameters

Elastic material parameters for the pseudo beam element and the plane stress elements: $f_t = 2.4\,\mathrm{MPa}$ the tension strength; $E_c = 31000\,\mathrm{MPa}$ the modulus of elasticity and $\nu = 0.15$

poisons ratio. The interface elements are modeled with a isotropic linear elastic stiffness modulus equal to 3.1×10^{11}N/mm^3 (pre-crack), the tensile strength $f_t = 2.4$MPa, a fracture energy $G_F = 0.1$ N/mm and a shear modulus after cracking equal to 3.1×10^{11} N/mm^3.

2.2 Crack Tip Definition

The basic idea of the presented model is to consider the hinge as two horizontal beams connected along the top and bottom surface at the level of the crack tip as illustrated in figure 1.6. Thus, the beam heights are variable through the analysis. Therefore, it is relevant to observe the mechanisms present at this level in the finite element model. The crack tip is interpreted as the first integration point of the interface elements which is not cracked. It is possible to log information about the crack status at each load step during the analysis, see appendix B.2.3. In iDiana it is possible to get information about stresses along lines which can be defined on the node level (through nodes). For the horizontal line this could be a node at the mid-section and another at the boundary. Since the integration points in the interface cohesive crack elements are only coinciding with the nodes at the element ends, see figure 2.2, the definition of the crack tip can be rephrased in a way that the crack tip is at the first node above or equal to the first integration point which is not cracked. For the finite element model represented by figure 2.4, 21 elements and additional 3 integration points are cracked. The crack tip level is therefore defined as a line through the top of the 22nd element. As illustrated in figure 2.2 the crack tip level were data are retrieved might vary depending of which of the four integration points that are cracked.

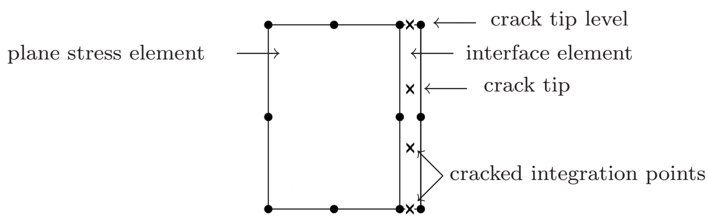

Figure 2.2: Definition of crack tip and crack tip level. Integration points in the interface element marked with a cross, and nodes are marked with a black bullet.

2.3 Finite Element Illustrations

In this section representative illustrations of the adaptive hinge, modeled by finite elements are presented. In figure 2.3 the retrieved moment-curvature relations are plotted with a small dot for each of the results, and a larger circle representing the two examples (s = 25 mm and s = 40 mm) considered in this section. The linear linear interpretation between the dots are illustratively added by the author.

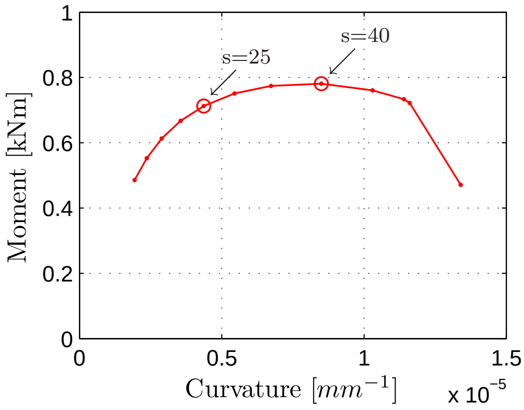

Figure 2.3: Moment-curvature curve representing the results retrieved from the finite element model.

The stress distributions σ_{yy}, σ_{xx} and σ_{xy} representing the vertical and horizontal normal stresses and the shear stresses are illustratively presented by means of color plots in figure 2.4.

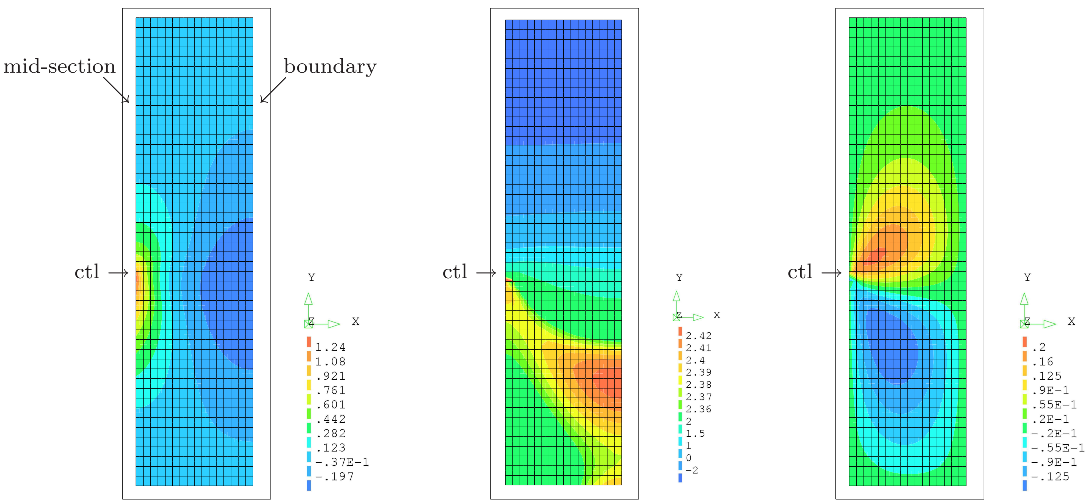

Figure 2.4: Stress distribution within a half hinge, $s = 25\,mm$. Definition of *crack tip level* (ctl), see section 2.2.

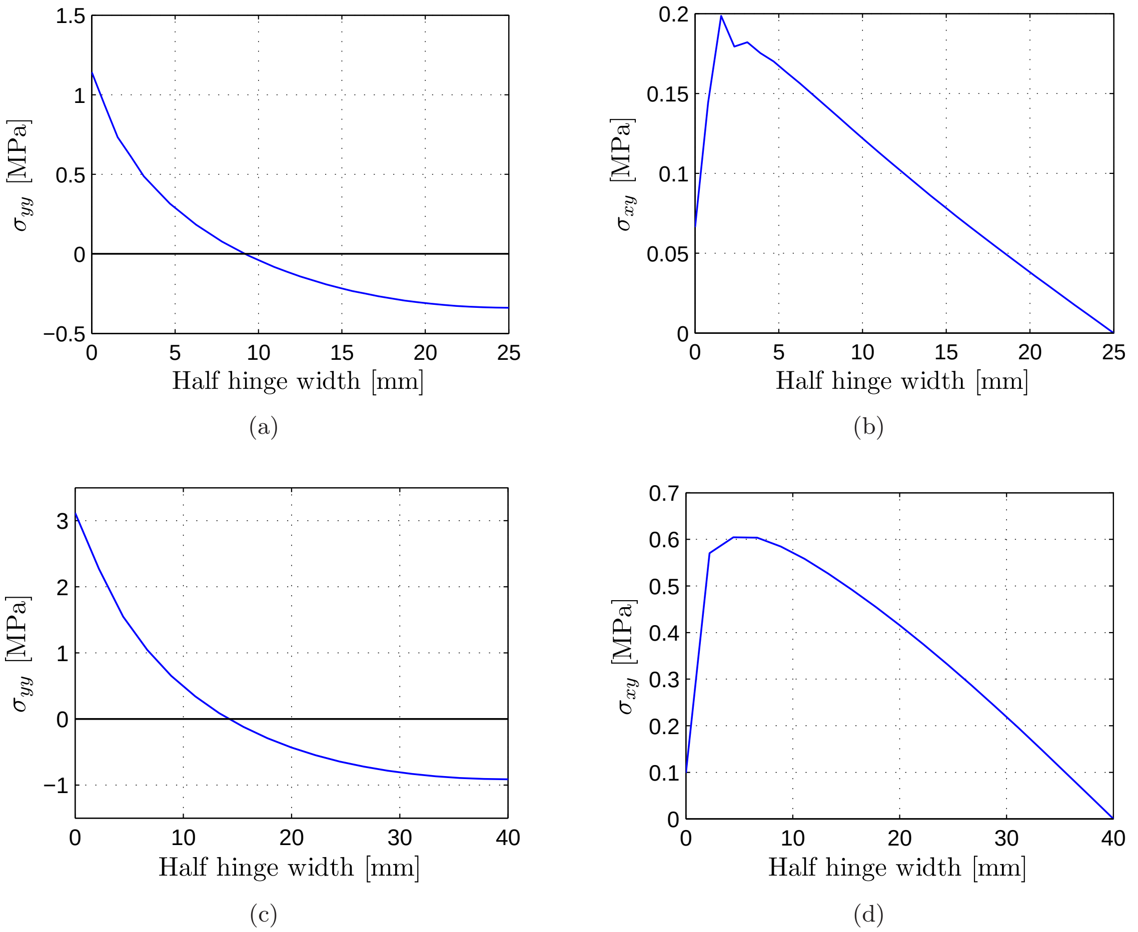

Figure 2.5: Vertical normal stress and shear stress distributions along a horizontal line at crack tip level going from the mid-section (0) to the boundary (25 or 40).

2.3.1 Crack Tip Level

With the basic idea about a model based on a two beam analogy and the stress distributions illustrated in figure 2.5, it seems evident that such a model must include both vertical normal stresses and shear stresses in the connection line between the two beams. With a hinge loaded with a constant moment, the resulting vertical force must equal zero. Therefore, it was evident that the resulting vertical force in the connection line would equal zero, but figure 2.5a and 2.5c are very important for inspiration to the shape of the stress distribution in the connection line. The statement about a zero resulting vertical force can be controlled knowing that the area on either side of the zero line must equal each other. This is represented by the integral (2.1) with x going from zero at the mid-section to s at the boundary

$$\int_0^s \sigma_{yy}(x)\, dx = 0 \tag{2.1}$$

where $\sigma_{yy}(x)$ represents the observed normal stress distribution. Due to the shape of the vertical stress distribution in the connection line it seems reasonable to model the distribution, of the vertical stresses σ_{yy}, with an analytical expression that fulfils the observed characteristics of the shape. The function describing the stress distribution as a function of x will be denoted $f(x)$. The shape of the stress distribution resembles a 2nd order polynomial with horizontal tangent at $x = s$, a function value at $x = 0$ that will be denoted σ_{yc} and $\int_0^s f(x)dx = 0$. Such a polynomial is given in (2.2).

$$f(x) = \frac{3}{2}\frac{\sigma_{yc}}{s^2}x^2 - 3\frac{\sigma_{yc}}{s}x + \sigma_{yc} \tag{2.2}$$

Figure 2.6 illustrates the polynomial approximations that have the same moment as the distributions found in the finite element model.

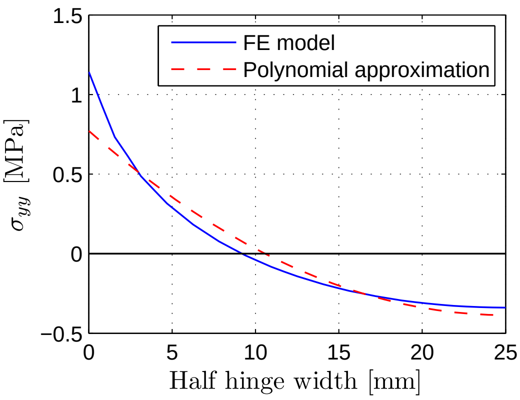

(a) $s = 25\,mm$

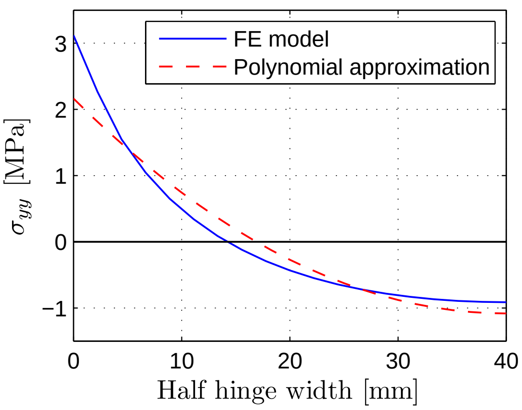

(b) $s = 40\,mm$

Figure 2.6: Polynomial approximations together with the finite element results.

Observations It should be noticed that the vertical stress at the crack tip exceeds the tensile strength which is only possible due to the definition of the model where the elastic plane stress elements do not allow cracking. As the crack develops there must exist a state where the stress in both vertical and horizontal direction equals the tensile strength. In this state the crack might theoretically develop in a random direction in a real structure. What is observed in experimental investigations is that the primary crack will continue in the vertical direction, which is probably a consequence of the overall deformation of the crack. What happens in a real structure is probably that the material will soften in the vertical direction which can be interpreted as micro-cracks that develop in the horizontal direction. In the model proposed in the following chapter, this observation is not accounted for.

2.3.2 Mid-section and Boundary

The stress distributions in the cracked mid-section and the boundary section for the two hinge sizes are illustrated in figure 2.7. In the mid-section a bi-linear stress distribution seems as an evident choice. For the boundary, some curved or multi linear distribution seems like a more precise choice, but in order to initially keep the model simple, a bi-linear distribution will be used for the boundary distribution as well.

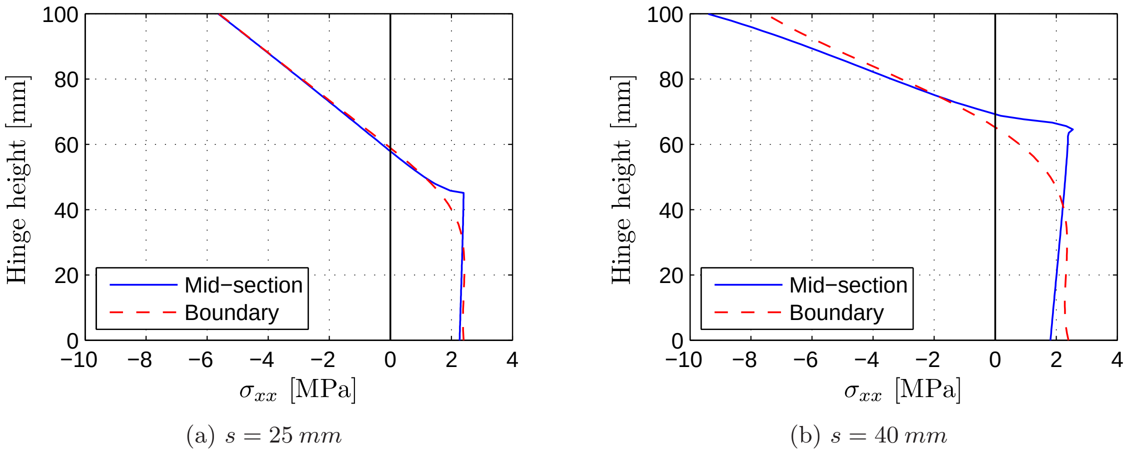

Figure 2.7: Stress distributions along the vertical mid-section and at the boundary.

Chapter 3

Adaptive Cracked Hinge Model

In previous chapters, the principles of an adaptive cracked hinge and the hinge boundary assumption were presented. Also an investigation of the mechanisms present in an adaptive cracked hinge, through a finite element analysis were presented.

In this chapter the non-linear adaptive cracked hinge model is developed. The model is established as a non-linear system of equilibrium equations describing the kinematic and static behavior of the hinge. In appendix A, all of the equations together with the derived variables are listed.

The presented model is limited to model a crack where bridging stresses are present in the entire length of the crack. Definition of a crack with bridging stresses and a stress free part is given in figure 1.1 on page 3.

In the figures, stress distributions are shown with a shape and an indication of positive or negative stresses. Distributed loads are shown with shape and small arrows and can be interpreted as the stresses multiplied with the thickness of the hinge.

All detailed derivations are left out in the main report, but can be found in the appendices (it is indicated where in the relevant sections).

Geometry and load definitions, see figure 1.5 on page 5.

3.1 Bi-Linear Stress Distribution

From the observations in the finite element model of the stress distributions in the cracked mid-section and at the hinge boundary, in section 2.3, bi-linear stress distributions were considered to be applicable distributions. Illustration of the principal stress distributions and definition of the parameters describing the distributions are given in figure 3.1. In the figure the stress definitions σ_{0c}, σ_{1c}, σ_{2c}, σ_{0b}, σ_{1b} and σ_{2b} are the stresses corresponding to the points p1 to p6 defined in figure 1.6b, s is half of the hinge width, c is the crack length, $a = h - c$ where h is the hinge height and the positive direction of the y-axis is indicated. From the assumptions presented in section 1.4 and 1.6 it follows that $\sigma_{1c} = \sigma_{0b} = f_t$.

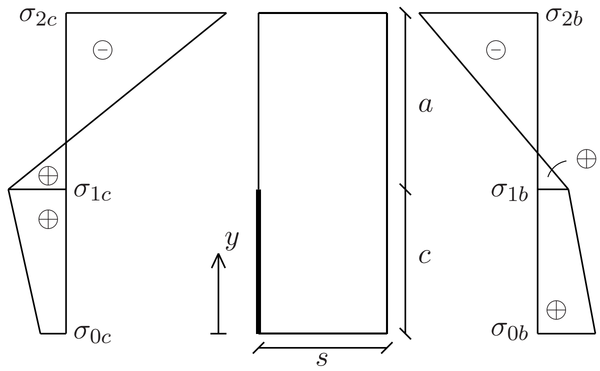

Figure 3.1: Right half of adaptive hinge defining geometry and showing the normal stress distribution at both the cracked mid-section and the boundary. Sign convention is negative for pressure and positive for tension.

3.2 Overall Deformation

From the overall kinematic assumption about rigid boundaries follows that the mean strain distribution is linear in the height direction of the hinge. From the mean strain at the middle of the hinge ε'_m and the curvature κ the mean strain distribution $\varepsilon'(y)$ is given by equation (3.1).

$$\varepsilon'(y) = \varepsilon'_m + \left(\frac{1}{2}h - y\right)\kappa \tag{3.1}$$

where h is the hinge height. Three of the "system" equations (3.2), (3.3) and (3.4) follows from the kinematic condition that the mean strain is linearly distributed. From this condition follows that the sum of the strain and crack opening must equal the mean strain. Equation (3.2) describes the deformation of the top of the hinge.

$$\varepsilon'_t = \frac{1}{2E_c}(\sigma_{2c} + \sigma_{2b}) \tag{3.2}$$

where ε'_t = mean strain at the top of the hinge (y=h in equation (3.1)); E_c = elastic modulus of the concrete. Equation (3.3) describes the deformation at the crack tip, point p2 in figure 1.6b.

$$\varepsilon'_c = \frac{1}{2E_c}(\sigma_{1c} + \sigma_{1b}) \tag{3.3}$$

where ε'_c = mean strain at the crack tip (y=c in equation (3.1)). The third equation (3.4) comes from the deformation criterion at the bottom of the hinge, where the sum of the crack opening and the elastic deformation of the material from the crack (point p1) to the boundary (point p6 in figure 1.6b) must equal the mean strain at the bottom of the hinge.

$$\varepsilon'_b s = w_0 + \frac{1}{2E_c}(\sigma_{0c} + \sigma_{0b})s \tag{3.4}$$

where ε'_b = mean strain at the crack tip (y=0 in equation (3.1)); w_0 is half of the crack mouth opening and E_c is the modulus of elasticity for the concrete. See definition of w_0 in figure 1.6b.

3.3 Static Equilibrium in the Mid-section

Equilibrium between the external forces and the internal stresses are fulfilled in the mid-section by equation (3.5) and (3.6). The normal force N in the mid-section is defined by the integral of the stresses over the height multiplied with the thickness of the hinge.

$$N = t\int_0^h \sigma_{mid-section}(y)\,dy \tag{3.5}$$

where $\sigma_{mid-section}$ is the bi-linear stress distribution illustrated in figure 3.1 represented by σ_{0c}, σ_{1c} and σ_{2c}.

The moment around an axis out of the plane at the height $\frac{h}{2}$, as indicated on figure 1.5, is found by integration of the stresses multiplied with the distance from the middle with y defined as illustrated in figure 3.1.

$$M = t\int_0^h \sigma_{mid-section}(\frac{h}{2} - y)\,dy \tag{3.6}$$

Equation (3.5) and (3.6) are principal and for the simple stress distributions used in the presented model, the integrals can be interpreted as summation of simple triangular areas, see appendix A.

3.4 Division into two Beams

In this model the new concept is to model the hinge as two independent beams connected along a horizontal line at the crack tip level as illustrated in figure 1.6a. The stress distribution in the connection line is assumed to be a uniform shear stress given by the normal force differences $\tau_{1b} = \Delta N_b/(s\,t)$ and $\tau_{1t} = \Delta N_t/(s\,t)$, and for the vertical stresses, a 2nd order polynomial is assumed to describe the shape of the distribution as described in section 2.3.1. The stresses acting on the two beam parts, which are part of the considered hinge half, are illustrated in figure 3.2.

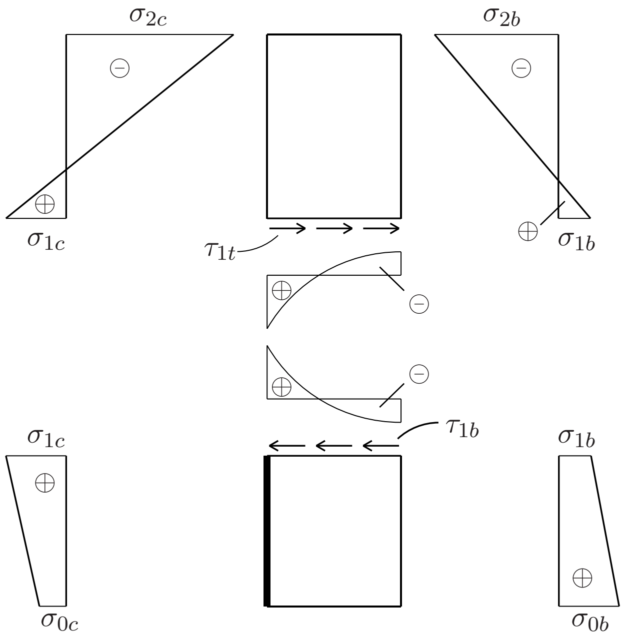

Figure 3.2: Right hinge half divided into two beam parts illustrating the stresses along the division line together with the stress distributions in the mid-section and the boundary.

The moment and normal force in the mid-section and at the boundary are equivalent following from the assumption about constant moment. This means that the right hinge half illustrated in figure 3.1 is in overall static equilibrium. The overall deformation is controlled by the curvature and the rigid boundaries. When the beam half is divided into two beams, both static and kinematic equilibrium must still be fulfilled.

3.5 Lower Beam

Figure 3.3 illustrates the stresses and equivalent forces that act on the lower beam part.

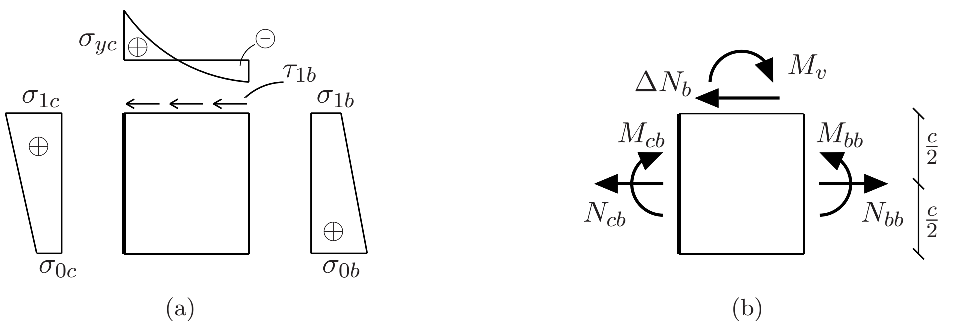

Figure 3.3: The bottom cracked part of the right hinge half from figure 3.1. Loads are illustrated in terms of (a) the stress distributions and (b) the corresponding forces.

3.5.1 Static Equilibrium

Static equilibrium of the lower beam part is described through equation (3.7)

$$M_{cb} + M_v - M_{bb} - \frac{1}{2}c\Delta N_b = 0 \tag{3.7}$$

where M_{cb} is the moment in the mid-section around an axis through the middle equal to $c/2$; M_v is the resulting moment from the vertical normal stress distribution given by equation (2.2); M_{bb} is the moment at the boundary around an axis through the middle equal to $c/2$; and $\Delta N_b = N_{cb} - N_{bb}$ is the axial normal force difference. Normal forces and moments are found as for the entire height in the mid-section exemplified by (3.5) and (3.6) using the crack length c instead of the height.

3.5.2 Horizontal Kinematic Equilibrium

For the description of the horizontal kinematic equilibrium of the lower beam, it is modeled as a clamped beam with a vertical beam axis as illustrated in figure 3.4a together with the distributed load (thickness $\times$ stress) acting upon the beam. The beam is handled as a shear flexible beam, where the horizontal displacement is the sum of bending- and shear deformation $w_{01} = w_{01,a} + w_{01,b}$ as a result of the horizontal stresses and a rigid body motion w_{02} as a result of the vertical displacement of the lower beam. Due to the changes of the beam geometry (crack length and half hinge width) during the continuous deformation of the hinge, bending and shear deformation have their primary relevance at different deformation stages. The beam axis is plane perpendicular to the original beam axis while considering the horizontal displacements in the bottom and the positive direction is downwards.

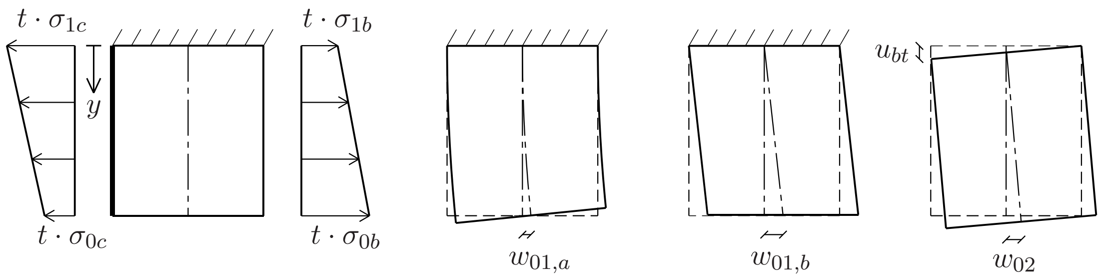

(a) Stresses (b) Bending (c) Shear (d) Rotation

Figure 3.4: Lower right beam part modeled as a clamped beam where the mid-section and boundary are substituted by equivalent distributed load (thickness $\times$ stress).

From the overall kinematic relation defined in equation (3.1) the horizontal displacement of the bottom of the boundary is given by $\varepsilon_b' s$ and the displacement at the mid-section can be interpreted as half the crack mouth opening w_0. The horizontal displacement at the bottom of the beam axis must equal the mean displacement evaluated from w_0 and ε_b'. The horizontal displacement equilibrium equation for the lower beam part is defined by equation (3.8).

$$w_{01} + w_{02} = \frac{w_0 + \varepsilon_b' s}{2} \tag{3.8}$$

where w_{01} is found from the principle of virtual work with the uniformly distributed loads illustrated in figure 3.4a. The bending and shear deformation mechanisms are shown in figure 3.4b and 3.4c. In this interpretation of the lower beam as a clamped beam along the connection line, the sign convention is opposite to the one presented in figure 3.1 which means that the positive direction is downwards. The basic principle of a virtual work equation including the displacement contribution from both the resulting moment distribution $M_0(y)$ and the resulting shear force distribution $V_0(y)$ is represented by equation (3.9).

$$w_{01} = t\left(\int_0^c \frac{V_1(y)V_0(y)}{GA_0}dy + \int_0^c \frac{M_1(y)M_0(y)}{E_c I_{vb}}dy\right) \tag{3.9}$$

where $V_1(y)$ and $M_1(y)$ are the shear and moment distribution from a virtual unit force; GA_0 is the shear stiffness consisting of the elastic shear modulus $G = \frac{Ec}{2(1+\nu)}$ where ν is poisons ratio, and a representative cross section area $A_0 = \frac{5}{6}A$, according to Krenk [2000]; $E_c I_{vb}$ is the bending stiffness, consisting of the elastic modulus E_c and the moment of inertia I_{vb}. The displacement from the rotation of the clamped support alias the vertical displacement of the lower beam w_{02} is defined by the geometry given in figure 3.4d.

$$w_{02} = \frac{c\, u_{bt}}{s} \tag{3.10}$$

where $u_{bt} = u_b + u_{V,b} + u_r$ is the total vertical displacement of the lower beam part, measured at the crack tip. Derivation of u_{bt} is presented later on in section 3.7.2.

Derivation of w_{01} is found in appendix D.

3.6 Upper Beam

Equivalent to figure 3.3, figure 3.5 defines the stress distribution and forces acting on the upper beam half. Equilibrium of the upper beam is ensured indirectly through the other equations presented in this chapter. The connection is ensured later on through equation (3.11).

3.7 Equilibrium between the Two Beams

3.7.1 Static

The overall static equilibrium is ensured through the differences of the axial normal forces where the difference must equal the external axial normal force N. Using the positive direction from the mid-section, the equilibrium condition is given by equation (3.11)

$$N = \Delta N_b - \Delta N_t \tag{3.11}$$

where ΔN_b is the normal force difference defined along with equation (3.7) and illustrated on figure 3.3b. ΔN_t is the normal force difference for the upper beam part A, $N_{bt} - N_{ct}$.

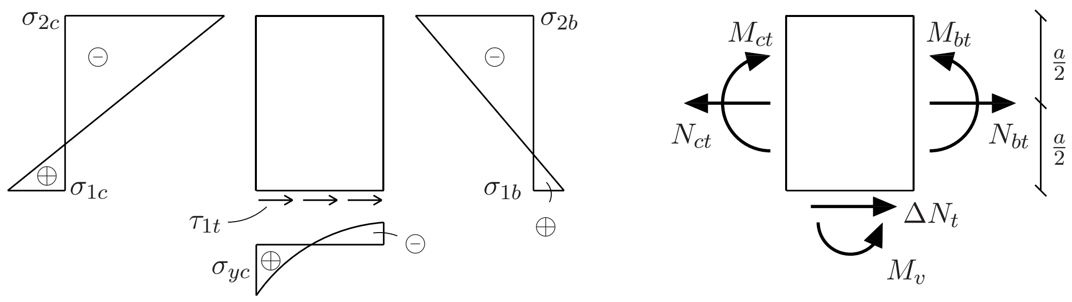

(a) Stresses (b) Forces

Figure 3.5: The uncracked top of the right hinge half from figure 3.1. Loads are illustrated in terms of (a) the stress distributions and (b) the corresponding forces.

3.7.2 Kinematic

The two beams, part A and part B in figure 1.6c, are handled as shear flexible beams where the deformation is the sum of bending-, shear deformation and for the lower beam part also a rigid body motion. The two beam parts must move together which is ensured through the assumption of a rigid boundary together with a displacement criterion that ensures that the middle vertical deflection (point p2 in figure 1.6b) is equal for part A and part B. The displacement criterion is described in equation (3.12). Illustrations of the support conditions and loadings for the two beam parts are illustrated in figure 3.6 for the upper beam part and figure 3.7 for the lower beam part, where the supports defined in figure 1.6c are substituted by a clamped support at the mid-section.

$$u_b + u_{V,b} + u_r = u_t + u_{V,t} \tag{3.12}$$

where u_b is the vertical bending deflection of the bottom beam part; $u_{V,b}$ is the vertical shear displacement of the lower beam part; u_r is the rotation of the lower beam part due to the crack opening as illustrated in figure 3.7b; u_t is the bending deflection of the upper beam part and $u_{V,t}$ is the vertical shear displacement of the upper beam part. Like the horizontal displacement described in section 3.5.2 the bending- and shear deformation is found by means of the principle of virtual work. Derivation of the moment- and shear force distribution is found in appendix K. The rigid body motion which results in u_r is given by the geometry in figure 3.7b as (3.13).

$$u_r = w_0 \frac{s}{c} \tag{3.13}$$

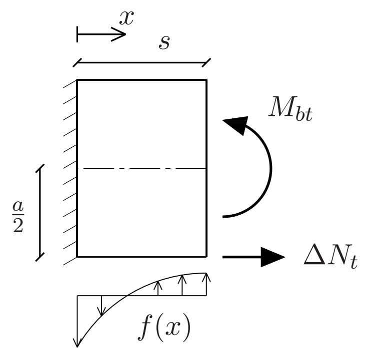

Figure 3.6: Upper beam part interpreted as a clamped beam loaded with a moment M_{bt}, excentric normal force difference ΔN_t and a distributed load $f(x)$

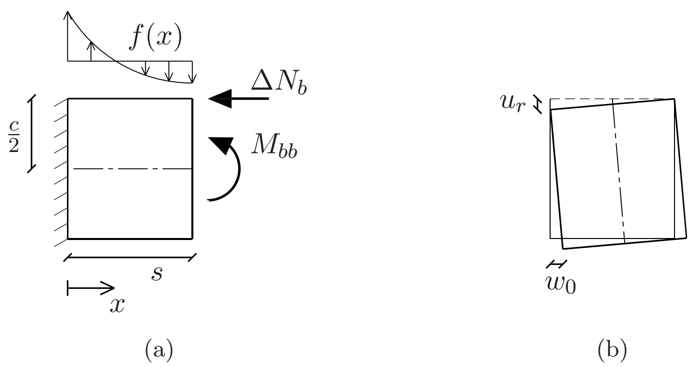

Figure 3.7: The lower cracked beam part, (a) interpreted as a clamped beam loaded with a moment M_{bb}, excentric normal force difference ΔN_b and a distributed load $f(x)$ and (b) rigid body motion.

3.8 Summary of the Model

The numerical cracked hinge model is a non-linear system of equilibrium equations, in this chapter presented in the form given in (3.2), (3.3), (3.4), (3.5), (3.6), (3.7), (3.11), (3.12) and (3.8), see appendix A for a full overview.

With the system of the nine equations follows nine unknowns and two control parameters. The unknowns are not predefined but can be chosen among several since several of them are internally dependant of each other. There are also different possibilities for the control parameters. The control parameters are chosen to be the half hinge width s and the normal force N but instead of s, the curvature could be an obvious choice. However, working with the implementation has shown some problems using the curvature as a control parameter. The unknowns are listed below.

M moment

κ curvature

c crack length

w_0 half the crack mouth opening

σ_{1b} normal stress at the boundary at the crack tip level

σ_{2c} normal stress at the top of the mid-section

σ_{2b} normal stress at the top of the boundary

ε'_m mean strain at half the hinge height

σ_{yc} vertical tensile stress at the crack tip

3.9 Model Limitations

The presented model assumes a non-zero stress value at the crack mouth which means that half the crack mouth opening is limited by $w_0 \geq w_1$. It has been shown by Ulfkjaer et al. [1995] that the limit where part of the crack becomes stress free for a linear softening relation corresponds to the elastic moment. This is also the limit where the boundary assumption no longer can be fulfilled, since the tensile stress can not reach the tensile strength anywhere in the structure when the moment is below the elastic moment everywhere.

Chapter 4

Numerical Solution

4.1 Implementation in MATLAB

4.1.1 Non-linear Solver

The MATLAB build in non-linear equation solver `fsolve` has the wanted solver characteristics. `fsolve` solves a problem as specified by (4.1) for x

$$F(x) = 0 \tag{4.1}$$

where x is a vector and $F(x)$ is a function that returns a vector value. `fsolve` must be feeded with an initial guess x_0 and a function where the equations to be solved are defined. The unknowns are represented by x and `fsolve` search for a solution x that fulfil equation (4.1), in a way that all of the equations defined equals zero plus minus some predefined tolerances. Two stopping criteria are used for `fsolve`. The first stopping criteria is defined by the norm of $(x_i - x_{i+1})$ meaning the length of the resulting vector, interpreted as a lower bound on the size of a step, in MATLAB denoted *TolX*. The default value which is used is $\mathit{TolX} = 10^{-6}$. The other stopping criteria, denoted *TolFun*, is a lower bound on the change in the value of the objective function during a step, meaning that, if $|f(x_i) - f(x_{i+1})| < \mathit{TolFun}$, the iteration ends. The default value which is used is $\mathit{TolFun} = 10^{-6}$. Definitions from, see Mathworks in the bibliography.

In the implemented solution the unknowns x are scaled to the order of one to ensure that no numerical problems occurs. Experience with the implemented solution has shown that no scaling of the function values has been necessary to have converging results. The iteration is stopped if either of the stopping criteria is reached.

4.1.2 Implementation

The above described solver can solve the non-linear system of equations described in chapter 3. The control parameters defining the equilibrium state that is searched for are the half hinge width s and the normal force N. In the presented solution the normal force is zero. For each value of s going from zero to an upper limit restricted by the limitations of the presented model an equilibrium solution is searched. To recall the limitations of the model, it has a limit at the state where point p1 in figure 1.6b becomes stress free which correspond to $w_0 \geq w_1$.

The diagram in figure 4.1 illustrates the procedure solving the non-linear system of equations for one pair of s and N. In appendix I.1 the three MATLAB files used to retrieve equilibrium solutions for an interval of half hinge widthes s which results in solutions within the limitations of the model are found. The implemented solution consists of `run.m`, which defines the geometry, material parameters and creates a data file containing the equilibrium results for the nine unknowns for each value of s. The file `solve.m` defines the loop over a specified interval of s. Within this loop a break criterion is also defined and activated when w_0 exceeds the limits of the model. The file `petersen.m` defines the nine equations and calculates the known variables.

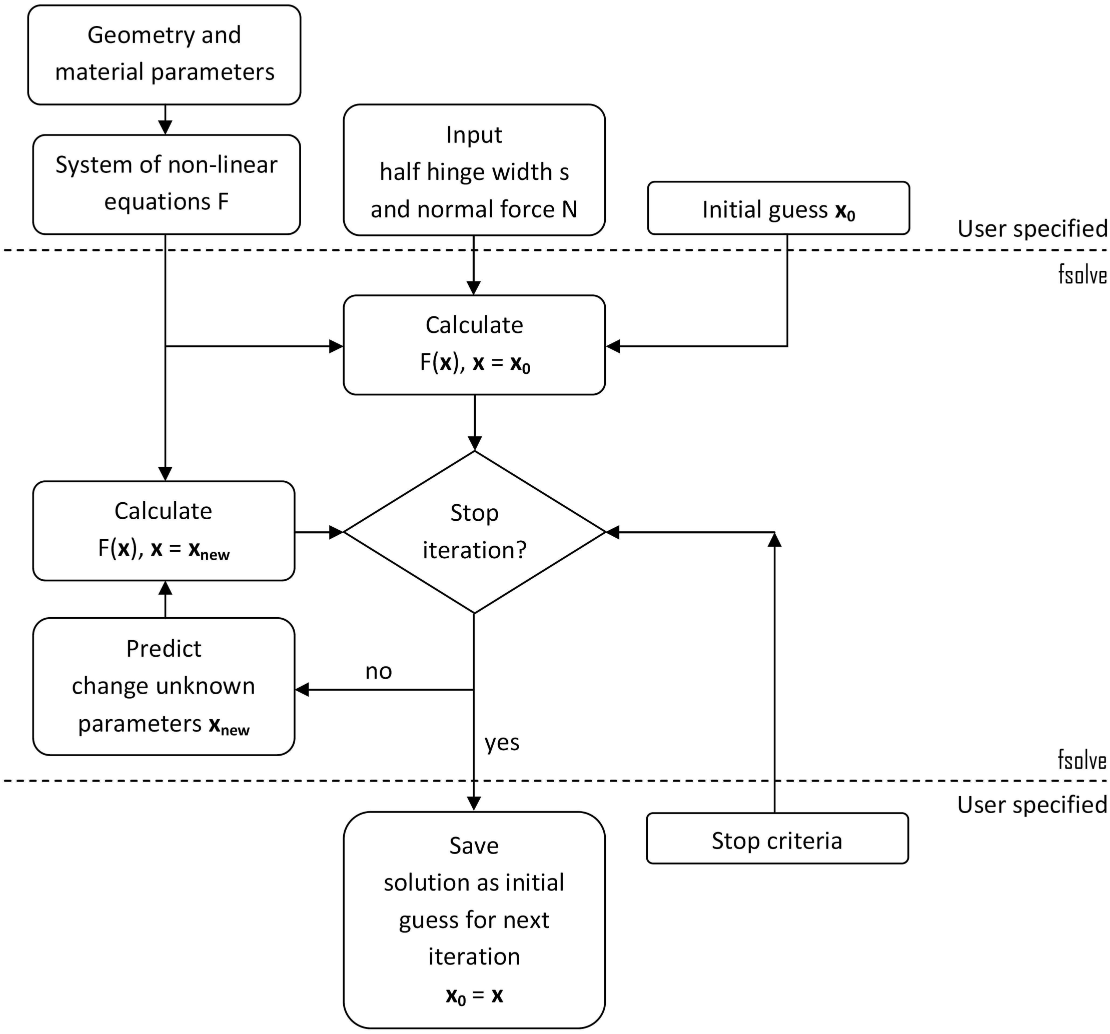

Figure 4.1: Illustration of the implemented procedure for one set of the control parameters s and N. The stippled lines indicate the boundary between the user specified part of the procedure and what is solved by the non-linear solver fsolve. The input to fsolve is the two control parameters s and N, the non-linear system of equations F with input of the geometry and material definitions and an initial guess of the nine unknowns defined in the vector x_0. The first guess is user defined and is parameters corresponding to the elastic solution for the non-zero elastic parameters and for the others, a small but non-zero number is used (suggestions are given in the Matlab script, appendix I.1.1). The default stop criteria as described above is used, but can be changed manually. When an equilibrium solution is found, this solution is saved as a solution for the unknown parameters, but also as the initial guess for the next pair of s and N.

4.2 Hinge Model by Olesen

The explicit formulation of a hinge model with constant width presented by Olesen [2001] is used for comparison in the following section. A description of the model for the phase of the crack development where bridging stresses are present is given in appendix C and the MATLAB scripts are found in appendix I.3.

4.3 Comparison

With the finite element model (DIANA) as a basis for comparison, the presented solution for the adaptive cracked hinge model (Petersen) is compared with both the finite element model, to illustrate the degree of agreement, and the solution for the explicit formulation (Olesen) in order to illustrate the advantages of an adaptive hinge. The finite element model has a minimum of 32 interface cohesive crack elements over the height. The dots on the DIANA-curves indicates the retrieved results, and the connection lines are illustratively added by the author. The graphs presented are focused on the comparison between the finite element model and the solution for the adaptive cracked hinge, and the axes might cut off without inclusion of all data points from the explicit formulation of the hinge with constant width.

The geometry of the adaptive cracked hinge considered is defined by the height $h = 100$mm and the thickness $t = 100$ mm. The concrete is characterized by the material parameters f_t the tensile strength, E_c the modulus of elasticity and poisons ratio ν, see table 4.1.

Table 4.1: Material parameters

f_t [MPa]	E_c [MPa]	ν
2.4	31000	0.15

The following normalization is used

$$M' = \frac{6M}{th^2 f_t} \quad , \quad \kappa' = \frac{\kappa E_c h}{2 f_t} \tag{4.2}$$

where M' is the normalized moment M/M_E where M_E represents the elastic moment; κ' is the normalized curvature κ/κ_E where κ_E represents the curvature corresponding to the elastic moment. Also the relative measures c/h which is the crack length relative to the hinge height and s/h which is the half hinge width relative to the hinge height are used.

While solving the non-linear system of equations representing the adaptive cracked hinge, the solution were based on increments of the half hinge width s, but considering concrete beam structures it is more relevant to observe the behavior of the hinge as a function of the curvature. The moment-curvature relation in normalized form is presented in figure 4.2. With the normalization it is seen that the bearing capacity is increased with a factor two for the current geometry and material definition compared to the elastic bearing capacity. The figure also illustrate that the adaptive hinge and the hinge with constant width are entirely different in their nature after peak. The presented model has a quick descent on the curve shortly after peak, where the explicit formulation is more flat, which means that the hinge with constant width will overestimate the bearing capacity post peak and as observed the adaptive cracked hinge model is a little to conservative after peak compared to the finite element model.

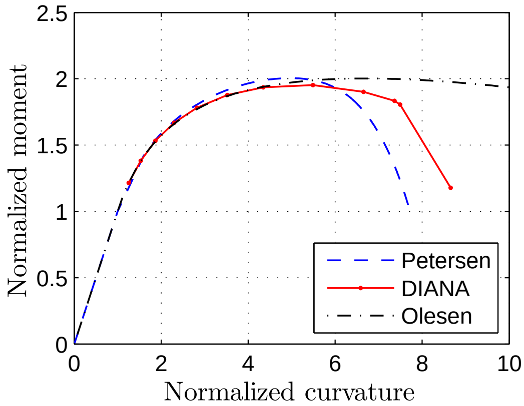

Figure 4.2: Moment-curvature curves.

In figure 4.3, three other characteristic relations for the adaptive hinge are presented.

The relation between the crack mouth opening displacement and the curvature, figure 4.3a, show large differences between the presented model and the explicit formulation. The crack mouth opening displacement increases fast at a certain curvature corresponding to the initial post peak state whereas the explicit formulation shows a more flat relation. Pre-peak the adaptive hinge underestimates the crack mouth opening displacement, but post-peak there is a little overestimation using the adaptive cracked hinge model (Petersen). The hinge with constant width is seen to underestimate the crack mouth opening displacement almost from crack initiation.

Figure 4.3b illustrates a good agreement between all three models, but here it is important to be aware of the different half hinge widths, which also could be interpreted as an indicator of many or few cracks, since a larger half hinge width is equivalent to fewer cracks. The last observation is naturally only relevant for the two models with varying hinge widths.

In figure 4.3c the relative half hinge width is plotted against the normalized curvature. It is seen how the relative half hinge width increases considerably at the same normalized curvature at which the moment decreases rapidly in figure 4.2. The fact that the half hinge width increases rapidly is expected since the moment drops radically towards the elastic moment, which is the limit where the boundary assumption can be fulfilled. It could have been expected that the development of the half hinge width would have a vertical tangent at the limit of the elastic moment. That is not the case, and therefore, it seems evident to use this limit to define a new boundary condition or maybe a fixed hinge width when the crack become stress free at the crack mouth.

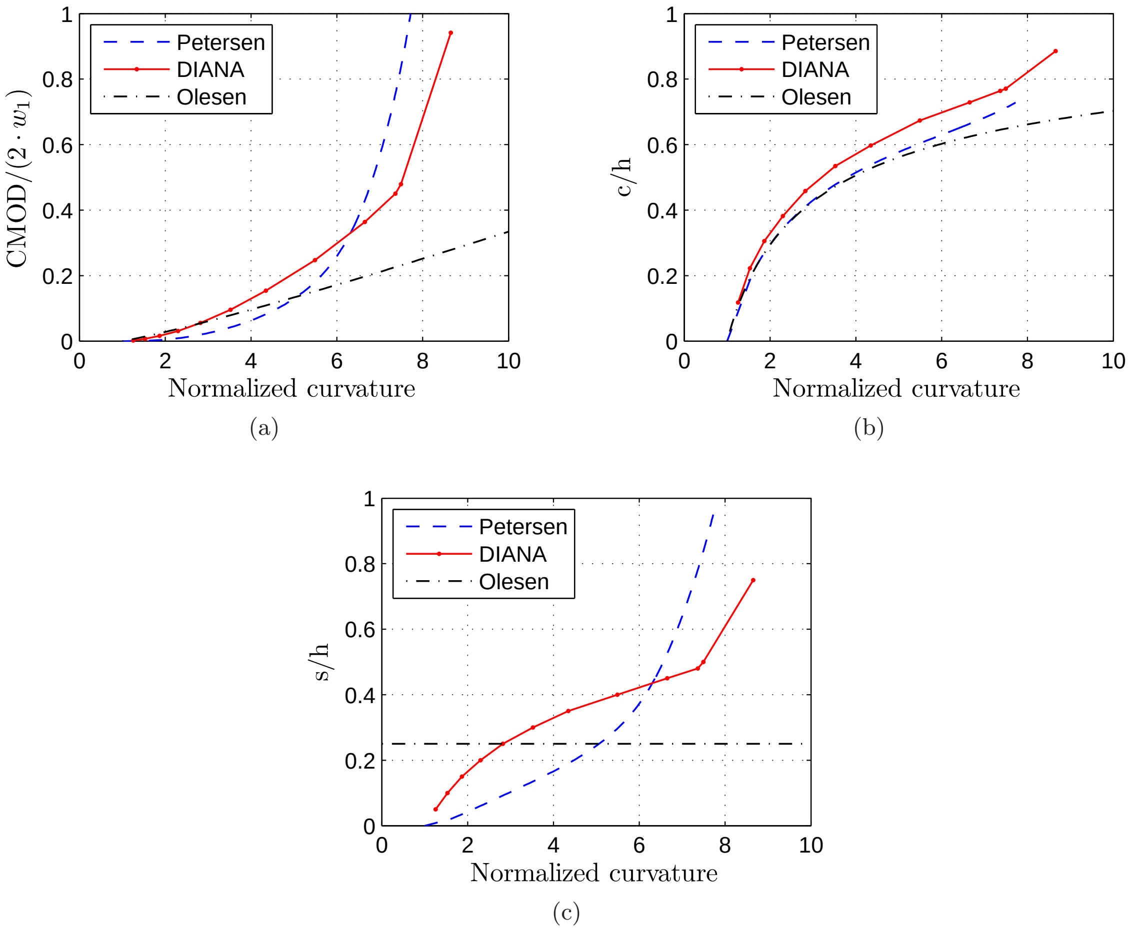

Figure 4.3: Characteristic hinge parameters relative to the curvature.

The finite element curve in figure 4.4 indicates that there might be a certain level of linearity in the relation between the relative crack length and the relative half hinge width, in the pre-peak phase. This linearity is not used in the presented model, but it could be a relevant investigation to see if it was possible to implement it into the presented model.

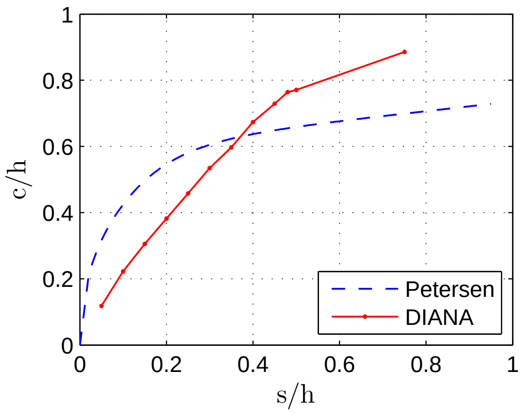

Figure 4.4: Relative crack length versus the relative half hinge width.

Comparison of figure 4.2, 4.3a and 4.5 shows that it is important to see the bearing capacity (moment) and crack mouth opening displacement (CMOD) related to the curvature. The latter is especially demonstrated looking at figure 4.5 where it seems that both the presented model (Petersen) and the explicit formulation (Olesen) gives a good prediction of the crack mouth opening displacement with reference to the moment and knowledge about the pre- or post peak result. But figure 4.3a clearly shows that the crack mouth opening displacement is developed entirely different as a function of the curvature. Therefore if results about crack mouth opening displacement is wanted it must be given based on the current curvature of the concrete beam structure.

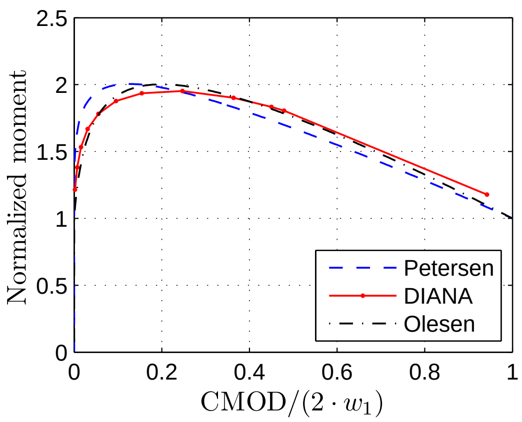

Figure 4.5: Moment-cmod curves for a cracking hinge.

4.4 Parameter Variation

Variation of the fracture energy is covered for the normalized moment-curvature curve and the normalized moment- relative crack mouth opening in figure 4.6 and 4.7. The interval of the variation of the fracture energy for plain concrete is defined on the basis of experimental results by Kragh-Poulsen [2009] which indicate a fracture energy of $G_F = 0.149\,\mathrm{N/mm}$ and literature studies by Østergaard [2003] indicates values of fracture energy at approximately $G_F = 0.1\,\mathrm{N/mm}$. An interval from 0.8-1.6 N/mm is considered here.

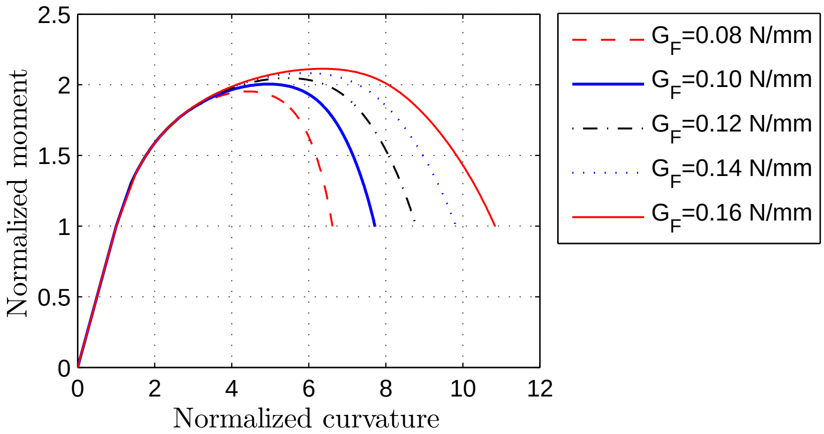

Figure 4.6: Moment-curvature curves. Variation of the fracture energy G_F.

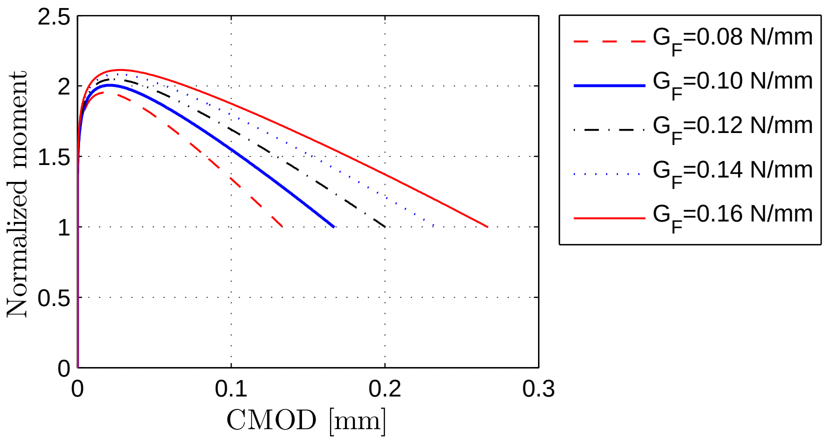

Figure 4.7: Moment-cmod curves. Variation of the fracture energy G_F.

The graphs illustrate higher peak bearing capacity with increasing fracture energy, which is as expected since the fracture energy is defined as the necessary amount of energy to create a crack of a unit area and a greater load is therefore needed for increased fracture energy to propagate the crack in the beam. Figure 4.6 also show that the beam structure can sustain more deformation with increased fracture energy. A simple geometrically comprehension of the consequence of increased fracture energy can be seen from figure 1.2 on page 3, where an increased fracture energy will increase the half crack opening w_1 at which the crack become stress free at the crack mouth. In figure 4.7 the moment is plotted against the crack mouth opening displacement and the described consequence of increased fracture energy is directly observed as increased bearing capacity, but also larger crack mouth opening displacements are reached before the moment return to the limit corresponding to the elastic moment.

Chapter 5

Introduction of a Simple Reinforcement Bar

In this chapter the principles for an extension of the presented model is given. The most simple case of a reinforced adaptive cracked hinge is created with an extension of the already established non-linear system of equilibrium equations that describes the unreinforced hinge. The reinforcement bar is geometrically connected to the hinge boundaries, see figure 5.1, and the deformation correspond to the overall horizontal displacement at the level of the reinforcement bar. There are no connection between the reinforcement bar and the concrete, between the boundaries, which imply that important topics as de-bonding and pull-out are not covered by the model. Looking at a half hinge the connection of the reinforcement bar can be interpreted as a simple connection at the mid-section and the boundary.

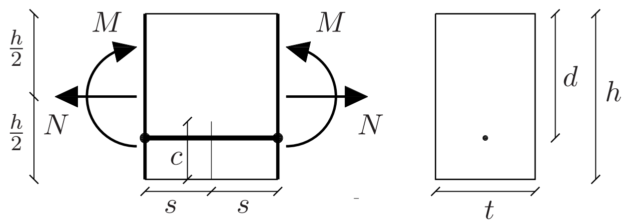

Figure 5.1: Undeformed reinforced hinge with geometry and load definitions.

5.1 Extension of the Model

In the case of an extension with the described simple model for a reinforcement bar the only equilibrium equations that are effected are (3.5) and (3.6) representing the equilibrium in the mid-section between the external normal force, moment and the internal stresses. The modifications are shown in (5.1) and (5.2).

$$N = F_{bar} + t \int_0^h \sigma_{mid-section}(y)\, dy \tag{5.1}$$

$$M = (d - \frac{1}{2}h)\, F_{bar} + t \int_0^h \sigma_{mid-section}(\frac{h}{2} - y)\, dy \tag{5.2}$$

where the force F_{bar}, (5.4) present in the reinforcement bar is added. The force in the reinforcement bar is determined buy the mean strain at the height of the reinforcement bar ε'_d given by (5.3). d represents the distance from the top of the hinge to the reinforcement bar and h is the hinge height.

$$\varepsilon'_d = \varepsilon'_m + (d - \frac{1}{2}h)\kappa \tag{5.3}$$

where ε'_m is the mean strain at the middle of the hinge $\frac{1}{2}h$.

$$F_{bar} = \varepsilon'_d E_s \pi \left(\frac{D}{2}\right)^2 \tag{5.4}$$

where E_s is the modulus of elasticity for the reinforcement bar and D is the diameter of the reinforcement bar.

The model is still limited to describe a reinforced adaptive cracked hinge where there are stresses in the entire crack length.

The MATLAB scripts which implement the changes are found in appendix I.2.

5.2 Comparison

To illustrate the effect of the reinforcement bar four different mechanical reinforcement degrees ($\Phi_1 - \Phi_4$) are used. These are the mechanical reinforcement degrees corresponding to minimum reinforcement for pure bending Φ_{min} (5.5), reinforcement corresponding to a balanced cross section Φ_{bal} (5.6) and two mechanical reinforcement degrees that represents the interval in between the lower and upper limit of the normal reinforced cross section in pure bending, definitions according to Heshe et al. [2005].

$$\Phi_{min} = 0.45\frac{f_t}{f_c} \tag{5.5}$$

where f_t is the tensile strength of the concrete and f_c is the compression strength.

$$\Phi_{bal} = 0.8\frac{\varepsilon_{cu}}{\varepsilon_{cu} + \varepsilon_y} \tag{5.6}$$

where ε_{cu} is the strain corresponding to crushing of the concrete and ε_y is the strain corresponding to yielding of the reinforcement. The cross sectional reinforcement area A_s is found by 5.7.

$$A_s = \Phi t d \frac{f_c}{f_y} \tag{5.7}$$

where t represents the thickness of the hinge; d represents the depth of the reinforcement and f_y is the yield strength of the reinforcement.

The reinforced adaptive cracked hinge considered has the same height $h = 100$ mm and thickness $t = 100$ mm as the adaptive cracked hinge considered in chapter 4. The reinforcement is placed in the distance $d = 75$ mm from the top. The material parameters for the concrete and reinforcement are given in table 5.1 where E_c and E_s are the modulus of elasticity for the concrete and the reinforcement, ν is poisons ratio.

Table 5.1: Material parameters

f_t [MPa]	f_c [MPa]	f_y [MPa]	E_c [MPa]	E_s [MPa]	ν
2.4	30	550	31000	210000	0.15

With the described geometry and material parameters the mechanical reinforcement degrees are given in table 5.2.

Table 5.2: Mechanical reinforcement degrees used for the reinforced adaptive cracked hinges.

Φ_1	Φ_2	Φ_3	Φ_4
0.036	0.096	0.156	0.216

The unreinforced solution together with the four reinforced solutions are graphically illustrated in figure 5.2. The figure illustrates how the moment as a function of the curvature increases with the mechanical reinforcement degree as expected, but also an increased curvature before the limit of a stress free crack mouth is reached is observed.

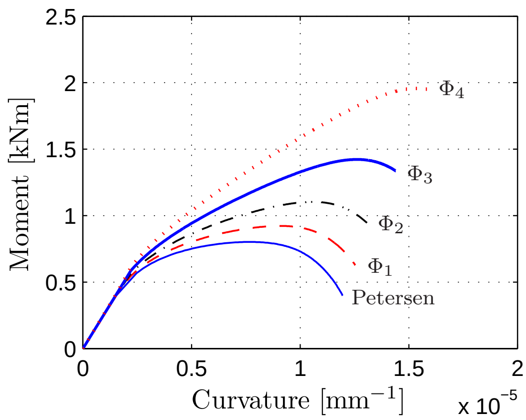

Figure 5.2: Moment-curvature curves for the unreinforced hinge (Petersen) and the four reinforced cases represented by $\Phi_1 - \Phi_4$.

The moment-curvature relation for the four mechanical reinforcement degrees are illustrated in figure 5.3 together with the same relation for a cracked cross section with no tensile strength in the crack, which is defined by the $\alpha\rho - method$ as it is described in Heshe et al. [2005] section 5.2.4. From the curves in figure 5.3 it is seen that the reinforced

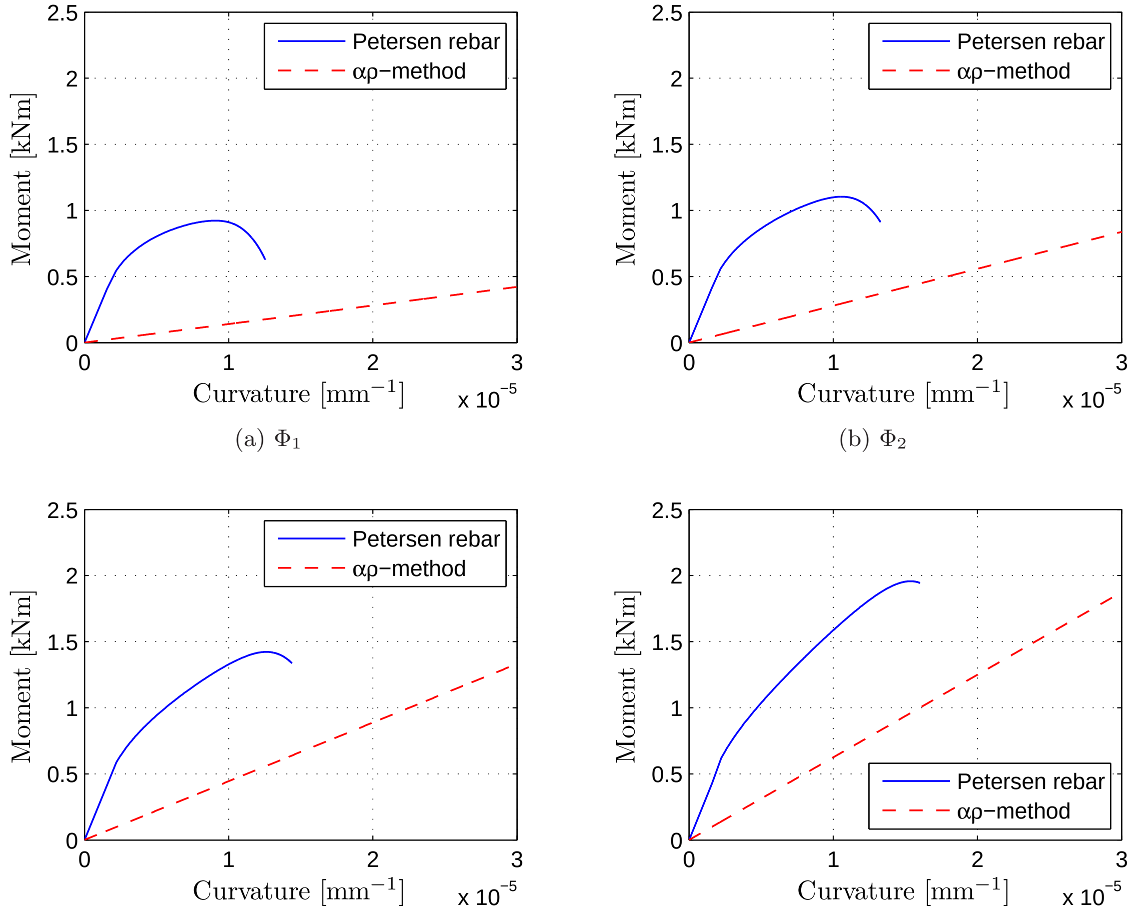

(a) Φ_1 (b) Φ_2 (c) Φ_3 (d) Φ_4

Figure 5.3: Reinforced hinge by Petersen compared to the elastic solution of a cracked cross section based on the $\alpha\rho - method$

cracked hinge model add relatively much to the bearing capacity, which are as expected since at a given curvature there will be a rather large contribution from the cracked concrete. As it where illustrated in chapter 4 the bearing capacity for concrete alone, with the current geometry and material definition, is increased with a factor two.

It is expected that the curve for the reinforced adaptive hinge will converge towards the solution given by the $\alpha\rho - method$ when the crack gradually becomes stress free. The presented model is limited to the solution where the crack mouth, point p1 in figure 1.6b, become stress free. Therefore the solutions will not really begin to converge before the model is developed further.

In appendix F four graphic presentantions representing the relation between the four characteristic model parameters, the moment M, the crack length c, the half hinge width s, the crack mouth opening displacement $CMOD$, and the curvature κ for each of the four mechanical reinforcement degrees are given.

In the current chapter it has been shown that extension of the presented model seems relatively easy to implement. This is important for further development of the model, since the model presented can be a base wherefrom new equations or extension of the existing equations can be handled.

Chapter 6

Conclusion

6.1 Conclusion

In this thesis, a non-linear solution for an adaptive cracked hinge has been developed and the extension of the model to cover a simple reinforced non-linear adaptive cracked hinge has been handled. The adaptive cracked hinge model has been compared to both a finite element model and an explicit formulation of a cracked hinge with constant hinge width.

A new approach to the topic of hinge models, modeling the fictitious crack development in a concrete beam structure was presented. Using a two-beam analogy where the upper and lower beam are connected along a line at the vertical level of the crack tip it was necessary to gain knowledge about the mechanisms present in this horizontal plane. Studies of the established finite element model showed that both vertical stresses and shear stresses are present in such a horizontal plane. The finite element model also delivered results which indicated that bi-linear normal stress distributions at the vertical mid-cross section and the boundary cross section would be reasonable model assumptions.

With the knowledge from the finite element model and the following assumptions, a non-linear system of equations describing the adaptive cracked hinge were established. A non-linear solution showed good correlation between the presented model and the finite element model. Comparison of the presented model with the explicit formulation demonstrated some of the forces using an adaptive hinge to describe the behavior of cracking concrete beam structures. Considering the bending stiffness relation in terms of a moment-curvature curve the post peak behavior was entirely different comparing the presented model with the explicit formulation. The presented model has a quick descent on the curve shortly after peak, where the explicit formulation is more flat. The relation between the crack mouth opening displacement and the curvature also showed large differences between the presented model and the explicit formulation. The crack mouth opening displacement increased fast at a certain curvature corresponding to the initial post peak state whereas the explicit formulation showed a more flat relation.

In the serviceability limit state for undetermined concrete beam structures a good description post peak is important, since the forces will redistribute when the stiffness changes. For unreinforced concrete beam structures the important parameter is curvature, since it can be used to describe the support conditions (rotation) and thereby give a good estimate of the deflections.

Introduction of the simple reinforcement bar is the more simple example of a reinforced adaptive cracked hinge model based on the presented model. It should be emphasized that the presented simple model for the reinforcement bar due not take important characteristics of the concrete-reinforcement interaction as de-bonding and pull-out into account. Comparison of the simple reinforced adaptive cracked hinge model with an elastic solution of a cracked beam cross section, in form of a moment-curvature relation showed expected behavior of the reinforced hinge, since the moment for the reinforced hinge were considerably higher with a drop shortly before the crack become stress free at the crack mouth. The moment for the reinforced hinge should converge towards the elastic solution when the crack gradually became stress free, but due to the limitations of the adaptive cracked hinge model (bridging stresses in the entire length of the crack) this behavior was not clearly obtained.

6.2 Future work

There is a great potential in the establishment of a good solution for a reinforced adaptive cracked hinge model, since it can become very useful in determination of deflections and crack mouth opening displacements which are both important characteristics in the serviceability limit state.

With the implementation of a simple reinforcement bar into the presented model it was shown that an extend of the presented model seems fairly easy. The primary work in the establishment of a good reinforced adaptive cracked hinge model is therefore to establish the equations necessary to describe de-bonding and pull-out interaction between the concrete and the reinforcement bar through the width of the adaptive hinge.

Other topics for future work is the extend of the model exterior of the current limits. Relevant topics to be mentioned are the possibility to model a stress free crack and the introduction of a multi-linear softening relation.

The presented model also includes the normal force, but due to time limitations it has not been possible to cover this part of the model, and therefore this should also be a topic of future work.

Bibliography

DIANA. *User's Manual Version 9.3*. TNO DIANA, October, 2008.

Gert Heshe, Aage Peter Jensen, Poul Kring Jakobsen, and René Christensen. *Betonkonstruktioner, teori og udførelse*. Department of Civil Engineering - Technical University of Denmark and Aalborg University, 2005.

Arne Hillerborg, P. E. Petersson, and M. Modéer. Analysis of crack formation and crack growth in concrete by means of fracture mechanics and finite elements. *Cement and Concrete Research*, 6:773–782, 1976.

Jens-Christian Kragh-Poulsen. *Forskydningsbaereevnen af fiberarmerede betonbjaelker*. Master Thesis, Department of Civil Engineering, Technical University of Denmark, 2009.

S. Krenk. *Mechanics and Analysis of Beams, Columns and Cables*. Polyteknisk Press, Copenhagen, 1 edition, 2000.

Mathworks. *Optimization Toolbox - User Guide*. available (5'th of January 2010) at *http://www.mathworks.com/access/helpdesk/help/toolbox/optim/optim_ product_page.html*.

J. F. Olesen. *Cracks in reinforced FRC beams subject to bending and axial load*. Proceedings of the Fourth International Conference on Fracture Mechanics of Concrete and Concrete Structures, available at *www.ICF11.com*.

J.F. Olesen. Fictitious crack propagation in fiber-reinforced concrete beams. *Journal of Engineering Mechanics*, 127(3):272–280, 2001.

Henrik Stang, John Forbes Olesen, Peter Noe Poulsen, and Lars Dick-Nielse. On the application of cohesive crack modeling in cementitious materials. *Materials and Structures*, 40(4):365–374, 2007.

Lennart Østergaard. *Early-Age Fracture Mechanics and Cracking of Concrete, Experiments and Modelling*. PhD thesis, Department of Civil Engineering, Technical University of Denmark, 2003.

J. P. Ulfkjaer, S. Krenk, and R. Brincker. Analytical model for fictitious crack propagation in concrete beams. *Journal of Engineering Mechanics*, 121(1):7–15, 1995.

Appendix A

Equations and Variables for the Adaptive Cracked Hinge

The control parameters are the half hinge width s and the normal force N. The variables are given in the entire derived length which fits the geometry and definitions described in chapter 3. The nine equations are given as they where stated in chapter 3.

A.1 Equations

$$\varepsilon_t' = \frac{1}{2E_c}(\sigma_{2c} + \sigma_{2b}) \tag{A.1}$$

$$\varepsilon_c' = \frac{1}{2E_c}(\sigma_{1c} + \sigma_{1b}) \tag{A.2}$$

$$\varepsilon_b' s = w_0 + \frac{1}{2E_c}(\sigma_{0c} + \sigma_{0b})s \tag{A.3}$$

$$N = t\int_0^h \sigma_{mid-section}(y)\,dy \tag{A.4}$$

$$M = t\int_0^h \sigma_{mid-section}(\frac{h}{2} - y)\,dy \tag{A.5}$$

$$M_{cb} + M_v - M_{bb} - \frac{1}{2}c\Delta N_b = 0 \tag{A.6}$$

$$N = \Delta N_b - \Delta N_t \tag{A.7}$$

$$u_b + u_{V,b} + u_r = u_t + u_{V,t} \tag{A.8}$$

$$w_{01} + w_{02} = \frac{w_0 + \varepsilon_b' s}{2} \tag{A.9}$$

A.2 Unknowns

The unknowns are chosen to be:

M moment

κ curvature

c crack length

w_0 half the crack mouth opening

σ_{1b} normal stress at the boundary at the crack tip level

σ_{2c} normal stress at the top of the mid-section

σ_{2b} normal stress at the top of the boundary

ε'_m mean strain at half the hinge height

σ_{yc} vertical tensile stress at the crack tip

A.3 Known Parameters

Some material parameters and geometry definitions must be pre defined. The material parameters are f_t the tensile strength of the concrete; E_c the elastic stiffness modulus of the concrete; ν poisons ratio; G_F the fracture energy and the geometry are defined by h the height of the hinge and t the thickness of the hinge.

A.4 Definition of the Variables

Two of the variables are locked by the hinge assumptions.

$$\sigma_{1c} = f_t \quad \text{and} \quad \sigma_{0b} = f_t \tag{A.10}$$

In figure A.1 the stress distribution at the mid-section in figure 3.1 is illustrated in terms of equivalent triangular areas, which is the basis for the derived moment and normal forces.

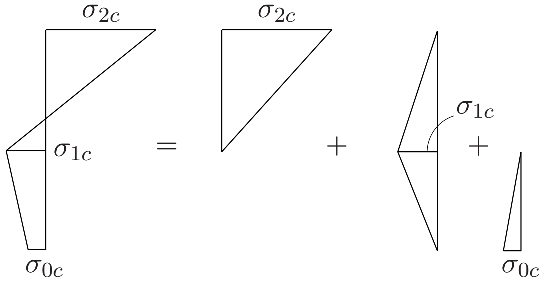

Figure A.1: Illustration of equivalent triangular stress distribution, With the definition in figure A.1, equation (A.4) and (A.5) are equivalent to the two following formulations

$$N = \frac{1}{2}t(\sigma_{2c}a + \sigma_{1c}h + \sigma_{0c}c) \tag{A.11}$$

$$M = \frac{1}{2}hN + \frac{1}{2}t\Big((-\sigma_{2c})a\Big(h - \frac{1}{3}a\Big) - \sigma_{1c}a\Big(h - \frac{2}{3}a\Big) - \sigma_{1c}c\frac{2}{3}c - \sigma_{0c}c\frac{1}{3}c\Big) \tag{A.12}$$

The mean curvature is linear and given by (3.1) from which the following three equations are derived.

$$\begin{aligned} \varepsilon'_t &= \varepsilon'_m - \frac{1}{2}h\kappa \\ \varepsilon'_c &= \varepsilon'_m + (\frac{1}{2}h - c)\kappa \\ \varepsilon'_b &= \varepsilon'_m + \frac{1}{2}h\kappa \end{aligned} \tag{A.13}$$

a is a geometric definition

$$a = h - c \tag{A.14}$$

The stress at the crack mouth is given by

$$\sigma_{0c} = ft - ft\frac{w_0}{w_1} \tag{A.15}$$

The shear stiffness is derived by

$$G = \frac{Ec}{2(1+\nu)} \tag{A.16}$$

Normal force difference of the upper beam.

$$N_{ct} = \frac{1}{2}at(\sigma_{1c} + \sigma_{2c}) \tag{A.17}$$

$$N_{bt} = \frac{1}{2}at(\sigma_{1b} + \sigma_{2b}) \tag{A.18}$$

$$\Delta N_t = N_{bt} - N_{ct} \tag{A.19}$$

Displacement of the upper beam at the boundary:

$$I_t = \frac{1}{12}ta^3 \tag{A.20}$$

$$u_t = -\frac{1}{24}\frac{s^2(ta^2\sigma_{1b} - ta^2\sigma_{2b} + 4a\Delta N_t + t\sigma_{yc}s^2)}{E_cI_t} \tag{A.21}$$

$$u_{V,t} = -\frac{1}{8}\frac{t\sigma_{yc}s^2}{G\frac{5}{6}ta} \tag{A.22}$$

$$u_{tt} = u_t + u_{V,t} \tag{A.23}$$

The variables for (A.6) are:

$$M_{cb} = \frac{1}{2}c\frac{1}{2}tc(\sigma_{1c} + \sigma_{0c}) + \frac{1}{2}t\left(-\sigma_{1c}c\frac{2}{3}c - \sigma_{0c}c\frac{2}{3}c\right) \tag{A.24}$$

$$M_v = \int_0^s f(x)x dx = \frac{1}{8} t\sigma_{yc}s^2 \tag{A.25}$$

$$M_{bb} = \frac{1}{2}c\frac{1}{2}tc(\sigma_{1b} + \sigma_{0b}) + \frac{1}{2}t\left(-\sigma_{1b}c\frac{2}{3}c - \sigma_{0b}c\frac{2}{3}c\right) \tag{A.26}$$

$$\Delta N_b = N_{cb} - N_{bb} = \frac{1}{2}tc(\sigma_{1c} + \sigma_{0c} - (\sigma_{1b} + \sigma_{0b})) \tag{A.27}$$

Vertical displacement of the bottom beam at the boundary:

$$I_b = \frac{1}{12}tc^3 \tag{A.28}$$

$$u_b = \frac{1}{24}\frac{s^2(-tc^2\sigma_{0b} + tc^2\sigma_{1b} - 4c\Delta N_b + t\sigma_{yc}s^2)}{EcI_b} \tag{A.29}$$

$$u_{V,b} = \frac{1}{8}\frac{t\sigma_{yc}s^2}{G\frac{5}{6}tc} \tag{A.30}$$

$$u_r = -w_0\frac{s}{c} \tag{A.31}$$

$$u_{bt} = u_b + u_{V,b} + u_r \tag{A.32}$$

Horizontal displacement at a vertical axis at the bottom of the bottom beam

$$A_0 = \frac{5}{6}ts \tag{A.33}$$

$$I_{vb} = \frac{1}{12}ts^3 \tag{A.34}$$

$$\begin{aligned} w_{01} = &-\frac{1}{120}\frac{1}{GA_0EI_{vb}}(tc^2(4c^2GA_0\sigma_{1c}EI_{vb} + 11c^2GA_0\sigma_{0c} - 20\sigma_{1b}EI_{vb} \\ &+ 40EI_{vb}\sigma_{0c} - 40EI_{vb}\sigma_{0b} - 11c^2GA_0\sigma_{0b} - 4c^2GA_0\sigma_{1b})) \end{aligned} \tag{A.35}$$

$$w_{02} = c\frac{-u_{bt}}{s} \tag{A.36}$$

Appendix B

Finite Element Model - Details

B.1 Model

The finite element model needed to model the characteristics of an adaptive cracked hinge is special in its nature since a new model is needed for each size of the hinge width that are considered. For each model a non-linear analysis is performed but only one load step will fulfill the boundary assumption of the adaptive hinge. More exactly the load step where the tensile stress in the bottom of the boundary (point p6 in figure 1.6b) equals the tensile strength.

Models can be constructed by means of the graphical user interface iDiana but a better approach is to use a file of the `.fga` format where the model can be defined and read directly into iDiana by means of the `utility read batch file.fga` command. An example of such a file is found in appendix J.2.

B.1.1 Geometry

Due to the above discussion the width of the model is variable. The finite element analysis performed represents the half hinge widths s = [5 10 15 20 25 30 35 40 45 48 50 75]. The geometry is tabulated in table B.1.

Table B.1: Model geometry

Width [mm]	Height [mm]	Depth [mm]
$2 \times s$	100	100

Due to symmetry it is sufficient to model one half of the hinge, with width s, assuming that the crack will occur in the middle.

B.1.2 Mesh

The mesh for the model was restricted by the limits of the DIANA Teacher Edition. The element limit is 1000 elements and there are no restrictions on the number of nodes. Therefore, rectangular elements are preferred compared to triangular elements which will yield less elements. In order to achieve smooth stress plots particularly in the cracking cross section the finer mesh possible is used within the limitations. This results in a mesh with 48 interface elements in the hinge height for all of the models except for the one where $s = 75$. For this, 32 interface elements in the hinge height are used. All of the elements outside the discrete crack are rectangular and the size is defined by the number of elements in the height direction and over half the hinge width.

Table B.2: Number of elements, in the height and the width directions, in the models.

Half hinge width [mm]	Elements in the height	Elements over half hinge width
5	48	8
10	48	8
15	48	8
20	48	16
25	48	16
30	48	18
35	48	18
40	48	18
45	48	18
48	48	18
50	48	18
75	32	30

Plane Stress Elements

For the elastic part of the beam, the *CQ16M - quadrilateral, 8 nodes element*, which is an eight-node quadrilateral isoparametric plane stress element is used. The element is based on quadratic interpolation and Gauss integration. By default, a 2×2 integration is applied.

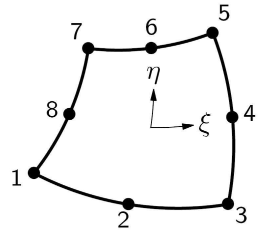

Figure B.1: *CQ16M - quadrilateral, 8 nodes element*. Illustration from DIANA [October, 2008]

Interface Elements

The discrete crack is discretized with the element *CL12I - line, 3+3, 2-D* which is an interface cohesive crak element between two lines in a two-dimensional configuration with 3 nodes on each line. This element fits the plane stress element. The element is based on quadratic interpolation and a 4-point Newton-Cotes integration scheme is applied, see figure .

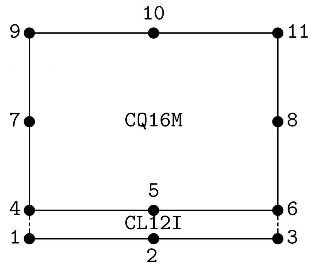

Figure B.2: Example of the interface element connected with the elastic element. Illustration from DIANA [October, 2008]

Relevant to notice about the integration scheme is the placement of the two middle integration points which are not equivalent to the nodes. This is an issue determining the crack tip level as explained in section 2.2.

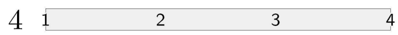

Figure B.3: 4-point Newton-Cotes integration scheme.

Beam Elements

The beam element is a curved 3 nodes beam element based on the Mindlin-Reissner theory which does take shear deformation into account. The beam element is based on an isoparametric formulation which assumes that the displacements and rotations of the beam axis normals are independent and are respectively interpolated from the nodal displacements and rotations. In DIANA the name of the beam element is *CL9BE curved, 3 nodes, 2-D*. A 2-point Gauss integration scheme along the bar axis is applied.

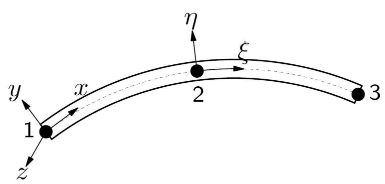

Figure B.4: Illustration of the Mindlin-Reissner beam element. Illustration from DIANA [October, 2008]

B.1.3 Material and Physical Properties

Table B.3: Material parameters for the elastic part (Plane stress and the beam elements).

E_c [MPa]	ν
31000	0.15

Where E_c is the modulus of elasticity for the concrete and ν is Poisson's ratio.

Table B.4: Material parameters for the interface

D_{11} [N/mm^3]	D_{22} [N/mm^3]	f_t [MPa]	G_f [N/mm]	G_{cr} [MPa]
3.1×10^{11}	3.1×10^{11}	2.4	0.1	3.1×10^{11}

Where D_{11} and D_{22} are the DIANA name for the linear stiffness modulus in both normal and tangential direction; f_t, G_f and G_{cr} are the non-linear material parameters for discrete cracking in the interface, tensile strength, fracture energy and the shear modulus after cracking. The linear stiffness modulus should be infinity since the interface elements have no width. It is not possible to run an analysis with interface elements having infinite stiffness and therefore a stiffness is defined and evaluated considering which geometric size they correspond to. This is evaluated using the relation stated in equation (B.1).

$$D = \frac{\Delta\sigma}{\Delta u} = \frac{f_t}{\frac{f_t}{E_c} \cdot u_{stiff}} = \frac{E_c}{u_{stiff}} \tag{B.1}$$

where E_c is the modulus of elasticity of the concrete; u_{stiff} is the relative width corresponding to the stiffness D. With the defined values $u_{stiff} = 0.1$ mm considered close enough to zero width, compared to half hinge widthes of 5-75 mm.

B.1.4 Boundary Conditions

The hinge is simply supported. Modeling only half of the beam, this correspond to a vertical support at the boundary and horizontal support along the symmetry axis. The support at the symmetry axis is a line support connected to one side of the interface elements.

For the adaptive cracked hinge model presented the boundary is assumed to remain plane. Therefore a translational constraint of the boundary in the finite element model is established. The pseudo beam element illustrated in figure 2.1 on page 9, has both translational and rotational degrees of freedom. By means of a build in semi-automatic constraint in the finite element program it is possible to constraint the translational degree of freedom of the plane stress elements to the rotational degree of freedom of the pseudo beam element. The effect of this constraint is that all the element nodes which are placed on the boundary line will follow the rotation of the pseudo beam node on the boundary line. With this boundary constraint a constant moment with a linear stress distribution of the hinge height is achieved through the two concentrated loads, indicated with arrows in opposite direction in figure 2.1 on page 9.

The described constraint is a linear constraint and definitions can be found in the DIANA manual, DIANA [October, 2008] in the part with Analysis Procedures - Part I - 2.2.8.2 Loose Elements.

The DIANA procedure for the linear constraint, can not make an automatic constraint when more than two elements are to be connected to the beam element. Therefore a small extension of the `.dat` file which contain information about the model, must be included. This constraint is in DIANA referred to as a TYING. The tying can be applied in an extra .dat file which must be selected in the DIANA analysis setup in the selection box for input data files. The needed commands for the model with $s = 25\,mm$ are given below

```
'TYINGS'
ELEMEN
/ 3-50 / 1
```

With this tying command all nodes of the specified slave plane stress elements which are on the beams y-axis will be tied automatically to the beam's degrees of freedom, according to DIANA [October, 2008] in the part mentioned above. The connection is graphically illustrated in figure B.5.

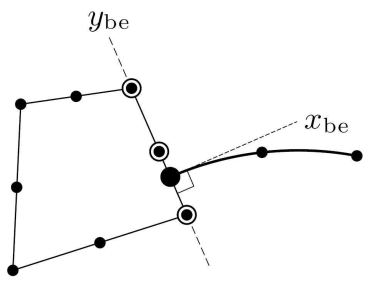

Figure B.5: Example of the connection between the plane stress elements and the beam element. Using the loose element tying type, all element nodes on the beams y-axis will be tied to the beam's degrees of freedom. Illustration from DIANA [October, 2008] - Element Library - Part I: Structural Elements

To ensure the correct behavior of the load and the boundary constraints, the influence of the beam connection has been tested in a simple finite element model, see section B.3.

B.2 Non-Linear Analysis

A physical non-linear analysis is used. The analysis uses a incremental-iterative solution procedure with a load controlled using a CMOD Arc-length control where CMOD indicates that it is the displacement difference between two points that is used. The step sizes used for the Arc-length control are explicitly specified for the elastic part and until an undefined limit before the peak. After this point an iterative based method is used to adapt the step size depending on the number of iterations in the previous calculation, see the Diana manual DIANA [October, 2008] Part IV Non-Linear Static and Transient Analysis for extended definitions. In Part X Background Theory - Chapter 30 Solution Procedures for Non-Linear Systems, descriptions of the incremental-iterative solution procedures are described. In the following sections the utilized methods are briefly described and a short comprehensive description is also given.

The analysis procedures can be defined within the graphical interface of Diana, but a better outline of the analysis procedure is achieved using a command file of the `.dcf` format to define the analysis procedure. An example of the command file used for the Diana models is given in appendix J.1.

B.2.1 Equilibrium Iteration

For the equilibrium iteration process the Regular Newton-Raphson method is used. This method yields a quadratic convergence characteristic.

B.2.2 Incremental Procedures

The Arc-length control together with the Updated Normal Plane method is used for the incremental procedure. This method can adapt the step size depending on the results in the current step. For the Updated Normal Plane method the geometrical meaning of the constraint means that the iterative increment must be perpendicular to the total increment at the previous iteration. This means that the solution is projected on the plane, normal to the previous solution.

B.2.3 Output

The status of the interface elements can be given in an output file using the approach described in the Diana manual DIANA [October, 2008] Part IV Non-Linear Static and Transient Analysis - 12.4.4.2 Crack Status. In the current model the crack status is collected through the following commands using the model section `CRK_SRFC` which contains the interface elements. The cracking status is collected in the integration points as indicated on the last line.

```
BEGIN OUTPUT
    TABULA
    FILE "Crack_status"
    SELECT  ELEMEN CRK_SRFC /
    TEXT "Crack status"
    STATUS CRACK INTPNT
END OUTPUT
```

Similar to this output command, data output for different parts of the model can be achieved in a tabular form as seen in the file in appendix J.1.

B.3 Model Tests and Convergence Analysis

B.3.1 Convergence Analysis

A simple convergence analysis has been performed considering the load, curvature and the stress distribution in the mid-section to see the effect of different number of interface cohesive crack elements over the hinge height. In appendix G the plots for 16, 32 and 48 interface cohesive crack elements over the hinge height illustrating the normal stress distributions are given. It is seen that the distribution due not vary considerably, and actually the finer mesh results in the more disturbed distribution. This indicate that it is important even with fine mesh to graphically observe that the stress distribution in the cracked mid-section is acceptably smooth. When average stresses in the cracked mid-section is used, for the fine mesh, a smooth curve is obtained, which could indicate that the disturbance observed in the plots are very concentrated and due not effect the rest of the hinge considerably.

In the models used for comparison with the adaptive cracked hinge model 48 interface cohesive crack elements are used, except for the model with half hinge width equal to 75 mm, there only 32 elements where used. In table B.5 results from the three analysis are presented. Along with the results it should also be mentioned that small variation of the tensile stress at the bottom point of the boundary of the utilized analysis step were observed.

From the investigations it is concluded that the utilized mesh of 32 and 48 elements are sufficiently fine for the performed finite element analysis.

Table B.5: Results of simulations with different number of interface cohesive crack elements over the hinge height. The analysis procedure and Arc-length step sizes are identical for the simulations.

No. of elements	Moment	Curvature	Analysis step
16	$6.364 \cdot 10^5$	$8.5025 \cdot 10^{-6}$	122
32	$6.368 \cdot 10^5$	$8.355 \cdot 10^{-6}$	121
48	$6.368 \cdot 10^5$	$8.3875 \cdot 10^{-6}$	119

B.3.2 Test of Linear Constraint

A test of the constraint with the pseudo beam element has been performed. The dimensions of the test structure, are 400 mm × 100 mm × 100 mm. The concentrated load equals 2.5 kN.

The translation of the nodes which are placed on the line at the top of the beam structure are constraint to the rotation of the pseudo beam element. With a concentrated force indicated with the arrow the vertical stress distribution should be linear if the constraint acts as it is supposed to do. The stresses at the top line are plotted in figure B.6b and it is seen that the constraint works properly.

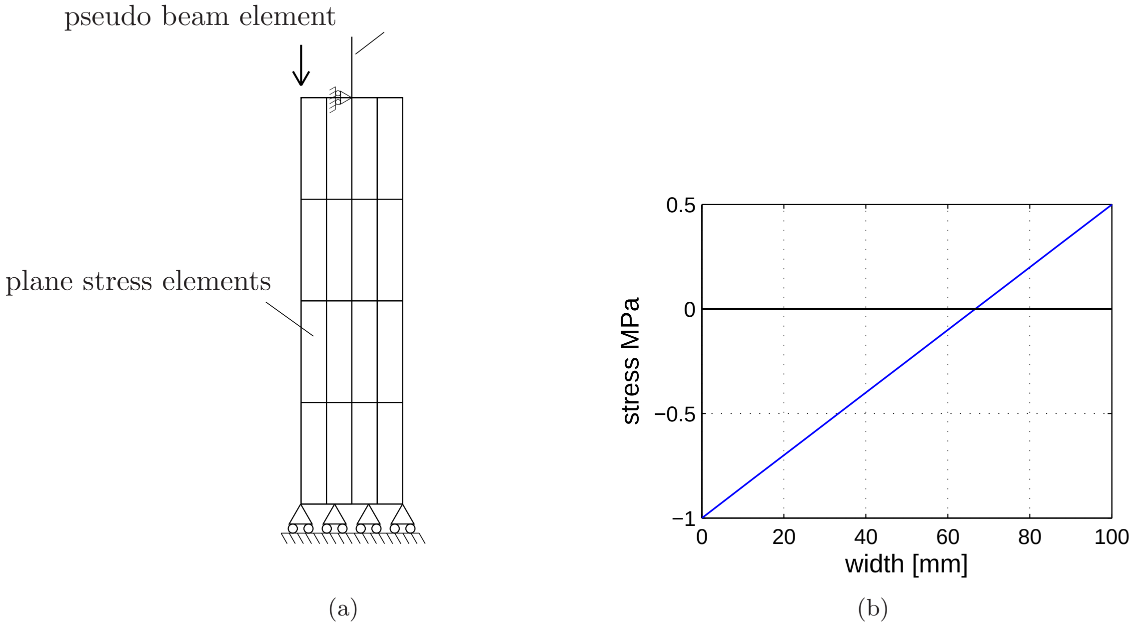

Figure B.6: (a) FE mesh, support and load for test example and (b) Resulting stress distribution.

B.4 FEM Results

In this section representative color plots of the stresses within a half hinge with width 75 mm is illustrated. Vector plots of the principal stresses for half hinge widthes of 25 mm, 40 mm and 75 mm are also illustrated where it is seen how the stresses tend to find their way over the top of the crack. Comparison of the FE normal stress distribution σ_{xx} with the adaptive cracked hinge results is found in appendix E.

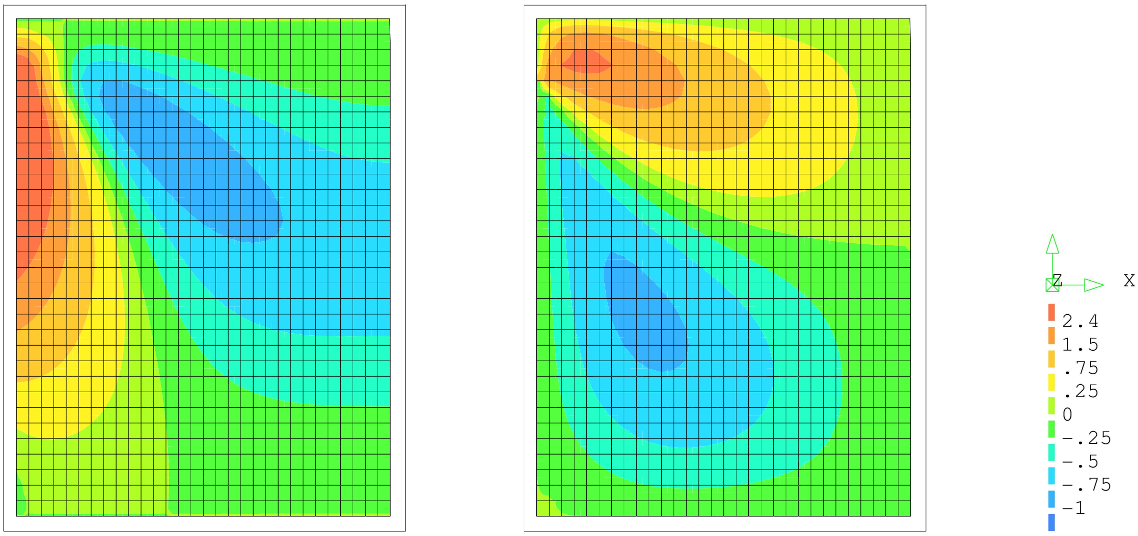

(a) σ_{yy} (b) σ_{xy}

Figure B.7: Contour plots, $s = 75$ mm

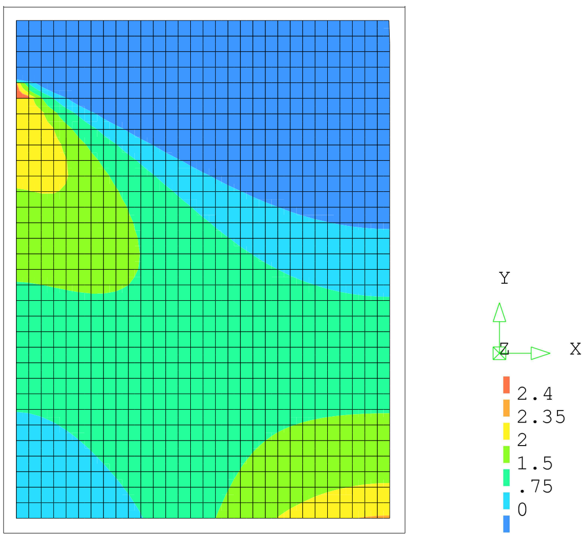

Figure B.8: Contour plot, s_{xx}, $s = 75$ mm

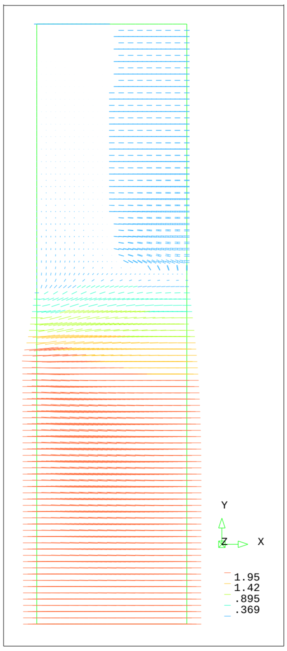

(a) $s = 25\,\mathrm{mm}$

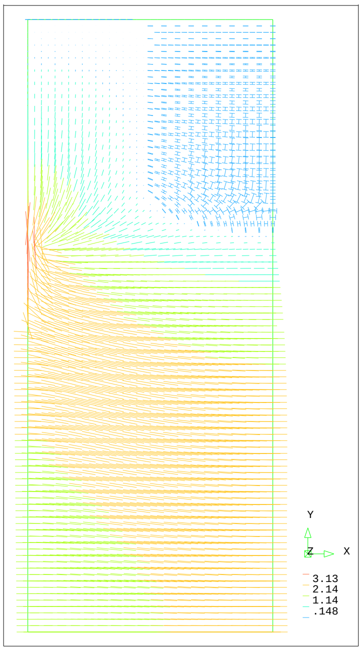

(b) $s = 40\,\mathrm{mm}$

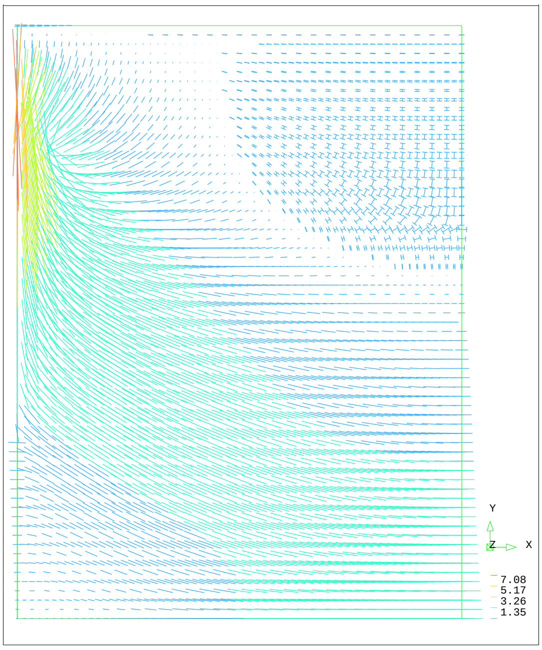

(c) $s = 75\,\mathrm{mm}$

Figure B.9: Vector plots of principal stresses.

Appendix C

Analytical Hinge Model

C.1 Geometry and Material Parameters

The analytical hinge model by Olesen [2001] is used for comparison regarding the results of the new model presented in the main report. The analytical hinge model has a fixed hinge width which in the article by Olesen [2001] is referred to by s as an definition of the entire hinge width. In this section, the terminology of s equal to half the hinge width is still used and accounted for in the described equations. A hinge width corresponding to $s = h/4$ has been able to model the peak load compared to finite element analysis and experimental results, see Ulfkjaer et al. [1995]. The geometry used for the results that have been compared to the other models is found in table C.1.

Table C.1: Geometry and material properties

L [mm]	h [mm]	t [mm]	E_c [MPa]	f_t [MPa]	G_F N/mm	s [mm]
200	100	100	31000	2.4	0.1	25

Where L is the length of the beam; h is the height of the beam; t is the thickness; E is Young's modulus of the concrete; f_t is the tensile strength and G_F is the fracture energy.

The linear stress-crack opening relation used was presented in section 1.4 on page 2.

C.2 Non-Linear Hinge Formulation by Olesen

In the current description of the non-linear hinge, only what is referred to as phase I in Olesen [2001], where the stress-crack opening relation is linear, will be described. Also the normal force is taken out of the equations. It is also emphasized that only what is needed to gain the needed results is presented. For any deeper description see Olesen [2001].

For the non-linear hinge formulation it is assumed that the boundaries of the non-linear hinge remains plane also referred to as rigid which is illustrated in figure (C.1) together with a definition of the geometry, loading and overall deformation.

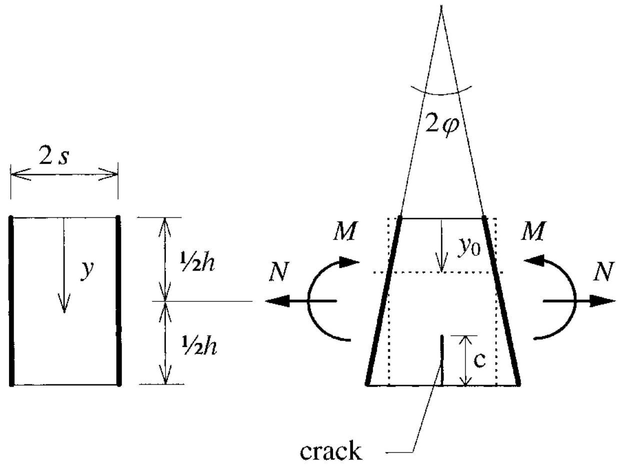

Figure C.1: Geometry, loading and deformation of cracked hinge, illustration from Olesen [2001], slightly modified

The non-linear hinge is modeled as incremental layers of springs which act without transferring shear between each other. The incremental layer is fixed to the boundary as illustrated on figure C.2.

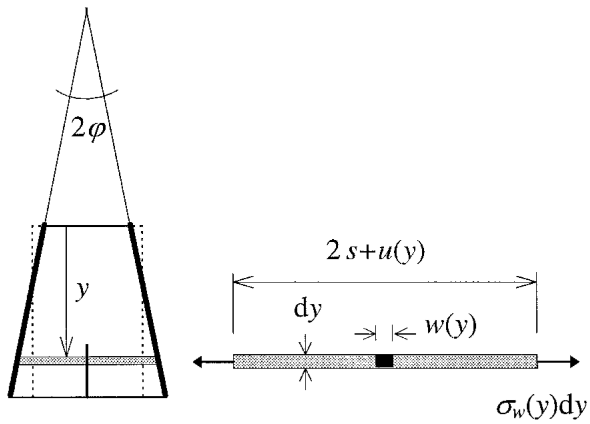

Figure C.2: Geometry, loading and deformation of crack incremental horizontal strip of hinge, illustration from Olesen [2001], slightly modified

The following normalizations are introduced

$$\mu = \frac{6}{f_t h^2 t} M, \quad \theta = \frac{hE}{2(2s) f_t} \phi, \quad \alpha = \frac{c}{h} \tag{C.1}$$

where c is the crack length. The normalized crack length α is given by (C.2).

$$\alpha = 1 - \beta - \sqrt{(1-\beta)\left(\frac{1}{\theta} - \beta\right)} \tag{C.2}$$

where β is a dimensionless parameter given by (C.3).

$$\beta = \frac{f_t \frac{1}{(2\,w_1)} 2\,s}{E_c} \tag{C.3}$$

The normalized moment μ is given by (C.4).

$$\mu = 4\left(1 - 3\alpha + 3\alpha^2 - \frac{\alpha^3}{1-\beta}\right)\theta - 3 + 6\alpha \tag{C.4}$$

The crack mouth opening displacement $CMOD$ is given by

$$CMOD = \frac{2sf_t}{E_c}\frac{2\alpha\theta}{1-\beta} \tag{C.5}$$

For the comparison the curvature is used and it can be derived by (C.6).

$$\kappa = \frac{\phi}{s} \tag{C.6}$$

The analysis of the non-linear hinge is carried out with θ as the controlling parameter.

C.3 Implementation in Matlab

The above formulation for modeling the fictitious crack is implemented in a small MATLAB-program. The procedure is as shown in table C.2. Remark that instead of a phase changing criteria as used in the original model presented in the article Olesen [2001] a simple break criterion is used at the limit $M = M_E$ which can be used since the considered phase only consider moments above the elastic moemnt and it has the same effect as a break criterion with $CMOD > 2w_1$ where $2w_1$ is the stress free crack opening.

Table C.2: MATLAB procedure

1)	Define geometry and material parameters
2)	Loop over θ
	For $\theta = 1 : n$
	Calculate α, μ and $CMOD$ by use of (C.2), (C.4) and (C.5), respectively.
	Calculate M for the current iteration from (C.1)
	Collect the current value of θ in a vector
	if $M < M_E$
	break, end
	End
3)	Calculate the crack length c, the moment M and the curvature κ from (C.1) and (C.6).

The implemented MATLAB-code can be found in appendix I.3.

Appendix D

Horizontal Displacement of the Lower Beam Part

In this appendix the principle derivations for the horizontal displacement of the lower beam part are performed by means of the principle of virtual work. Not all variables are entirely described but the meaning should comprehensive. The symbols which are only presented in this appendix is not found in the symbols list.

Positive direction of the following formulations are to the left and thereby the negative direction referring to the positive direction of w_{01} in figure 3.4.

$$f_A(y) = t\left(\sigma_{1c} - \frac{y}{c}(\sigma_{1c} - \sigma_{0c})\right) \tag{D.1}$$

$$f_B(y) = t\left(-\sigma_{1b} - \frac{y}{c}(\sigma_{0b} - \sigma_{1b})\right) \tag{D.2}$$

D.1 Shear Force Contribution

$$V_y = -\int f(y)dy \tag{D.3}$$

Solving an indeterminate integral results in one unknown constant. This constant is found from the boundary condition that $V(c) = 0$ which leads to the following expressions for the shear force distribution as a result of the two load distributions (D.1) and (D.2).

$$V_A(y) = \frac{1}{2}tc(\sigma_{1c} + \sigma_{0c}) - t\sigma_{1c}y + \frac{1}{2}\frac{t(\sigma_{1c} - \sigma_{0c})y^2}{c} \tag{D.4}$$

$$V_B(y) = -\frac{1}{2}tc(\sigma_{1b} + \sigma_{0b}) + t\sigma_{1b}y + \frac{1}{2}\frac{t(\sigma_{0b} - \sigma_{1b})y^2}{c} \tag{D.5}$$

$V_1(y)$ is the shear force distribution from a unit load at the end of the beam where the displacement is wanted.

$$V_1(y) = 1 \tag{D.6}$$

$$u_A = \int_0^c \frac{V_1\,(y)\,V_A\,(y)}{GA_0} dy = \frac{1}{6}\,\frac{tc^2\,(\sigma_{1c} + 2\,\sigma_{0c})}{GA_0} \tag{D.7}$$

$$u_B = \int_0^c \frac{V_1\,(y)\,V_B\,(y)}{GA_0} dy = -\frac{1}{6}\,\frac{tc^2\,(2\,\sigma_{0b} + \sigma_{1b})}{GA_0} \tag{D.8}$$

$$u_V = u_A + u_B = \frac{1}{6}\,\frac{tc^2\,(\sigma_{1c} + 2\,\sigma_{0c} - 2\,\sigma_{0b} - \sigma_{1b})}{GA_0} \tag{D.9}$$

D.2 Moment Contribution

$$M_y = -\int\int f(y)dydy \tag{D.10}$$

Solving a double indeterminate integral results in two unknown constant. These constants are found from the boundary condition that $V(c) = 0$ and $M(c) = 0$ which leads to the following expressions for the moment distribution as a result of the two load distributions (D.1) and (D.2).

$$M_A(y) = \frac{1}{2}tc(\sigma_{1c} + \sigma_{0c})y - \frac{1}{2}t\sigma_{1c}y^2 + \frac{1}{6}\frac{t(\sigma_{1c} - \sigma_{0c})y^3}{c} - \frac{1}{6}tc^2(\sigma_{1c} + 2\sigma_{0c}) \tag{D.11}$$

$$M_B(y) = -\frac{1}{2}tc(\sigma_{1b} + \sigma_{0b})y + \frac{1}{2}t\sigma_{1b}y^2 + \frac{1}{6}\frac{t(\sigma_{0b} - \sigma_{1b})y^3}{c} + \frac{1}{6}tc^2(2\sigma_{0b} + \sigma_{1b}) \tag{D.12}$$

$M_1(y)$ is the moment distribution from a unit load at the end of the beam where the displacement is wanted.

$$M_1(y) = y - c \tag{D.13}$$

$$u_{MA} = \int_0^c \frac{M_1\,(y)\,M_A\,(y)}{EI} dy = \frac{1}{120}\,\frac{tc^4\,(4\,\sigma_{1c} + 11\,\sigma_{0c})}{EI} \tag{D.14}$$

$$u_{MB} = \int_0^c \frac{M_1\,(y)\,M_B\,(y)}{EI} dy = -\frac{1}{120}\,\frac{tc^4\,(11\,\sigma_{0b} + 4\,\sigma_{1b})}{EI} \tag{D.15}$$

$$u_M = u_{MA} + u_{MB} = \frac{1}{120}\,\frac{tc^4\,(4\,\sigma_{1c} + 11\,\sigma_{0c} - 11\,\sigma_{0b} - 4\,\sigma_{1b})}{EI} \tag{D.16}$$

D.3 Total Horizontal Displacement of the Lower Beam

$$\begin{aligned} u_h &= u_V + u_M \\ &= \frac{1}{120}\,\frac{1}{GA_0EI}(c^2t(11\,c^2GA_0\sigma_{0c} - 11\,c^2GA_0\sigma_{0b} - 4\,c^2GA_0\sigma_{1b} - 20\,\sigma_{1b}EI \\ &+ 4\,c^2GA_0\sigma_{1c} + 20\,\sigma_{1c}EI + 40\,EI\,\sigma_{0c} - 40\,EI\,\sigma_{0b})) \end{aligned} \tag{D.17}$$

Since u_h is derived with a positive direction opposite to the positive direction of w_{01}, $w_{01} = -\,u_h$ equivalent to:

$$\begin{aligned} w_{01} = -\frac{1}{120}\,\frac{1}{GA_0EI}(c^2t(11\,c^2GA_0\sigma_{0c} - 11\,c^2GA_0\sigma_{0b} - 4\,c^2GA_0\sigma_{1b} - 20\,\sigma_{1b}EI \\ + 4\,c^2GA_0\sigma_{1c} + 20\,\sigma_{1c}EI + 40\,EI\,\sigma_{0c} - 40\,EI\,\sigma_{0b})) \end{aligned} \tag{D.18}$$

Appendix E

Petersen - Comparison Plots

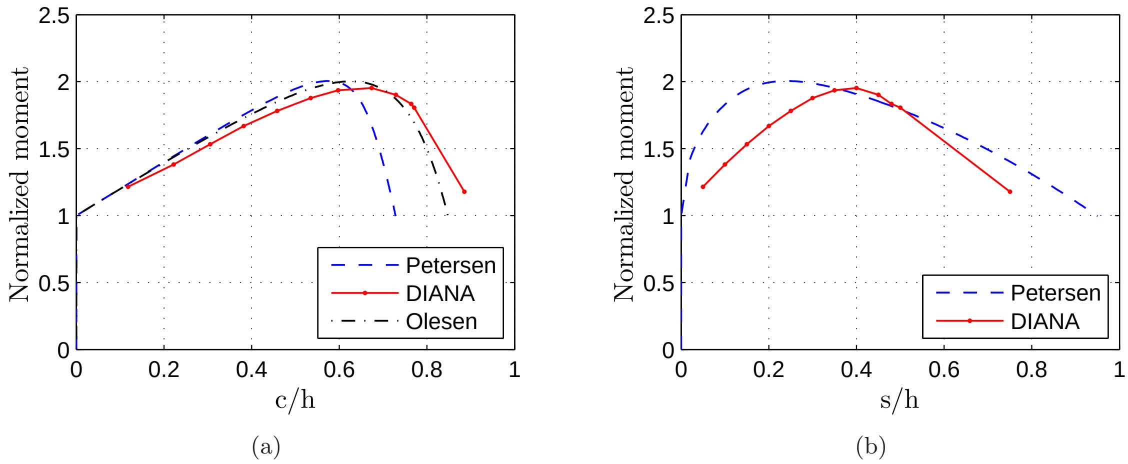

Figure E.1: Normalized moment as a function of (a) the relative crack length and (b) the relative half hinge width

On the following pages the development of the stresses in the mid-section and at the boundary for both the adaptive cracked hinge model and the finite element model are presented.

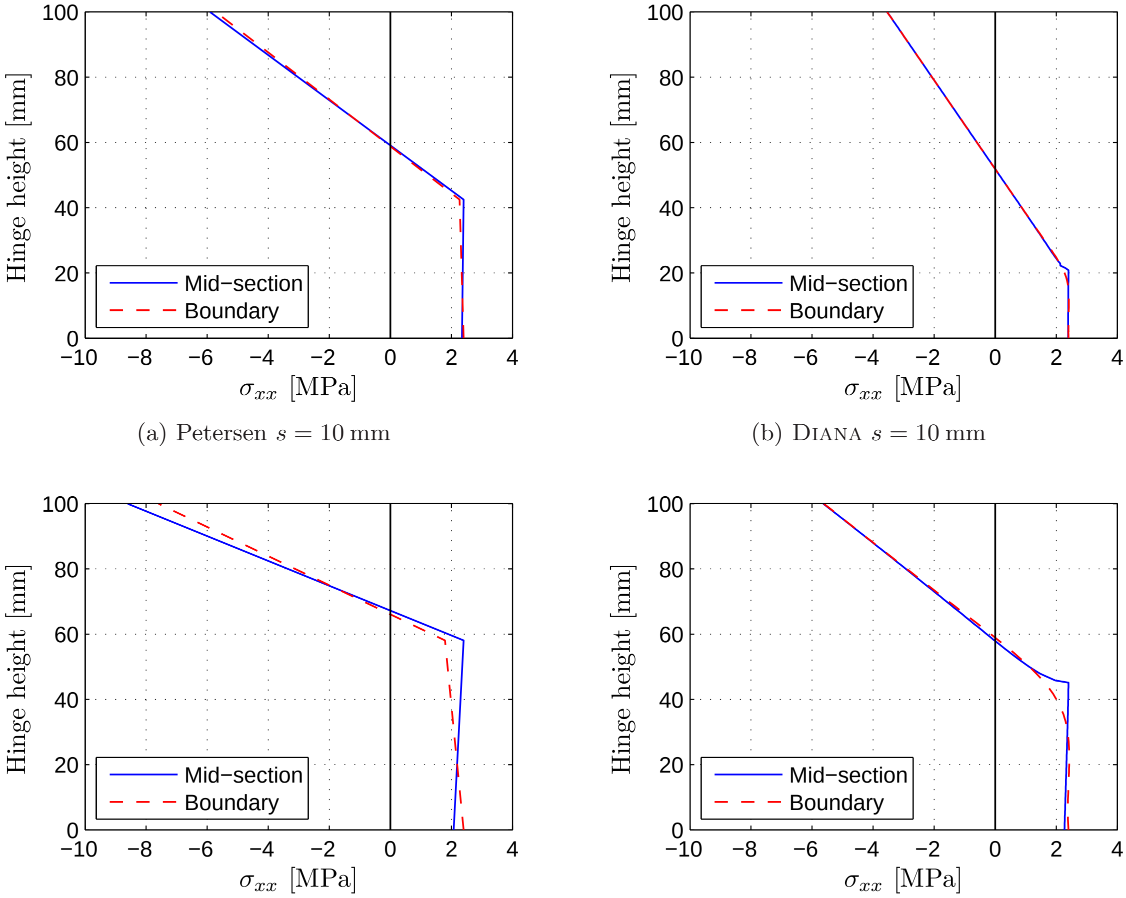

(a) Petersen $s = 10$ mm

(b) Diana $s = 10$ mm

(c) Petersen $s = 25$ mm

(d) Diana $s = 25$ mm

Figure E.2: Stress distributions

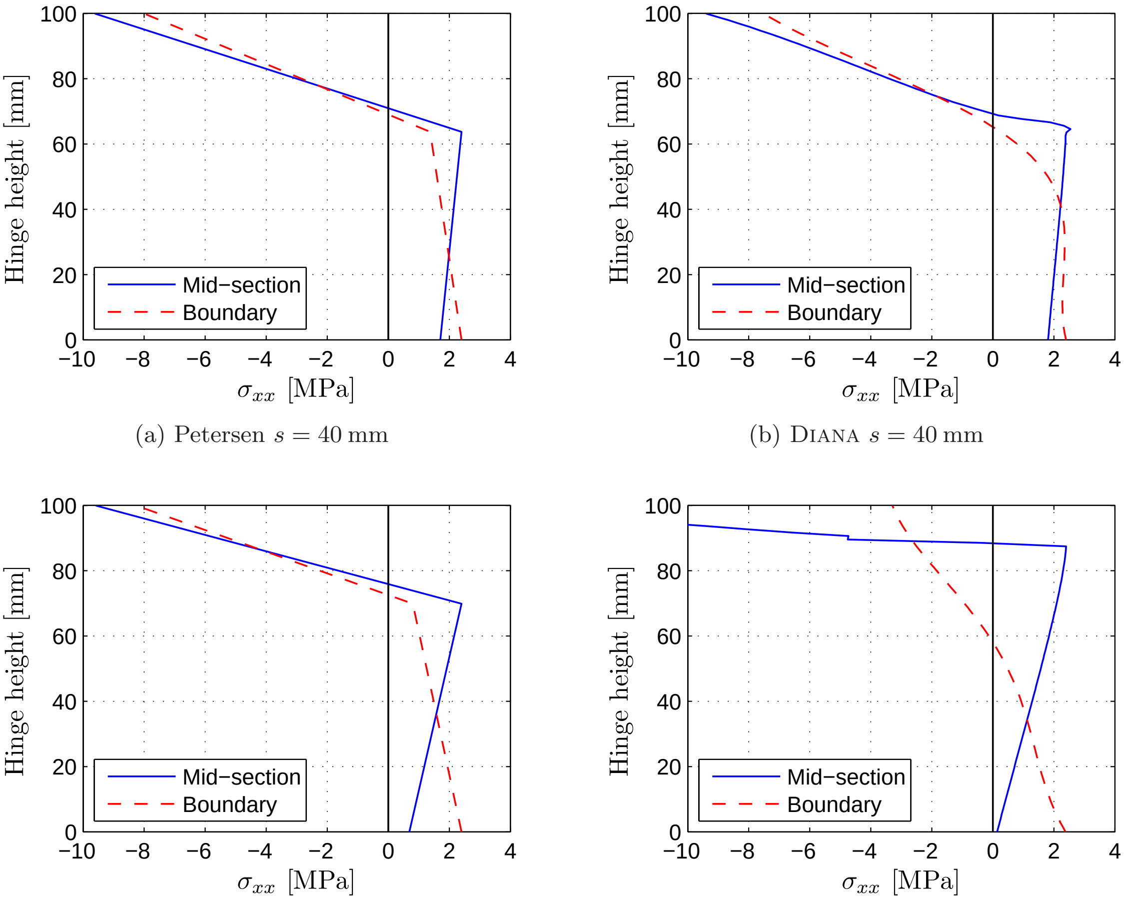

(a) Petersen $s = 40$ mm (b) DIANA $s = 40$ mm

(c) Petersen $s = 75$ mm (d) DIANA $s = 75$ mm

Figure E.3: Stress distributions

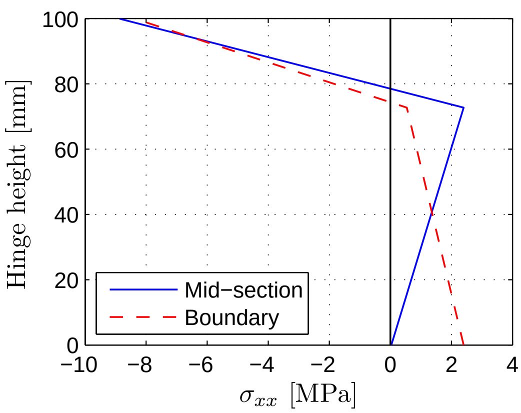

Figure E.4: Stress distribution at the limit of the presented model where there are still stresses in the entire length of the crack. $s = 94$ mm

Appendix F

Petersen with Reinforcement Bar - Characteristic Plots

F.1 Minimum Mechanical Reinforcement Degree

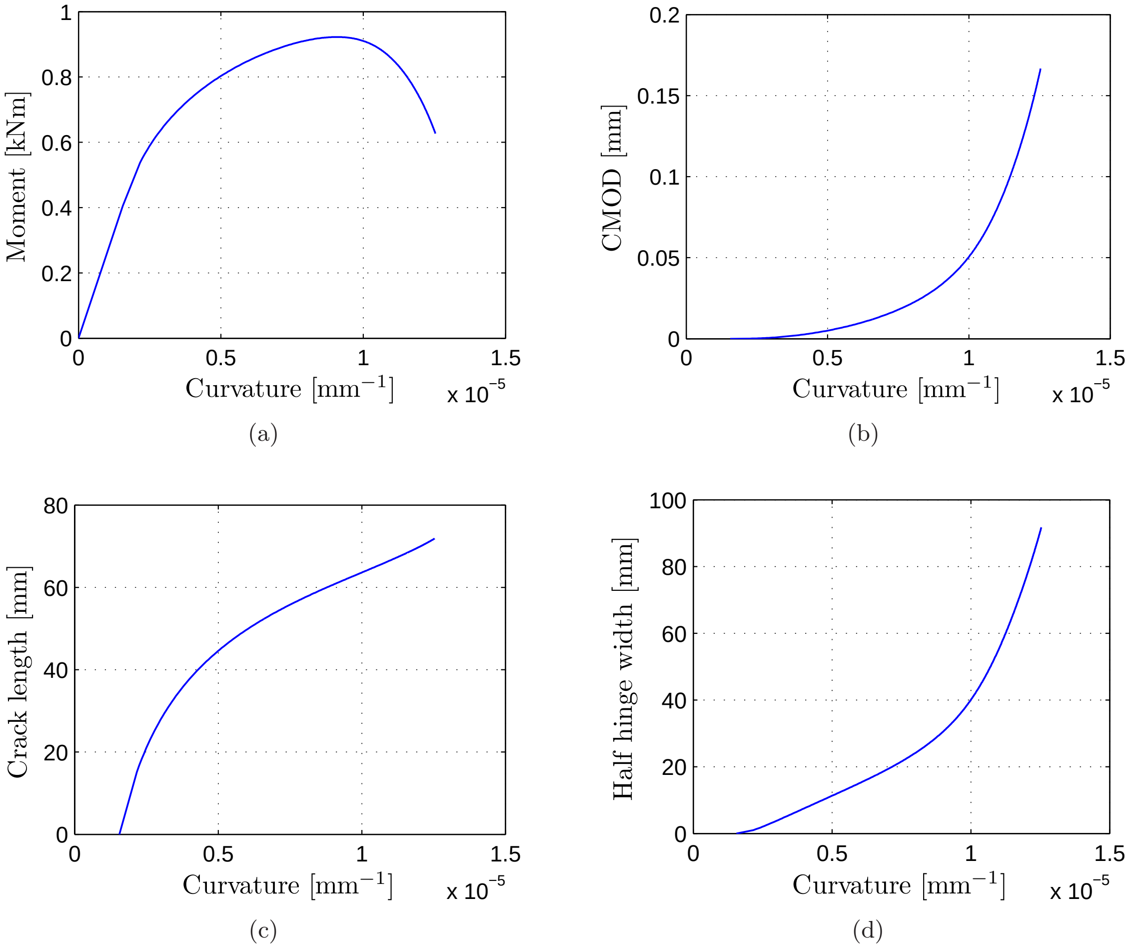

(a) (b) (c) (d)

Figure F.1: $\Phi_{min} = 0.0360$

F.2 Normal Mechanical Reinforcement Degree - Low End

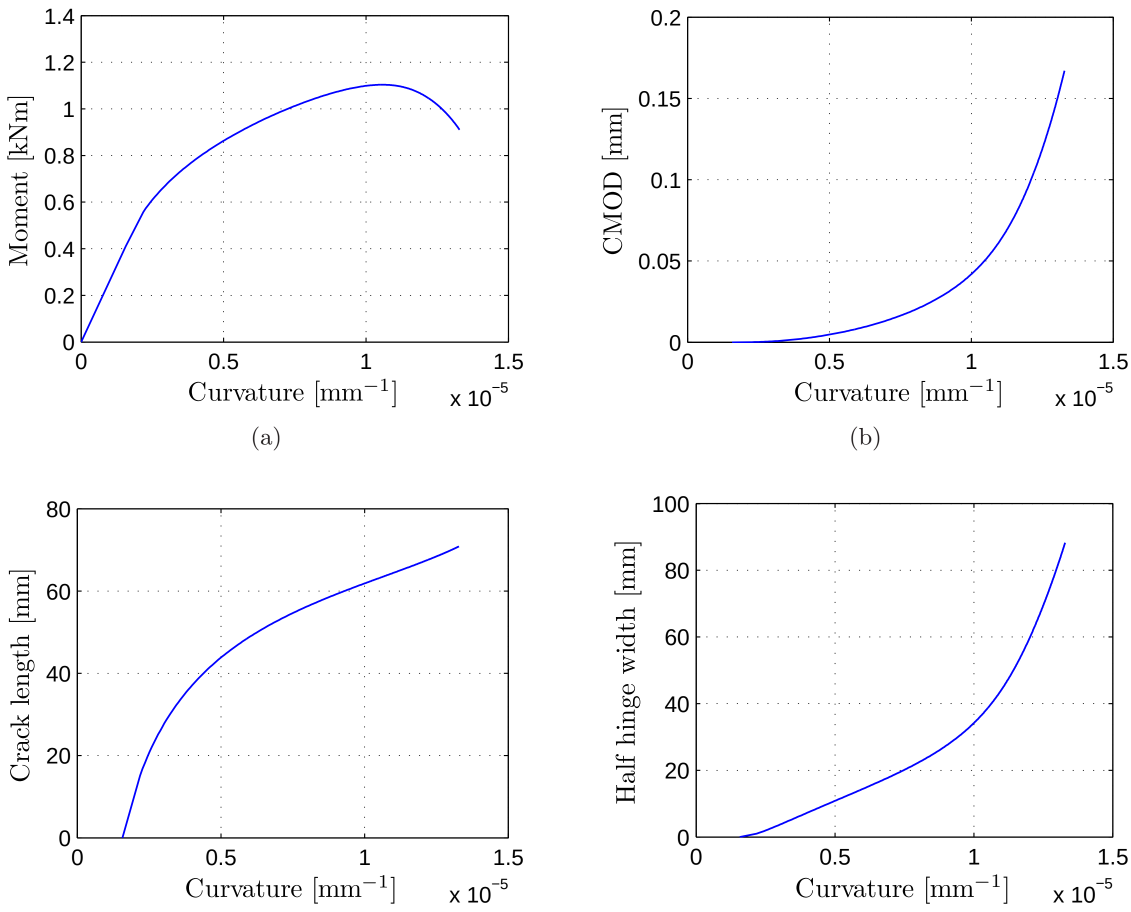

(a) (b) (c) (d)

Figure F.2: $\Phi = 0.0959$

F.3 Normal Mechanical Reinforcement Degree - High End

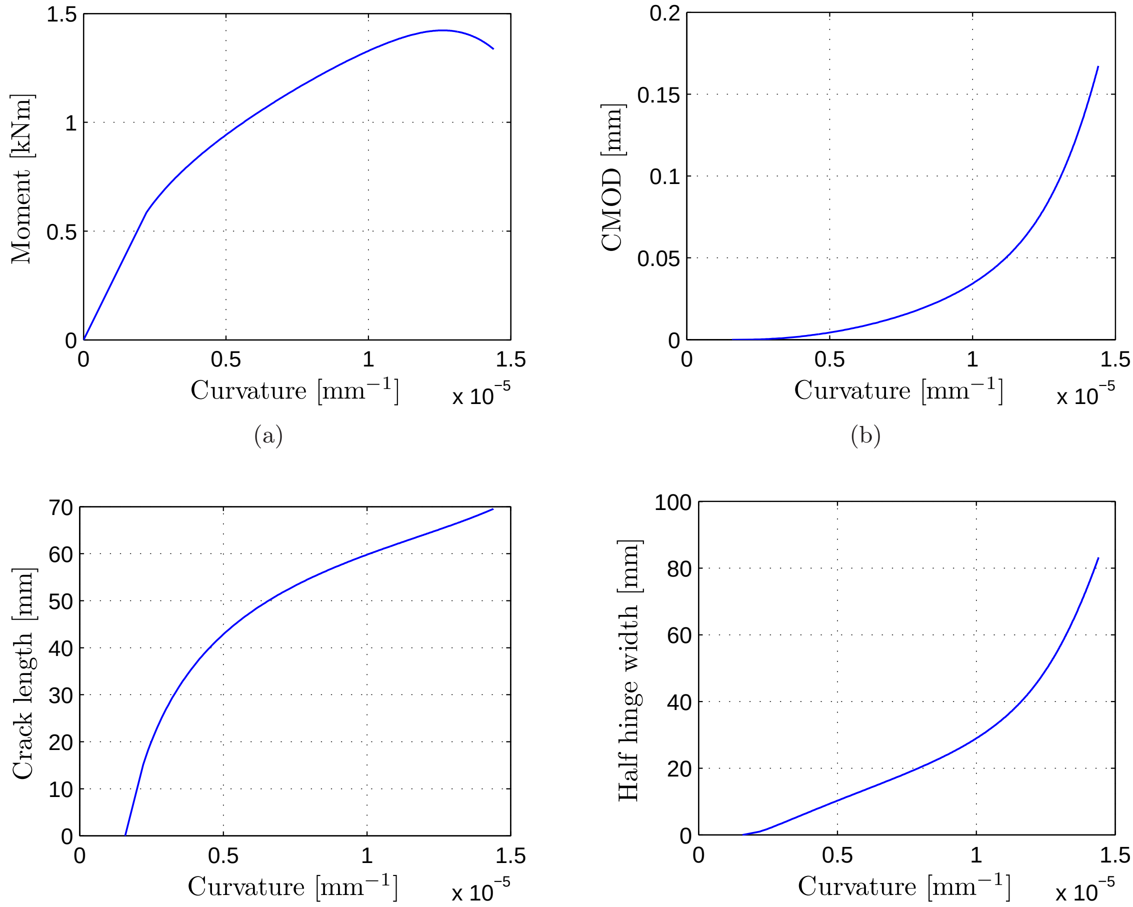

(a) (b) (c) (d)

Figure F.3: $\Phi = 0.1559$

F.4 Balanced Mechanical Reinforcement Degree

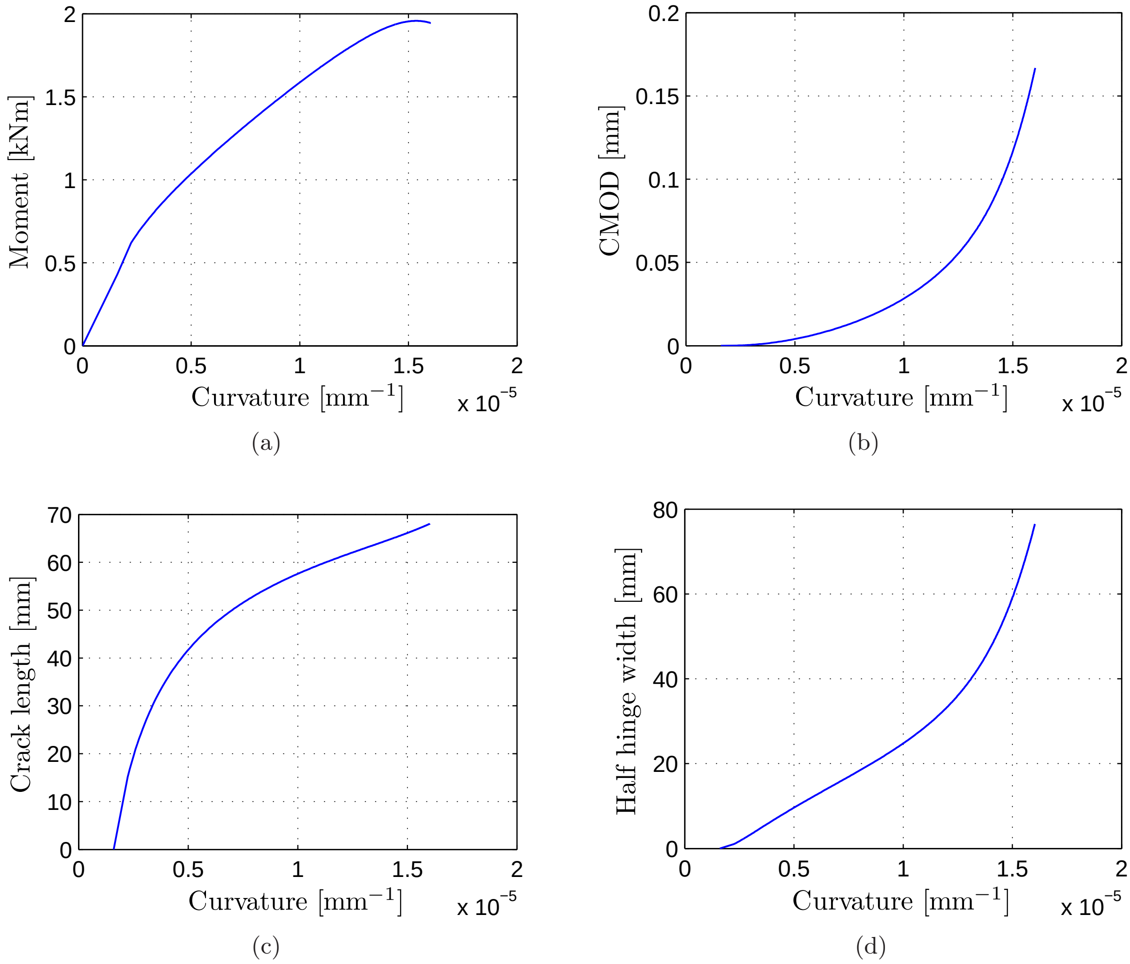

Figure F.4: $\Phi_{bal} = 0.2158$

Appendix G

FEM Convergence Analysis Plots

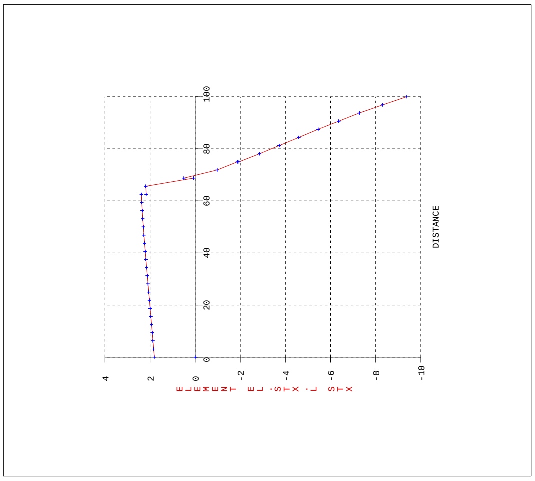

(a)

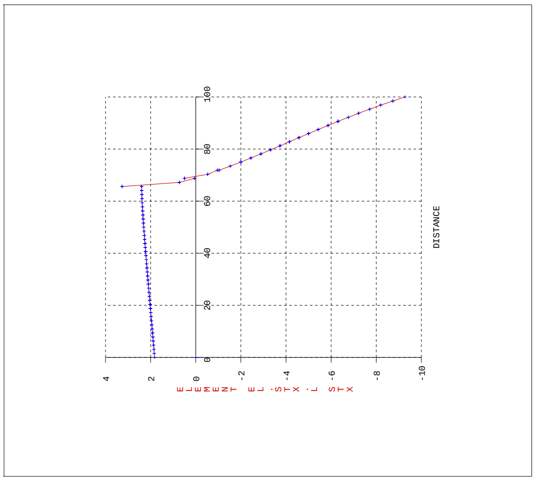

(b)

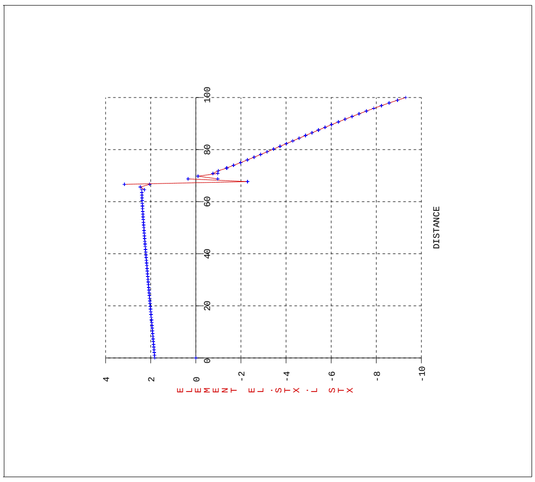

(c)

Figure G.1: Number of interface cohesive crack elements over the height (a) 16 elements (b) 32 elements (c) 48 elements

Appendix H

CD: Content

H.1 Report

H.2 Figures

H.3 MATLAB scripts

H.4 DIANA files

Appendix I

MatLab Scripts

I.1 Adaptive cracked hinge by Petersen

I.1.1 run.m

```
%%%%%%%%%%%%%%%%%%%%%%%%%%%%%%%%%%%%%%%%%%%%%%%%%%%%%%%%%%%%%%%%%%%%%%%%
% file: run.m
%
% Numerical adaptive hinge model by Petersen
% A linear softening relation is used
%
% Input file where the following must be defined:
% Geometry
% Material parameters
% Initial guess for the unknown variables
% Control parameters:
%   - Using a smaller minimum value for s will demand a smaller step size.
%   - Runs easy with smin=1 and step=0.25
%
% Version 1.0  -  13-01-2010  -  Nicky Viebæk Petersen
%%%%%%%%%%%%%%%%%%%%%%%%%%%%%%%%%%%%%%%%%%%%%%%%%%%%%%%%%%%%%%%%%%%%%%%%
%% Clearing sequence
clear all;
close all; clc;
%% Known parameters
% Geometry
parameters.h            =100;        % Hinge height
parameters.t            =100;        % Hinge thickness
% Material parameters
parameters.ft           =2.4;        % Tensile strength
parameters.Ec           =31000;      % Elastic modulus for concrete
parameters.nu           =0.15;       % Poissons ratio
Gf                      =0.1         % Fracture energy
parameters.w1           =2*Gf/parameters.ft;% w1=2*Gf/ft linear softening relation
%% Initial guess for the unknwon variables
parameters.X0_sig_2C    =-2.4;       % Stress at the top of the mid-section
                                     % Elastic value
parameters.X0_sig_2B    =-2.4;       % Stress at the top of the boundary
                                     % Elastic value
parameters.X0_sig_1B    =2.4;        % Stress at the boundary at crack tip level
                                     % Elastic value
parameters.X0_sig_yc    =0.1;        % Vertical stress at crack tip
                                     % Small value
parameters.X0_eps_mm    =7.74e-006;  % Mean strain at half hinge height
```

```
                                                    % 1/1000*eps_mt, elastik
parameters.X0_kappa      =1.55e-6;     % Curvature
                                                    % Elastic value
parameters.X0_c          =10;          % Crack length
                                                    % Initial guess must have som value
parameters.X0_w0         =0.000083;    % Crack mouth opening
                                                    % 1/1000*w1
parameters.X0_Mc         =4.0e+005;    % Moment
                                                    % Elastic value
%% Control parameters - s will raise
parameters.smin          =1;                  % Minimum half hinge width
parameters.step          =0.25;               % Step size
parameters.smax          =2*parameters.h      % Maximum possible half hinge width
parameters.Nc            =0;                  % Normal force, constant
%% Run petersen.m
[M kappa c w0 s sig_2C sig_2B sig_1B sig_yc eps_mm]=solve(parameters);
%% Create data file
INPUT = fopen('petersen.data','w');
fprintf( INPUT, '%g ', 0 );
fprintf( INPUT, '%g ', 0 );
fprintf( INPUT, '%g ', 0 );
fprintf( INPUT, '%g ', 0 );
fprintf( INPUT, '%g ', 0 );
fprintf( INPUT, '%g ', 0 );
fprintf( INPUT, '%g ', 0 );
fprintf( INPUT, '%g ', 0 );
fprintf( INPUT, '%g ', 0 );
fprintf( INPUT, '%g\n', 0 );
for i=1:length(kappa)
fprintf( INPUT, '%g ', M(i) );
fprintf( INPUT, '%g ', kappa(i) );
fprintf( INPUT, '%g ', c(i) );
fprintf( INPUT, '%g ', w0(i) );
fprintf( INPUT, '%g ', s(i) );
fprintf( INPUT, '%g ', sig_2C(i) );
fprintf( INPUT, '%g ', sig_2B(i) );
fprintf( INPUT, '%g ', sig_1B(i) );
fprintf( INPUT, '%g ', sig_yc(i) );
if i==length(kappa)
    fprintf( INPUT, '%g', eps_mm(i) );
else
    fprintf( INPUT, '%g\n', eps_mm(i) );
end
end
fclose(INPUT);
```

I.1.2 solve.m

```
function [M kappa c w0 sh sig_2C sig_2B sig_1B sig_yc eps_mm]=solve(parameters)
%%%%%%%%%%%%%%%%%%%%%%%%%%%%%%%%%%%%%%%%%%%%%%%%%%%%%%%%%%%%%%%%%%%%%%%%%%%%%%%
% file: solve.m
%
% Numerical adaptive hinge model by Petersen
% A linear softening relation is used
%
% The initial guess is multiplied with what "fsolve" get as initial guess
% after the equation file eq_s.m is called. This is done in order to easen
% the iteration proces scaling all the parameters to one doing the
% iterations.
%
% Version 1.0  -  13-01-2010  -  Nicky Viebæk Petersen
%%%%%%%%%%%%%%%%%%%%%%%%%%%%%%%%%%%%%%%%%%%%%%%%%%%%%%%%%%%%%%%%%%%%%%%%%%%%%%%
% Half hinge width
s=parameters.smin:parameters.step:parameters.smax;
```

```

X0=ones(9,1);
%%
% First value for all variables is the elastic solution.
sig_2C(1)            =-parameters.ft;
sig_2B(1)            =-parameters.ft;
sig_1B(1)            =parameters.ft;
sig_yc(1)            =0;
eps_mm(1)            =0;
M(1)                 =1/6*parameters.t*parameters.h^2*parameters.ft;
kappa(1)             =M(1)/(parameters.Ec*1/12*parameters.t*parameters.h^3);
c(1)                 =0;
w0(1)                =0;
sh(1)                =0;
% Solutions for all the desired hinge width's are found through a loop
% sequense
Me=1/6*parameters.t*parameters.h^2*parameters.ft;
for i =1:length(s)
    parameters.s=s(i);
    options=optimset('MaxFunEvals',10000,'MaxIter',1000);
    [X,FVAL,EXITFLAG]=fsolve(@(x) petersen(x,parameters),X0,options);
% All unknown parameters are taken out at each step.
    sig_2C(i+1)             =X(1)*parameters.X0_sig_2C;
    sig_2B(i+1)             =X(2)*parameters.X0_sig_2B;
    sig_1B(i+1)             =X(3)*parameters.X0_sig_1B;
    sig_yc(i+1)             =X(4)*parameters.X0_sig_yc;
    eps_mm(i+1)             =X(5)*parameters.X0_eps_mm;
    kappa(i+1)              =X(6)*parameters.X0_kappa;
    c(i+1)                  =X(7)*parameters.X0_c;
    w0(i+1)                 =X(8)*parameters.X0_w0;
    M(i+1)                  =X(9)*parameters.X0_Mc;
    sh(i+1)                 =parameters.s;
% The initial guess for the follwing calculation is the results of the
% current calculation.
    parameters.X0_sig_2C    =X(1)*parameters.X0_sig_2C;
    parameters.X0_sig_2B    =X(2)*parameters.X0_sig_2B;
    parameters.X0_sig_1B    =X(3)*parameters.X0_sig_1B;
    parameters.X0_sig_yc    =X(4)*parameters.X0_sig_yc;
    parameters.X0_eps_mm    =X(5)*parameters.X0_eps_mm;
    parameters.X0_kappa     =X(6)*parameters.X0_kappa;
    parameters.X0_c         =X(7)*parameters.X0_c;
    parameters.X0_w0        =X(8)*parameters.X0_w0;
    parameters.X0_Mc        =X(9)*parameters.X0_Mc;
% Break criterions
if parameters.X0_Mc<Me || parameters.X0_w0>=parameters.w1
    s_Stop=parameters.s
    break , end
end
```

I.1.3 petersen.m

```
function [F]=petersen(X,parameters)
%%%%%%%%%%%%%%%%%%%%%%%%%%%%%%%%%%%%%%%%%%%%%%%%%%%%%%%%%%%%%%%%%%%%%%%%%%%
% The function eq_s is a function which defines the equations and
% unknowns for a system of nonlinear equations.

% Control parameters are half hinge width (s) and normalforce (Nc)

% Version 1.0 - 13-01-2010 - Nicky Viebæk Petersen
%%%%%%%%%%%%%%%%%%%%%%%%%%%%%%%%%%%%%%%%%%%%%%%%%%%%%%%%%%%%%%%%%%%%%%%%%%%
%% Known parameters
s        =parameters.s;
Nc       =parameters.Nc;
ft       =parameters.ft;
```

```
Ec        =parameters.Ec;
h         =parameters.h;
w1        =parameters.w1;
t         =parameters.t;
nu        =parameters.nu;
%% Definition of the unknowns. In the first run the startguess is used
sig_2c    =X(1)*parameters.X0_sig_2C;
sig_2b    =X(2)*parameters.X0_sig_2B;
sig_1b    =X(3)*parameters.X0_sig_1B;
sig_yc    =X(4)*parameters.X0_sig_yc;
eps_mm    =X(5)*parameters.X0_eps_mm;
kappa     =X(6)*parameters.X0_kappa;
c         =X(7)*parameters.X0_c;
w0        =X(8)*parameters.X0_w0;
Mc        =X(9)*parameters.X0_Mc;
%% Locked parameters
sig_1c    =ft;                      % Stress at the crack tip
sig_0b    =ft;                      % Stress at the bottom at the boundary
%% Calculated parameters:
eps_mt    =eps_mm-1/2*h*kappa;      % Mean curvature at the top of the hinge
eps_mc    =eps_mm+(1/2*h-c)*kappa;  % Mean curvature at the middle height of the hinge
eps_mb    =eps_mm+1/2*h*kappa;      % Mean curvature at the bottom of the hinge
a         =h-c;                     % Geometric size
sig_0c    =ft-ft/w1*w0;             % Crack stress at the bottom
G         =Ec/(2*(1+nu));           % Shear stifness
% Upper beam
N_ct      =1/2*a*t*(sig_1c+sig_2c);
N_bt      =1/2*a*t*(sig_1b+sig_2b);
dN_t      =N_bt-N_ct;
% Upper beam - displacement at the boundary
I_t       =1/12*t*a^3;
u_t       =-1/24*s^2*(t*a^2*sig_1b-t*a^2*sig_2b+4*a*dN_t+t*sig_yc*s^2)/(Ec*I_t);
u_tau_t   =-1/8*t*sig_yc*s^2/(G*5/6*t*a);
u_ttot    =u_t+u_tau_t;
% Bottom beam
N_cb      =1/2*c*t*(sig_0c+sig_1c);
M_cb      =1/2*c*N_cb+t*(-1/2*sig_1c*c*2/3*c-1/2*sig_0c*c*1/3*c);
N_bb      =1/2*c*t*(sig_0b+sig_1b);
M_bb      =1/2*c*N_bb+t*(-1/2*sig_1b*c*2/3*c-1/2*sig_0b*c*1/3*c);
dN_b      =N_cb-N_bb;
% Moment that keep the beams together
M_v       =1/8*t*sig_yc*s^2;
% Bottom beam - displacement at the boundary
I_b       =1/12*t*c^3;
u_b       =1/24*s^2*(-t*c^2*sig_0b+t*c^2*sig_1b-4*c*dN_b+t*sig_yc*s^2)/(Ec*I_b);
u_tau_b   =1/8*t*sig_yc*s^2/(G*5/6*t*c);
u_r       =-w0*s/c;
u_btot    =u_b+u_tau_b+u_r;
% Horizontal displacement of the bottom beam
A0        =5/6*t*s;
I_vb      =1/12*t*s^3;
w01       =-1/120*1/(G*A0*Ec*I_vb)*(t*c^2*(4*c^2*G*A0*sig_1c+20*sig_1c*Ec*I_vb ...
    +11*c^2*G*A0*sig_0c-20*sig_1b*Ec*I_vb+40*Ec*I_vb*sig_0c-40*Ec*I_vb*sig_0b ...
    -11*c^2*G*A0*sig_0b-4*c^2*G*A0*sig_1b));
w02       =c*(-u_btot)/s;
%% Equations to solve
% Strain at the top of the hinge
F(1)      =1/(2*Ec)*(sig_2c+sig_2b)-eps_mt;
% Strain at crack tip level
F(2)      =1/(2*Ec)*(sig_1c+sig_1b)-eps_mc;
% Deformation at the bottom of the hinge
F(3)      =w0+1/(2*Ec)*(sig_0c+sig_0b)*s-eps_mb*s;
% Normal force equilibrium at the mid-section
F(4)      =1/2*t*(sig_2c*a+sig_1c*h+sig_0c*c)-Nc;
```

```
% Moment equilibrium at the mid-section
F(5)      =1/2*h*Nc+1/2*t*((-sig_2c)*a*(h-1/3*a)-sig_1c*a*(h-2/3*a)...
    -sig_1c*c*2/3*c-sig_0c*c*1/3*c)-Mc;
% Equilibrium of the bottom beam
F(6)      =M_cb+M_v-M_bb-1/2*c*dN_b;
% Deformation equilibrium of the bottom beam (horizontal)
F(7)      =w01+w02-(w0+eps_mb*s)/2;
% Equilibrium between the normal force differences
F(8)      =dN_b-dN_t-Nc;
% Equilibrium between the beams, vertical displacement
F(9)      =u_b+u_tau_b+u_r-u_t-u_tau_t;
```

I.2 Reinforced adaptive cracked hinge by Petersen

I.2.1 runbar.m

```
%%%%%%%%%%%%%%%%%%%%%%%%%%%%%%%%%%%%%%%%%%%%%%%%%%%%%%%%%%%%%%%%%%%%%%%%%%%%%%%%
% file: run.m
%
% Numerical adaptive hinge model by Petersen
% A linear softening relation is used
%
% Input file where the following must be defined:
% Geometry
% Material parameters
% Initial guess for the unknown variables
% Control parameters:
%   - Using a smaller minimum value for s will demand a smaller step size.
%   - Runs easy with smin=1 and step=0.25
%
% Version 1.0  -  13-01-2010  -  Nicky Viebæk Petersen
%%%%%%%%%%%%%%%%%%%%%%%%%%%%%%%%%%%%%%%%%%%%%%%%%%%%%%%%%%%%%%%%%%%%%%%%%%%%%%%%
%% Clearing sequence
clear all;
close all; clc;
%% Known parameters
% Geometry
parameters.h            =100;           % Hinge height
parameters.t            =100;           % Hinge thickness
% Material parameters
parameters.ft           =2.4;           % Tensile strength
parameters.Ec           =31000;         % Elastic modulus for concrete
parameters.nu           =0.15;          % Poissons ratio
Gf                      =0.1;           % Fracture energy
parameters.w1           =2*Gf/parameters.ft;% w1=2*Gf/ft linear softening relation
% Parameters for reinforcement bar
parameters.d            =25;
parameters.Es           =210000;
% Calculate diameter of reinforcement bar
parameters.fyk          =550;
parameters.fck          =30;
[D Phi]                 =diameter(parameters);
parameters.D            =D(4);
% calculate area
parameters.As           = pi*(parameters.D/2)^2;
%%
alpha                   = parameters.Es/parameters.Ec;
d_ar                    = parameters.h-parameters.d;
xp                      = 1/2*(2*parameters.Es*parameters.As*d_ar...
    +parameters.t*parameters.Ec*parameters.h^2)...
    /(parameters.Es*parameters.As+parameters.t*parameters.Ec*parameters.h);
M_E=-1/6*parameters.ft/parameters.Ec*(6*parameters.Es*parameters.As...
    *(parameters.h-d_ar)*d_ar-6*parameters.Es*parameters.As...
    *(parameters.h-d_ar)*xp...
    +parameters.t*parameters.Ec*parameters.h^3-3*parameters.t...
    *parameters.Ec*parameters.h^2*xp)/(parameters.h-xp);
I_tr=1/12*parameters.t*parameters.h^3+(parameters.h/2-xp)^2*parameters.t*parameters.h...
    +(alpha-1)*parameters.As*(d_ar-xp)^2;
kappa_E=M_E/(parameters.Ec*I_tr);
parameters.M_E=M_E;
parameters.kappa_E=kappa_E;
%% Initial guess for the unknwon variables
parameters.X0_sig_2C    =-2.4;          % Stress at the top of the mid-section Elastic value
```

```
parameters.X0_sig_2B      =-2.4;                  % Stress at the top of the boundary Elastic value
parameters.X0_sig_1B      =2.4;                   % Stress at the boundary at crack tip level Elastic value
parameters.X0_sig_yc      =0.1;                   % Vertical stress at crack tip Small value
parameters.X0_eps_mm      =7.74e-006;             % Mean strain at half hinge height 1/1000*eps_mt, elastik
parameters.X0_kappa       =1.55e-6;               % Curvature Elastic value
parameters.X0_c           =10;                    % Crack length Initial guess must have som value
parameters.X0_w0          =0.000083;              % Crack mouth opening 1/1000*w1
parameters.X0_Mc          =4.0e+005;              % Moment Elastic value
%% Control parameters - s will raise
parameters.smin           =1;                     % Minimum half hinge width
parameters.step           =0.25;                  % Step size
parameters.smax           =2*parameters.h         % Maximum possible half hinge width
parameters.Nc             =0;                     % Normal force, constant


%% Run petersen.m
[M kappa c w0 s sig_2C sig_2B sig_1B sig_yc eps_mm]=solvebar(parameters);
%% Calculate elastic solution of a reinforced cracked cross section
M_ar=0:(max(M)/1000):max(M);
% Calculate kappa
[kappa_ar x]=alpharho(M_ar,parameters);
%% Create data file
INPUT = fopen('petersenbar4.data','w');
fprintf( INPUT, '%g ', 0 );
fprintf( INPUT, '%g ', 0 );
fprintf( INPUT, '%g ', 0 );
fprintf( INPUT, '%g ', 0 );
fprintf( INPUT, '%g ', 0 );
fprintf( INPUT, '%g ', 0 );
fprintf( INPUT, '%g ', 0 );
fprintf( INPUT, '%g ', 0 );
fprintf( INPUT, '%g ', 0 );
fprintf( INPUT, '%g\n', 0 );
for i=1:length(kappa)
fprintf( INPUT, '%g ', M(i) );
fprintf( INPUT, '%g ', kappa(i) );
fprintf( INPUT, '%g ', c(i) );
fprintf( INPUT, '%g ', w0(i) );
fprintf( INPUT, '%g ', s(i) );
fprintf( INPUT, '%g ', sig_2C(i) );
fprintf( INPUT, '%g ', sig_2B(i) );
fprintf( INPUT, '%g ', sig_1B(i) );
fprintf( INPUT, '%g ', sig_yc(i) );
if i==length(kappa)
    fprintf( INPUT, '%g', eps_mm(i) );
else
    fprintf( INPUT, '%g\n', eps_mm(i) );
end
end
fclose(INPUT);

INPUT = fopen('elasticbar4.data','w');
for i=1:length(kappa_ar)
fprintf( INPUT, '%g ', M_ar(i) );
if i==length(kappa_ar)
    fprintf( INPUT, '%g', kappa_ar(i) );
```

```
else
    fprintf( INPUT, '%g\n', kappa_ar(i) );
end
end
fclose(INPUT);
```

I.2.2 solvebar.m

```
function [M kappa c w0 sh sig_2C sig_2B sig_1B sig_yc eps_mm]=solvebar(parameters)
%%%%%%%%%%%%%%%%%%%%%%%%%%%%%%%%%%%%%%%%%%%%%%%%%%%%%%%%%%%%%%%%%%%%%%%%%%%%%%%
% file: solve.m
%
% Numerical adaptive hinge model by Petersen
% A linear softening relation is used
%
% The initial guess is multiplied with what "fsolve" get as initial guess
% after the equation file eq_s.m is called. This is done in order to easen
% the iteration proces scaling all the parameters to one doing the
% iterations.
%
% Version 1.0 - 13-01-2010 - Nicky Viebæk Petersen
%%%%%%%%%%%%%%%%%%%%%%%%%%%%%%%%%%%%%%%%%%%%%%%%%%%%%%%%%%%%%%%%%%%%%%%%%%%%%%%
% Half hinge width
s=parameters.smin:parameters.step:parameters.smax;

X0=ones(9,1);
%%
% First value for all variables is the elastic solution.
 sig_2C(1)          =-parameters.ft;
 sig_2B(1)          =-parameters.ft;
 sig_1B(1)          =parameters.ft;
 sig_yc(1)          =0;
 eps_mm(1)          =0;
 M(1)               =parameters.M_E;%1/6*parameters.t*parameters.h^2*parameters.ft
     ;
 kappa(1)           =parameters.kappa_E;%M(1)/(parameters.Ec*1/12*parameters.t*
     parameters.h^3);
 c(1)               =0;
 w0(1)              =0;
 sh(1)              =0;
% Solutions for all the desired hinge width's are found through a loop
% sequense
for i =1:length(s)
    parameters.s=s(i);
    %options=optimset('MaxFunEvals',10000,'MaxIter',1000);
    %[X,FVAL,EXITFLAG]=fsolve(@(x) petersen(x,parameters),X0,options);
    [X]=fsolve(@(x) petersenbar(x,parameters),X0);
% All unknown parameters are taken out at each step.
    sig_2C(i+1)          =X(1)*parameters.X0_sig_2C;
    sig_2B(i+1)          =X(2)*parameters.X0_sig_2B;
    sig_1B(i+1)          =X(3)*parameters.X0_sig_1B;
    sig_yc(i+1)          =X(4)*parameters.X0_sig_yc;
    eps_mm(i+1)          =X(5)*parameters.X0_eps_mm;
    kappa(i+1)           =X(6)*parameters.X0_kappa;
    c(i+1)               =X(7)*parameters.X0_c;
    w0(i+1)              =X(8)*parameters.X0_w0;
    M(i+1)               =X(9)*parameters.X0_Mc;
    sh(i+1)              =parameters.s;

% The initial guess for the follwing calculation is the results of the
% current calculation.
    parameters.X0_sig_2C     =X(1)*parameters.X0_sig_2C;
    parameters.X0_sig_2B     =X(2)*parameters.X0_sig_2B;
    parameters.X0_sig_1B     =X(3)*parameters.X0_sig_1B;
```

```
    parameters.X0_sig_yc     =X(4)*parameters.X0_sig_yc;
    parameters.X0_eps_mm     =X(5)*parameters.X0_eps_mm;
    parameters.X0_kappa      =X(6)*parameters.X0_kappa;
    parameters.X0_c          =X(7)*parameters.X0_c;
    parameters.X0_w0         =X(8)*parameters.X0_w0;
    parameters.X0_Mc         =X(9)*parameters.X0_Mc;
% Break criterions
if parameters.X0_w0>=parameters.w1 %|| parameters.X0_Mc<Me
    s_Stop=parameters.s
    break , end
end
```

I.2.3 petersenbar.m

```
function [F]=petersenbar(X,parameters)
%%%%%%%%%%%%%%%%%%%%%%%%%%%%%%%%%%%%%%%%%%%%%%%%%%%%%%%%%%%%%%%%%%%%%%%%%%%%
% The function eq_s is a function which defines the equations and
% unknowns for a system of nonlinear equations.

% Control parameters are half hinge width (s) and normalforce (Nc)

% Version 1.0   -   13-01-2010   -   Nicky Viebæk Petersen
%%%%%%%%%%%%%%%%%%%%%%%%%%%%%%%%%%%%%%%%%%%%%%%%%%%%%%%%%%%%%%%%%%%%%%%%%%%%
%% Known parameters
s       =parameters.s;
Nc      =parameters.Nc;
ft      =parameters.ft;
Ec      =parameters.Ec;
h       =parameters.h;
w1      =parameters.w1;
t       =parameters.t;
nu      =parameters.nu;
d       =parameters.d;
Es      =parameters.Es;
D       =parameters.D;
%% Definition of the unknowns. In the first run the startguess is used
sig_2c  =X(1)*parameters.X0_sig_2C;
sig_2b  =X(2)*parameters.X0_sig_2B;
sig_1b  =X(3)*parameters.X0_sig_1B;
sig_yc  =X(4)*parameters.X0_sig_yc;
eps_mm  =X(5)*parameters.X0_eps_mm;
kappa   =X(6)*parameters.X0_kappa;
c       =X(7)*parameters.X0_c;
w0      =X(8)*parameters.X0_w0;
Mc      =X(9)*parameters.X0_Mc;
%% Locked parameters
sig_1c  =ft;                        % Stress at the crack tip
sig_0b  =ft;                        % Stress at the bottom at the boundary
%% Calculated parameters:
eps_mt  =eps_mm-1/2*h*kappa;        % Mean curvature at the top of the hinge
eps_mc  =eps_mm+(1/2*h-c)*kappa;    % Mean curvature at the middle height of the
    hinge
eps_mb  =eps_mm+1/2*h*kappa;        % Mean curvature at the bottom of the hinge
a       =h-c;                       % Geometric size
sig_0c  =ft-ft/w1*w0;               % Crack stress at the bottom
G       =Ec/(2*(1+nu));             % Shear stifness
% Upper beam
N_ct    =1/2*a*t*(sig_1c+sig_2c);
N_bt    =1/2*a*t*(sig_1b+sig_2b);
dN_t    =N_bt-N_ct;
% Upper beam - displacement at the boundary
I_t     =1/12*t*a^3;
u_t     =-1/24*s^2*(t*a^2*sig_1b-t*a^2*sig_2b+4*a*dN_t+t*sig_yc*s^2)/(Ec*I_t);
u_tau_t =-1/8*t*sig_yc*s^2/(G*5/6*t*a);
```

```
u_ttot   =u_t+u_tau_t;
% Bottom beam
N_cb     =1/2*c*t*(sig_0c+sig_1c);
M_cb     =1/2*c*N_cb+t*(-1/2*sig_1c*c*2/3*c-1/2*sig_0c*c*1/3*c);
N_bb     =1/2*c*t*(sig_0b+sig_1b);
M_bb     =1/2*c*N_bb+t*(-1/2*sig_1b*c*2/3*c-1/2*sig_0b*c*1/3*c);
dN_b     =N_cb-N_bb;
% Moment that keep the beams together
M_v      =1/8*t*sig_yc*s^2;
% Bottom beam - displacement at the boundary
I_b      =1/12*t*c^3;
u_b      =1/24*s^2*(-t*c^2*sig_0b+t*c^2*sig_1b-4*c*dN_b+t*sig_yc*s^2)/(Ec*I_b);
u_tau_b  =1/8*t*sig_yc*s^2/(G*5/6*t*c);
u_r      =-w0*s/c;
u_btot   =u_b+u_tau_b+u_r;
% Horizontal displacement of the bottom beam
A0       =5/6*t*s;
I_vb     =1/12*t*s^3;
w01      =-1/120*1/(G*A0*Ec*I_vb)*(t*c^2*(4*c^2*G*A0*sig_1c+20*sig_1c*Ec*I_vb...
    +11*c^2*G*A0*sig_0c-20*sig_1b*Ec*I_vb+40*Ec*I_vb*sig_0c-40*Ec*I_vb*sig_0b...
    -11*c^2*G*A0*sig_0b-4*c^2*G*A0*sig_1b));
w02      =c*(-u_btot)/s;
% Reinforcement bar
eps_md   =eps_mm+(1/2*h-d)*kappa;
Fbar     =eps_md*Es*pi*(D/2)^2;
%% Equations to solve
% Strain at the top of the hinge
F(1)     =1/(2*Ec)*(sig_2c+sig_2b)-eps_mt;
% Strain at crack tip level
F(2)     =1/(2*Ec)*(sig_1c+sig_1b)-eps_mc;
% Deformation at the bottom of the hinge
F(3)     =w0+1/(2*Ec)*(sig_0c+sig_0b)*s-eps_mb*s;
% Normal force equilibrium at the mid-section
F(4)     =Fbar+1/2*t*(sig_2c*a+sig_1c*h+sig_0c*c)-Nc;
% Moment equilibrium at the mid-section
F(5)     =d*Fbar+1/2*h*Nc+1/2*t*((-sig_2c)*a*(h-1/3*a)-sig_1c*a*(h-2/3*a)-sig_1c*c
    *2/3*c-sig_0c*c*1/3*c)-Mc;
% Equilibrium of the bottom beam
F(6)     =M_cb+M_v-M_bb-1/2*c*dN_b;
% Deformation equilibrium of the bottom beam (horizontal)
F(7)     =w01+w02-(w0+eps_mb*s)/2;
% Equilibrium between the normal force differences
F(8)     =dN_b-dN_t-Nc;
% Equilibrium between the beams, vertical displacement
F(9)     =u_b+u_tau_b+u_r-u_t-u_tau_t;
```

I.3 Analytical solution for the hinge model by Olesen

I.3.1 runolesen.m

```
%%%%%%%%%%%%%%%%%%%%%%%%%%%%%%%%%%%%%%%%%%%%%%%%%%%%%%%%%%%%%%%%%%%%%%%%
% file: runolesen.m
% Hinge model by Olesen
% Use of linear relation for crack opening
%
% Paramter difinition and creation of output file
%
% Version 1.0 - 13-01-2010 - Nicky Viebæk Petersen
%%%%%%%%%%%%%%%%%%%%%%%%%%%%%%%%%%%%%%%%%%%%%%%%%%%%%%%%%%%%%%%%%%%%%%%
%% Clearing sequence
clear all;
% close all; clc;
%% parameters
olpara.h=100;
olpara.s=0.25*olpara.h;
olpara.t=100;
olpara.L=200;
olpara.ft=2.4;
olpara.w1=2*0.0833;
olpara.E=31000;
olpara.thetamax=100;
%% Call function
[M w_cmod kappa d]=olesen(olpara);
%% data files
INPUT = fopen('olesen.data','w');
fprintf( INPUT, '%g ', 0 );
fprintf( INPUT, '%g ', 0 );
fprintf( INPUT, '%g ', 0 );
fprintf( INPUT, '%g\n', 0 );
for i=1:length(kappa)
fprintf( INPUT, '%g ', M(i) );
fprintf( INPUT, '%g ', kappa(i) );
fprintf( INPUT, '%g ', d(i) );
fprintf( INPUT, '%g\n', w_cmod(i) );
end
fclose(INPUT);
```

I.3.2 olesen.m

```
function [M w_cmod kappa d]=olesen(olpara)
%%%%%%%%%%%%%%%%%%%%%%%%%%%%%%%%%%%%%%%%%%%%%%%%%%%%%%%%%%%%%%%%%%%%%%%%
% file: Olesen.m
% Hinge model by Olesen
% Use of linear relation for crack opening
%
% Version 1.0 - 13-01-2010 - Nicky Viebæk Petersen
%%%%%%%%%%%%%%%%%%%%%%%%%%%%%%%%%%%%%%%%%%%%%%%%%%%%%%%%%%%%%%%%%%%%%%%
%% Imput parameters for hinge-geometry
h=olpara.h;              % mm
s=2*olpara.s;            % mm
t=olpara.t;              % mm
L=olpara.L;              % mm
%% Imput parameters for concrete
ft=olpara.ft;            % MPa
w1=olpara.w1;            % mm
E=olpara.E;              % MPa
%% Initial parameters for Olesen-model
% Defining Theta
Theta=1:0.1:olpara.thetamax;
```

```
% Dimensionless parameters
beta=ft*(1/w1)*s/E;
%% Calculation procedure
Me=1/6*t*h^2*ft;
for i =1:length(Theta)
      alpha(i)=1-beta-sqrt((1-beta)*(1/Theta(i)-beta));
      mu(i)=4*(1-3*alpha(i)+3*alpha(i)^2-(alpha(i)^3/(1-beta)))...
            *Theta(i)-3+6*alpha(i);
      w_cmod(i)=s*ft/E*2*alpha(i)*Theta(i)/(1-beta);
      M=mu(i)*ft*h^2*t/6;
      Theta_out(i)=Theta(i);
      if M<Me;
            break, end
end
M=mu.*ft*h^2*t/6;
d=alpha.*h;
phi=s*ft*Theta_out/(h*E);
kappa=2*phi/s;
```

Appendix J

DIANA Files

J.1 Nonlin45.dcf

```
*FILOS
 INITIA
*INPUT
*NONLIN
BEGIN MODEL
 AUTOTY
 ASSEMB TOLERA=1.E-7
END MODEL
 BEGIN EXECUT
   BEGIN LOAD
     BEGIN STEPS
       BEGIN EXPLIC
         BEGIN ARCLEN
         UPDATE
           BEGIN CMOD
             BEGIN SET
               SIDE1  NODES 2730 /
               SIDE2  NODES 838 /
             END SET
           END CMOD
         END ARCLEN
         SIZES 0.2(5) 0.015(50) 0.005 (30)
       END EXPLIC
     END STEPS
   END LOAD
   BEGIN ITERAT
     MAXITE=5
     METHOD NEWTON REGULA
     BEGIN CONVER
       SIMULT
        FORCE NEWREF TERMIN TOLCON=1.E-2 TOLABT=1.E+4
        DISPLA NEWREF TERMIN TOLCON=1.E-2 TOLABT=1.E+4
     END CONVER
   END ITERAT
   BEGIN LOGGIN
    REPORT FULL ITERAT
    CRACKI
   END LOGGIN
  BEGIN OUTPUT FEMVIE
    DISPLA TOTAL TRANSL
    STRESS TOTAL CAUCHY
    STRESS TOTAL TRACTI
```

```
      FORCE REACTI TRANSL
      STATUS CRACK INTPNT
      DISPLA TOTAL ROTATI GLOBAL
    END OUTPUT
    BEGIN OUTPUT TABULA FILE "cmod.out"
       SELECT  NODES 838 /
       TEXT CMOD/2
       DISPLA  TOTAL  TRANSL  GLOBAL
    END OUTPUT
    BEGIN OUTPUT
       TABULA
       FILE "Stress_profile"
       SELECT  ELEMEN CRK_SRFC /
       TEXT "Stress"
       STRESS TOTAL TRACTI GLOBAL X COORDI intpnt
    END OUTPUT
     TEXT "elastic"
    BEGIN OUTPUT
       TABULA
       FILE "Stress_profile_boundary"
       SELECT  ELEMEN 3-50 /
       TEXT "Stress"
       STRESS TOTAL CAUCHY GLOBAL XX COORDI nodes
    END OUTPUT
    BEGIN OUTPUT
       TABULA
       FILE "Crack_status"
       SELECT  ELEMEN CRK_SRFC /
       TEXT "Crack status"
       STATUS CRACK INTPNT
    END OUTPUT
    BEGIN OUTPUT
       TABULA
       FILE "Beam_Rotation"
       SELECT  ELEMEN 1 /
       TEXT "Rotation"
           DISPLA TOTAL ROTATI GLOBAL
    END OUTPUT
   END EXECUT
  BEGIN EXECUT
     BEGIN LOAD
       BEGIN STEPS
         BEGIN ITERAT
          INISIZ=0.0001
          NITERA=2
          MAXSIZ=0.5
          MINSIZ=0.0000001
          NSTEPS=100
          GAMMA=0.5
          SIGN
           BEGIN ARCLEN
           UPDATE
             BEGIN CMOD
               BEGIN SET
                 BEGIN SIDE1
                   NODES 2730
                   TYPE TRANSL
                   DIRECT 1
                   ALPHA 1.0
                 END SIDE1
                 BEGIN SIDE2
                   NODES 838
                   TYPE TRANSL
                   DIRECT 1
```

```
                    ALPHA  -1.0
                  END SIDE2
                END SET
              END CMOD
            END ARCLEN
          END ITERAT
        END STEPS
      END LOAD
      BEGIN ITERAT
        MAXITE=15
        METHOD NEWTON REGULA
        BEGIN CONVER
          SIMULT
           FORCE NEWREF TERMIN TOLCON=1.E-2 TOLABT=1.E+4
           DISPLA NEWREF TERMIN TOLCON=1.E-2 TOLABT=1.E+4
        END CONVER
      END ITERAT
      BEGIN LOGGIN
       REPORT FULL ITERAT
       CRACKI
      END LOGGIN
BEGIN OUTPUT FEMVIE
 DISPLA TOTAL TRANSL
 STRESS TOTAL CAUCHY
 STRESS TOTAL TRACTI
 FORCE REACTI TRANSL
 STATUS CRACK INTPNT
     DISPLA TOTAL ROTATI GLOBAL
END OUTPUT
BEGIN OUTPUT
 TABULA
 FILE "cmod.out"
 SELECT  NODES 838 /
 TEXT CMOD/2
 DISPLA  TOTAL  TRANSL  GLOBAL
 END OUTPUT
  BEGIN OUTPUT
      TABULA
      FILE "Stress_profile"
      SELECT  ELEMEN CRK_SRFC /
      TEXT "Stress"
      STRESS TOTAL TRACTI GLOBAL X COORDI intpnt
  END OUTPUT
   TEXT "peak"
  BEGIN OUTPUT
      TABULA
      FILE "Stress_profile_boundary"
      SELECT  ELEMEN 3-50 /
      TEXT "Stress"
      STRESS TOTAL CAUCHY GLOBAL XX COORDI nodes
  END OUTPUT
  BEGIN OUTPUT
      TABULA
      FILE "Crack_status"
      SELECT  ELEMEN CRK_SRFC /
      TEXT "Crack status"
      STATUS CRACK INTPNT
  END OUTPUT
  BEGIN OUTPUT
      TABULA
      FILE "Beam_Rotation"
      SELECT  ELEMEN 1 /
      TEXT "Rotation"
     DISPLA TOTAL ROTATI GLOBAL
```

```
    END OUTPUT
  END EXECUT
*END
```

J.2 s45.fga

```
FEMGEN m9_45
PROPERTY FE-PROG DIANA STRUCT_2D
YES
UTILITY SETUP UNITS LENGTH MILLIMETER
UTILITY SETUP UNITS MASS KILOGRAM
UTILITY SETUP UNITS FORCE NEWTON
UTILITY SETUP UNITS TIME SECOND
UTILITY SETUP UNITS TEMP KELVIN
UTILITY SETUP UNDO ON
UTILITY SETUP BINSET OFF
MESHING OPTIONS CHECK STRUCTURED OFF

GEOMETRY POINT P1 0.0 0.0
GEOMETRY POINT P2 -45 0.0
GEOMETRY POINT P3 -45 100
GEOMETRY POINT P4 0.0 100
GEOMETRY POINT P5 -55 0.0
GEOMETRY POINT P6 -55 100
GEOMETRY POINT P7 10 50

GEOMETRY SURFACE 4POINTS S1 P1 P4 P3 P2
GEOMETRY SPLIT L1 P0 0.5
GEOMETRY LINE STRAIGHT P0 P7

CONSTRUCT SET OPEN SPEC
CONSTRUCT SET APPEND SURFACES ALL
CONSTRUCT SET CLOSE SPEC

GEOMETRY SURFACE 4POINTS CRACK P2 P3 P6 P5

CONSTRUCT SET OPEN CRK_SRFC
CONSTRUCT SET APPEND SURFACES CRACK
CONSTRUCT SET CLOSE CRK_SRFC

MESHING TYPES SPEC QU8 CQ16M
MESHING TYPES CRACK IL33 CL12I BASE L1
MESHING TYPES L7 BE3 CL9BE
MESHING DIVISION LINE L5 48
MESHING DIVISION LINE L6 48
MESHING DIVISION LINE L3 96
MESHING DIVISION LINE L4 36
MESHING DIVISION LINE L2 36
MESHING DIVISION SURFACE CRACK 96 1
MESH GENERATE
VIEW MESH

PROPERTY BOUNDARY CONSTRAINT L9 X
PROPERTY BOUNDARY CONSTRAINT P0 Y

PROPERTY LOADS FORCE P4 -4000 X
PROPERTY LOADS FORCE P1 4000 X

EYE FRAME


 property material macrack elastic interfac 3.1e+011 3.1e+011
 property material macrack statnonl interfac cracking discrete=
 linear secant cshear 2.4 0.1 3.1e+011
```

```
property material maconcre elastic isotrop 31000 0.15
property physical phcrack geometry interfac line membra 100
property physical phconcre geometry planstrs thregulr 100
PROPERTY PHYSICAL PHBEAM GEOMETRY BEAM CLASSIII PREDEFIN RECTAN 100 100

PROPERTY ATTACH SPEC MACONCRE PHCONCRE
PROPERTY ATTACH CRACK MACRACK PHCRACK
PROPERTY ATTACH L7 MACONCRE PHBEAM

GEOMETRY MOVE SPEC TRANSLATE P3 P6
YES
MESH GENERATE
EYE FRAME
VIEW MESH
LABEL MESH CONSTRNT
LABEL MESH LOADS
SAVE
YES

UTILITY WRITE DIANA
YES

FILE CLOSE

ANALYSE m9_45
```

Appendix K

Vertical Displacement of Beam Part A and Part B

On the following pages handwritten derivation of the vertical displacement of beam part A and B are found, derived by the principle of virtual work.

Deflection of the upper beam due to the shear force

$$V_{OT} = -\int f(x)\,dx \qquad \text{where } f(x) = -\frac{3}{2}\frac{\sigma_{yc}}{s^2}x^2 + \frac{3\,\sigma_{yc}}{s}x - \sigma_{yc}$$

$$= -\int t\left(-\frac{3}{2}\frac{\sigma_{yc}}{s^2}x^2 + \frac{3\sigma_{yc}}{s}x - \sigma_{yc}\right)dx$$

$$= t\left(\frac{3}{6}\frac{\sigma_{yc}}{s^2}x^3 - \frac{3}{2}\frac{\sigma_{yc}}{s}x^2 + \sigma_{yc}\,x\right) + C_1$$

The constant C_1 is found from the boundary condition

that $V(s) = 0$

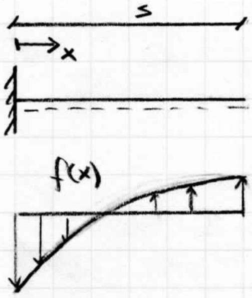

$$V_{OT}(s) = t\left(\frac{1}{2}\frac{\sigma_{yc}}{s^2}s^3 - \frac{3}{2}\frac{\sigma_{yc}}{s}s^2 + \sigma_{yc}\,s\right) + C_1 = 0$$

$$C_1 = t\left(\frac{3}{2}\sigma_{yc}\cdot s - \frac{1}{2}\sigma_{yc}\cdot s - \sigma_{yc}\cdot s\right)$$

$$= t\cdot\sigma_{yc}\cdot s\left(\frac{3}{2} - \frac{1}{2} - 1\right) \Rightarrow \underline{C_1 = 0}$$

Which means that

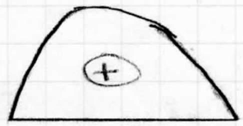

$$V_{OT} = t\left(\frac{1}{2}\frac{\sigma_{yc}}{s^2}x^3 - \frac{3}{2}\frac{\sigma_{yc}}{s}x^2 + \sigma_{yc}\,x\right)$$

Using the principle of virtual work to find the vertical displacement, a unit force is put on the beam at the point where the displacement is wanted

$$u_{v,t} = \int_0^s \frac{V_1 V_{OT}}{G A_{o,t}}\,dx \qquad V_1(x) = -1$$

$$= \frac{t}{G A_{o,t}}\int_0^s\left(-\frac{1}{2}\frac{\sigma_{yc}}{s^2}x^3 + \frac{3}{2}\frac{\sigma_{yc}}{s}x^2 - \sigma_{yc}\,x\right)dx$$

$$= \frac{t}{G A_{o,t}}\left(-\frac{1}{8}\frac{\sigma_{yc}}{s^2}s^4 + \frac{3}{6}\frac{\sigma_{yc}}{s}s^3 - \frac{1}{2}\sigma_y s^2\right)$$

$$= \frac{t}{G A_{o,t}}\sigma_{yc}s^2\left(\frac{3}{6} - \frac{1}{8} - \frac{1}{2}\right)$$

$$= \underline{-\frac{1}{8}\frac{t\,\sigma_{yc}\cdot s^2}{G A_{o,t}}}$$

where $A_{o,t} = \frac{5}{6}A_T = \frac{5}{6}t\cdot a$

Note: Positive direction downwards so the deflection is upwards

The deflection of the bottom is derived identically, but the load have a sign change and the represetative area $A_{o,b} = \frac{5}{6}ts$

$$u_{v,b} = +\frac{1}{8}\frac{t\,\sigma_{yc}\cdot s^2}{G A_{o,b}}$$

Clamped beam - upper beam

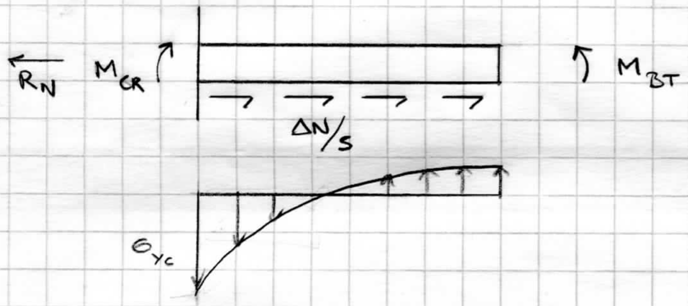

$L = L1 + L2 + L3$

The illustrated loads can be split up into three cases.

L1.

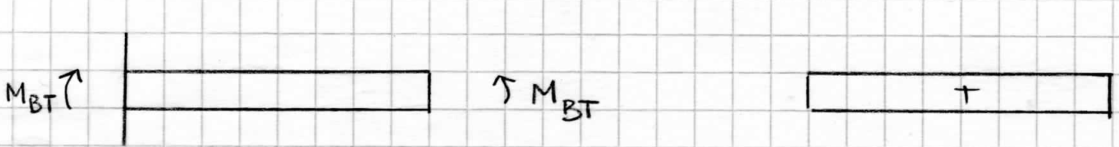

L2

L3

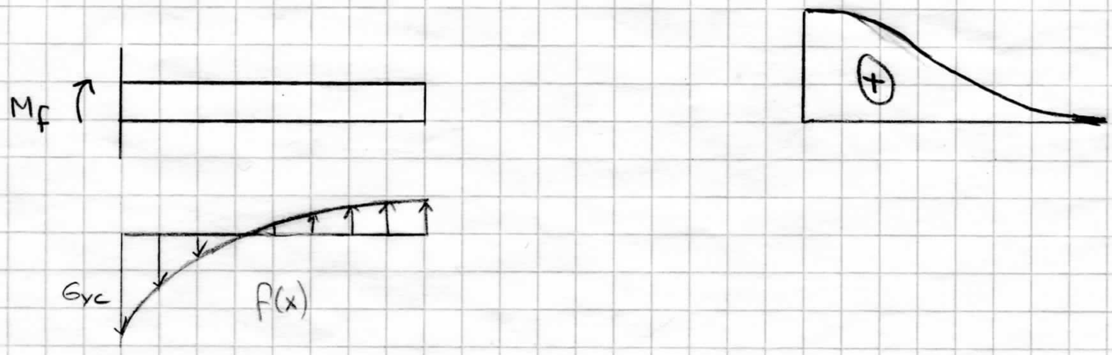

Unit load

Moment distribution for L1 - Constant moment

$$M_{OT,1} = M_{bt} = \frac{1}{2} a \frac{1}{2} a t \left(\sigma_{1b} + \sigma_{2b} \right) + \frac{1}{2} t \left((-\sigma_{2b}) a \frac{2}{3} a - \sigma_{1b} a \frac{1}{3} a \right)$$

Moment distribution for L2 - Horizontal line load

The line load act on the bottom of the beam, which is $\frac{1}{2}a$ from the beam axis. The moment distribution is linear with a moment at the clamped support

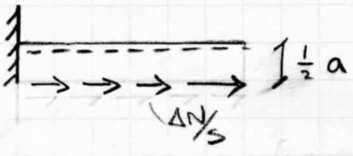

$$M_{OT,2}(0) = \frac{1}{2} a \Delta N$$

And a zero moment at the free end

Therefore,

$$M_{OT,2}(x) = \frac{1}{2} a \Delta N \left(1 - \frac{x}{s} \right)$$

Moment distribution for L3 - distributed load - upper beam

The sign ($\pm$) of the distributed load $f(x)$ depend on which beam part there is considered.

For the upper beam the following distribution is used

$$f(x) = -\frac{3}{2}\frac{6_{yc}}{s^2}x^2 + \frac{3\,6_{yc}}{s^2}x - 6_{yc}$$

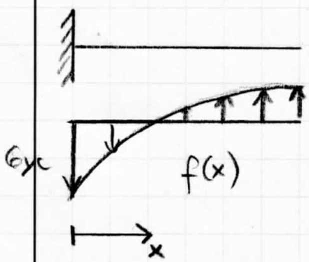

$$M_{OT,3} = \int V_{OT}\,dx = -\iint f(x)\,dx\,dx$$

$$= t\left(\frac{1}{8}\frac{6_{yc}}{s^2}x^4 - \frac{3}{6}\frac{6_{yc}}{s}x^3 + \frac{1}{2}6_{yc}x^2\right) + C_2$$

The constant C_2 is given by the boundary condition that $M_{OT,3}(s) = 0$

$$\Rightarrow C_2 = -t\left(\frac{1}{8}\frac{6_{yc}}{s^2}s^4 - \frac{3}{6}\frac{6_{yc}}{s}s^3 + \frac{1}{2}6_{yc}s^2\right)$$

$$= -t\,6_{yc}s^2\left(\frac{1}{8} - \frac{3}{6} + \frac{1}{2}\right)$$

$$= -\frac{1}{8}t\,6_{yc}s^2$$

$$\Rightarrow M_{OT,3} = t\left(\frac{1}{8}\frac{6_{yc}}{s^2}x^4 - \frac{1}{2}\frac{6_{yc}}{s}x^3 + \frac{1}{2}6_{yc}x^2\right) - \frac{1}{8}t\,6_{yc}s^2$$

Unit load

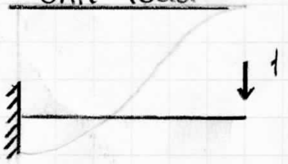

$$M_1(x) = 1\,(x-s)$$

Vertical displacement by virtual work, at the point of the unit load.

$$u_t \cdot 1 = \int_0^s \frac{M_1(x)\cdot M_{OT,1}(x)}{E_c I_T}dx + \int_0^s \frac{M_1(x)\cdot M_{OT,2}(x)}{E_c I_T}dx + \int_0^s \frac{M_1(x)\cdot M_{OT,3}(x)}{E_c I_T}dx$$

$$= -\frac{1}{24}\frac{s^2\left(-a^2 t\,6_{2b} + a^2 t\,6_{1b} + 4a\Delta N + t\,6_{yc}s^2\right)}{E_c I_T}$$

Remark that that this results in an upward displacement but it is the same for all the calculated displacements, and since it is an equality equation the positive direction do not influence.

Udkragt bjælke nederste del - illustration.

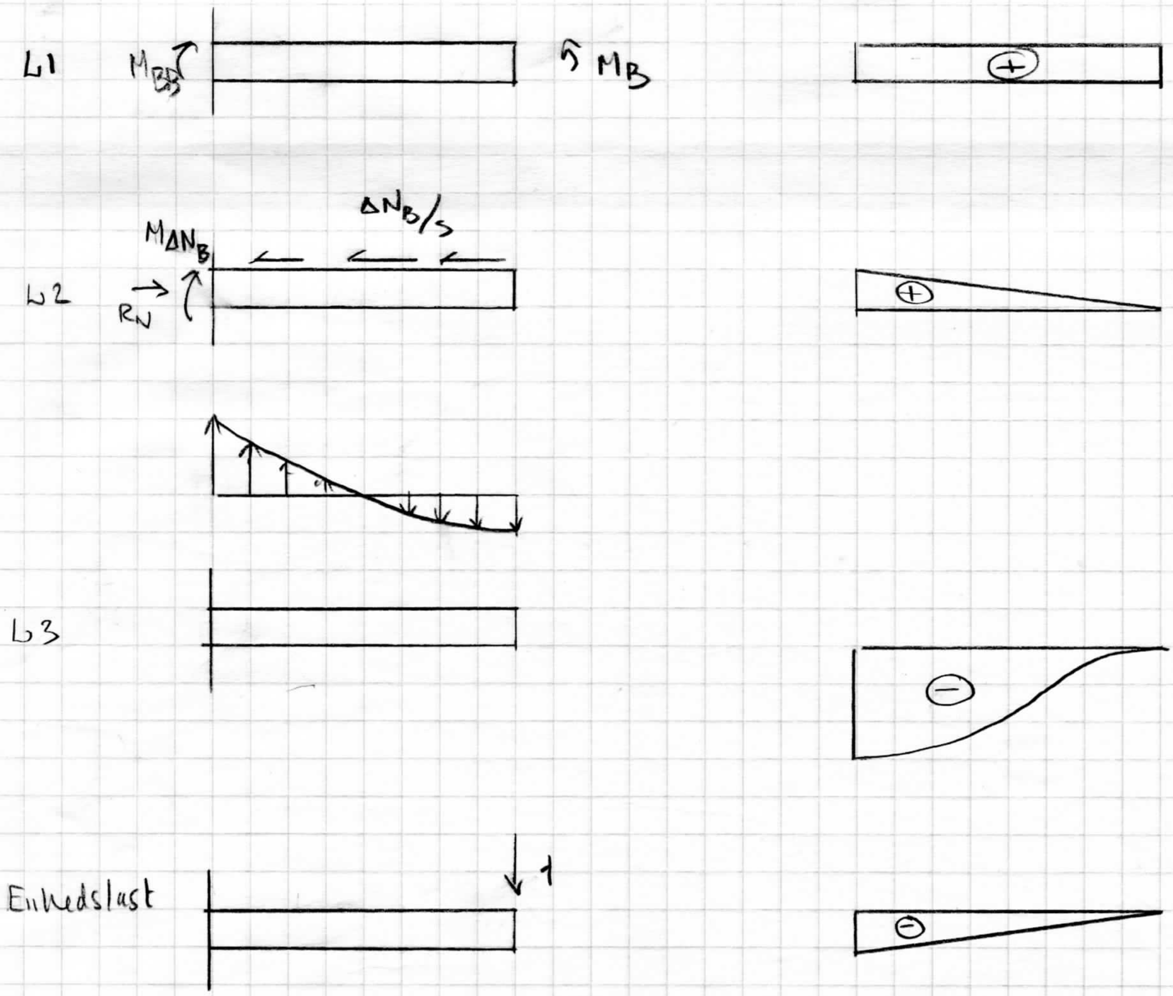

Udkraget bjælke nederste del

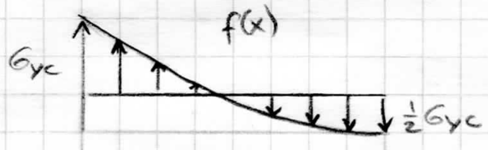

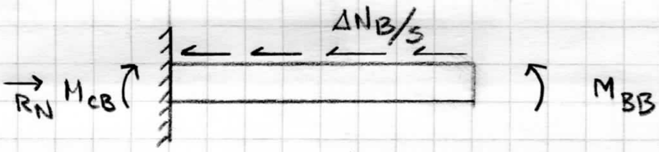

Lasten opdeles igen i 3 tilfælde for hvilke momentfordelingen beregnes for det enkelte tilfælde.

$$M'_A(x) = M_{BB} = \frac{1}{2} c \frac{1}{2} c t \cdot (\sigma_{OB} + \sigma_{1B})$$
$$+ t \cdot \left(-\frac{1}{2}\sigma_{1B} \cdot c \frac{2}{3} c - \frac{1}{2}\sigma_{OB} \cdot c \cdot \frac{1}{3} c\right)$$

$$M'_B(x) = M_{\Delta N} - \frac{1}{2} c \Delta N_B \frac{x}{s} = \frac{1}{2} c \Delta N_B \left(1 - \frac{x}{s}\right)$$

$$M'_C(x) = -\frac{1}{8} + \sigma_{yc} s^2 + t\left[-\frac{3}{8}\frac{\sigma_{yc} x_1^4}{s^2} + \left(\frac{\sigma_{yc}}{s} + \frac{1}{2}\frac{\sigma_{yc} x_1}{s^2}\right) x_1^3\right.$$
$$\left. + \left(-\frac{1}{2}\sigma_{yc} - \frac{3}{2}\frac{\sigma_{yc} x_1}{s}\right) x_1^2 + \sigma_{yc} x_1^2\right]$$

$$= -\frac{1}{8}\frac{t \cdot \sigma_{yc}(s^4 - x_1^4 + 4 x_1^3 \cdot s - 4 x_1^2 s^2)}{s^2}$$

Lodret flytning yderst – Bjælke bidrag – VAP anvendes

$$u_b = -\frac{1}{24}\frac{s^2 \cdot (-tc^2 \cdot \sigma_{OB} + tc^2 \cdot \sigma_{1B} - 4c\Delta N_B + t\,\sigma_{yc} \cdot s^2)}{EI}$$

Stiftlegeme rotation

$$u_r = -\frac{W_o}{c} \cdot s$$

Samlet lodret flytning – bund

$$u_{Tot} = u_b + u_r$$

Kontrolberegning - størrelse af lodret flytning

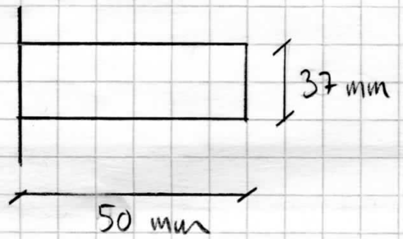

$E = 31000$

$I = \frac{1}{12} \cdot 100 \cdot 37^3$

$\sigma_{yc} = 2{,}2$ MPa

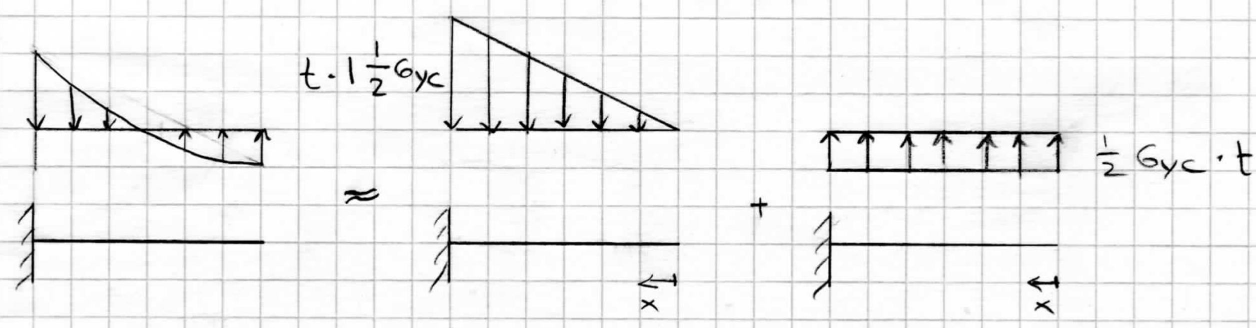

$u(0) = \frac{1}{30} \cdot \frac{q_1 l^4}{EI}$ $\qquad$ $u(0) = \frac{1}{8} \cdot \frac{q_2 l^4}{EI}$

Flytning af yderste punkt (positiv ned)

$$u = \frac{1}{30} \cdot \frac{q_1 l^4}{EI} - \frac{1}{8} \cdot \frac{q_2 l^4}{EI} = \frac{l^4}{EI}\left(\frac{q_1}{30} - \frac{q_2}{8}\right)$$

$$= \frac{50^4}{31000 \cdot \frac{1}{12} \cdot 100\ 37^3} \cdot \left(\frac{\frac{3}{2} \cdot 2{,}2 \cdot 100}{30} - \frac{\frac{1}{2} \cdot 2{,}2 \cdot 100}{8}\right)$$

$= \underline{-0{,}001314}$ (positiv ned)

$\boxed{\text{Matlab} \Rightarrow -0{,}004378 \text{ control value}}$

Bidrag fra normalkraft differencen

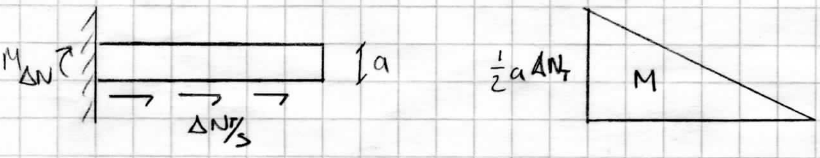

Denne last må svare til en lodret enkeltkraft der giver samme momentfordeling påsat yderst, virkende opad.

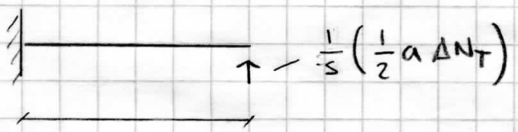

giver samme moment

$u(0) = \frac{1}{3} \frac{Q l^3}{EI}$

$\boxed{\text{Control value Matlab: } 0{,}0015257}$

$$u_{\Delta N} = \frac{1}{3} \cdot \frac{\frac{1}{5}\left(\frac{1}{2} \cdot 37 \cdot 1{,}295 \cdot 10^3\right) \cdot 5^3}{31000 \cdot \frac{1}{12} \cdot 100 \cdot 37^3} = \underline{0{,}0015257} \text{ (positiv op)}$$

Flytning ialt (2 bidrag) $\qquad u = 0{,}0015257 + 0{,}001314 = \underline{0{,}002839}$

Control calculation - Vertical displacement from constant moment

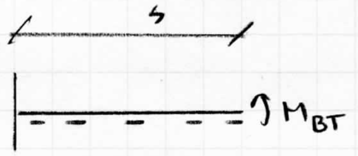

The simple example fra "Teknisk Ståbi" illustrated gives the wanted displacement at the midle if af beam of length $l = 2s$ is considered.

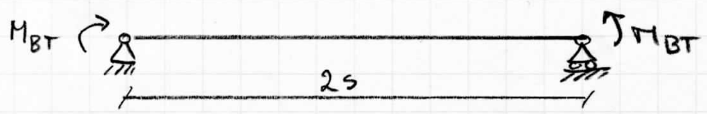

$$u_{Max} = \frac{1}{8} \frac{M l^2}{EI} = 0{,}0068$$

Matlab calculation gives: 0,006866 ✓